

UNCLASSIFIED

AD NUMBER

AD839355

LIMITATION CHANGES

TO:

Approved for public release; distribution is unlimited.

FROM:

Distribution authorized to U.S. Gov't. agencies and their contractors; Critical Technology; AUG 1968. Other requests shall be referred to Air Force Weapons Laboratory, WLRT, Kirtland AFB, NM 87117. This document contains export-controlled technical data.

AUTHORITY

afwl ltr, 30 nov 1971

THIS PAGE IS UNCLASSIFIED

AD839355

AFWL-TR-67-150

AFWL-TR-67-150

NUCLEAR INTERFERENCE STUDIES II :

A Physics Code for the Dynamics of High-Altitude Nuclear Bursts

W. McNamara
D. H. Archer
T. A. Hoffman

General Electric Company
TEMPO
Santa Barbara, California
Contract F29601-67-C-0059

TECHNICAL REPORT NO. AFWL-TR-67-150

August 1968

AIR FORCE WEAPONS LABORATORY
Air Force Systems Command
Kirtland Air Force Base
New Mexico

DDC
RECEIVED
SEP 13 1968
RECEIVED
C

This document is subject to special export controls and each transmittal to foreign governments or foreign nationals may be made only with prior approval of AFWL (WLRT) , Kirtland AFB, NM, 87117

**BEST
AVAILABLE COPY**

| | |
|---------------------------------|--|
| ACCESSION for | |
| CFSTI | WHITE SEC FOR <input type="checkbox"/> |
| DDC | BUFF SECTION <input checked="" type="checkbox"/> |
| UNANNOUNCED | <input type="checkbox"/> |
| JUSTIFICATION..... | |
| BY..... | |
| DISTRIBUTION/AVAILABILITY CODES | |
| DIST. | AVAIL. and/or SPECIAL |
| 2 | |

AIR FORCE WEAPONS LABORATORY
 Air Force Systems Command
 Kirtland Air Force Base
 New Mexico

When U. S. Government drawings, specifications, or other data are used for any purpose other than a definitely related Government procurement operation, the Government thereby incurs no responsibility nor any obligation whatsoever, and the fact that the Government may have formulated, furnished, or in any way supplied the said drawings, specifications, or other data, is not to be regarded by implication or otherwise, as in any manner licensing the holder or any other person or corporation, or conveying any rights or permission to manufacture, use, or sell any patented invention that may in any way be related thereto.

This report is made available for study with the understanding that proprietary interests in and relating thereto will not be impaired. In case of apparent conflict or any other questions between the Government's rights and those of others, notify the Judge Advocate, Air Force Systems Command, Andrews Air Force Base, Washington, D. C. 20331.

DO NOT RETURN THIS COPY. RETAIN OR DESTROY.

NUCLEAR INTERFERENCE STUDIES II:
A Physics Code for the Dynamics of
High-Altitude Nuclear Bursts

W. McNamara
D. H. Archer
T. A. Hoffman
General Electric Company
TEMPO
Santa Barbara, California
Contract F29601-67-C-0059

TECHNICAL REPORT NO. AFWL-TR-67-150

This document is subject to special export controls and each transmittal to foreign governments or foreign nationals may be made only with prior approval of AFWL (WLRT), Kirtland AFB, NMex 87117. Distribution is limited because of the technology discussed in the report.

FOREWORD

This report was prepared by General Electric, TEMPO, Santa Barbara, California, under Contract F29601-67-C-0059. The research was performed under Program Element 6.25.03.01R, and was funded by the Advanced Research Projects Agency under ARPA Order 727.

Inclusive dates of research were 1 March 1967 through 31 December 1967. The report was submitted 17 July 1968 by the AFWL Project Officer, Capt Paul B. Fleming (WLRT).

The contractor's report number is 67TMP-111 and represents in part, a documentation of work performed on this contract. Other reports of work accomplished during the term of this contract are: AFWL-TR-67-122 (67TMP-100) The Effect of Dispersion on the Ambiguity Function of a Train of Chirped Gaussian Pulses (U); AFWL-TR-67-123 (67TMP-104) Air-Debris Turbulent Interaction in High-Altitude Nuclear Detonations (U); AFWL-TR-67-138 (67TMP-118) Nuclear Precursors Today (U); AFWL-TR-67-139 (67TMP-106) Nuclear Precursors (U); AFWL-TR-67-151 (67TMP-127) Collision-Free Shock Calculations (U); AFWL-TR-67-153 (67TMP-124) Optical System Interference (U); AFWL-TR-67-154 (67TMP-105) Wideband Radar Simulation in a Nuclear Environment (U); AFWL-TR-67-155 (67TMP-129) Optical Countermeasures (U).

These reports represent the documentation of a continuing program in the analysis of radar and optical system performance in a nuclear-weapon environment.

This report has been reviewed and it approved.


PAUL B. FLEMING
Capt USAF
Project Officer


TRUMAN L. FRANKLIN
Colonel USAF
Chief, Theoretical Branch


CLAUDE K. STAMBAUGH
Colonel USAF
Chief, Research Division

ABSTRACT

(Distribution Limitation Statement No. 2)

A computational code is developed for investigating the dynamics of high-altitude nuclear bursts. The code can treat either one- or two-dimensional problems having either plane, cylindrical, or spherical symmetries. Electromagnetic and radiation transport effects are included, as are the effects of charge and current distributions. The numerical procedure computes the change during a time step of a property within a computational cell in terms of the fluxes of the property crossing the faces of the cell during the time step. The fluxes are computed by the method of characteristics. Use of a moving mesh permits the code to follow contact discontinuities in the field properties. Procedures for incorporating nonequilibrium thermodynamics are developed.

This page intentionally left blank.

CONTENTS

| <u>Section</u> | | <u>Page</u> |
|----------------|--|-------------|
| I | INTRODUCTION | |
| | 1. Problem Definition | 1 |
| | 2. Review of Existing Methods | 2 |
| | 3. Summary of the Present Approach | 3 |
| II | FORMULATION OF THE PROBLEM AND METHOD OF SOLUTION | |
| | 1. Statement of the Equations and Boundary Conditions | 5 |
| | 2. Normalization | 13 |
| | 3. Capabilities of Available Finite- Difference Methods | 14 |
| | 4. Method of Solution | 19 |
| III | FORMULATION OF THE PHYSICS CODE | |
| | 1. Integration of the Equations | 21 |
| | 2. Characteristic Solutions on Cell Boundaries | 29 |
| | 3. Constitutive Equations | 37 |
| | 4. Boundary Conditions | 47 |
| | 5. Mesh Geometry | 47 |
| | 6. Mesh Motion | 51 |
| | 7. Stability Analysis and Time-Step Calculation | 53 |
| | 8. Order of Computations in the Code | 55 |
| IV | DISCUSSION | |
| | 1. Method of Use | 57 |
| | 2. Further Development | 59 |

| Appendix | | <u>Page</u> |
|------------|---|-------------|
| I | Conservation Equations For a Reacting Nonequilibrium Mixture of Gases | 63 |
| II | Fortran Glossary and Flow Charts | 87 |
| III | Equations of Radiation Transport | 113 |
| IV | Maxwell's Equations | 123 |
| V | Integration of the Equations | 131 |
| VI | Characteristics | 143 |
| VII | Geometrical Formulae | 157 |
| VIII | Stability Analysis | 163 |
| References | | 167 |

FIGURES

| <u>Figure</u> | | <u>Page</u> |
|---------------|---|-------------|
| 1 | Computational Cells for Plane, Cylindrical, and Spherical Symmetries | 22 |
| 2 | Cross-Sectional Geometry of a Cell | 23 |
| 3 | Cell-Surface Coordinate System | 30 |
| 4 | Ionization Cross Sections as a Function of Velocity for Al^+ in Ar, N_2 , and Air | 39 |
| 5 | Ionization Rates for Atomic Oxygen and Nitrogen Versus Electron Temperatures | 41 |
| 6 | Cross Sections for the Dissociative Ionization of Molecular Nitrogen Yielding Product Ions With Kinetic Energies Greater than 0.25 ev | 42 |
| 7 | Cross Sections for the Dissociative Ionization of Molecular Oxygen Yielding Product Ions With Kinetic Energies Greater than 0.25 ev | 42 |
| 8 | Discontinuous Arcs | 49 |
| 9 | Node Velocity Geometry | 52 |
| 10 | Flow Chart of MAIN Program | 97 |
| 11 | Flow Chart of Subroutine ADVNCE | 98 |
| 12 | Flow Chart of Subroutine ARC | 99 |

| | | |
|----|---|-----|
| 13 | Flow Chart of Subroutine ARCGEO | 100 |
| 14 | Flow Chart of Subroutine COLUMN | 101 |
| 15 | Flow Chart of Subroutine DIFFEQ | 102 |
| 16 | Flow Chart of Subroutine FLUX | 103 |
| 17 | Flow Chart of Subroutine GMTRY | 104 |
| 18 | Flow Chart of Subroutine RAY | 105 |
| 19 | Flow Chart of Subroutine RESET | 106 |
| 20 | Flow Chart of Subroutine RAYGEO | 107 |
| 21 | Flow Chart of Subroutine SOURCE | 108 |
| 22 | Flow Chart of Subroutine THERMO | 109 |
| 23 | Flow Chart of Subroutine VOLUME | 110 |
| 24 | Flow Chart of Subroutine WALL | 111 |
| 25 | Surface Coordinate System | 144 |
| 26 | Three-Dimensional Surface Coordinate System | 154 |

NOTATIONS

Quantities with subscript asterisks are dimensional quantities; quantities without subscript asterisks are nondimensional quantities.

| | |
|-------------------|--|
| A | A_*/L_*^2 ; cross-sectional area of a cell of revolution |
| a_α | $\frac{a_\alpha}{U_*}$; speed of sound of species α |
| \vec{B} | $B_* / [E_* (\mu_{o*} \epsilon_{o*})^{1/2}]$; magnetic flux density |
| B_o | $4\sigma_* T_*^4 / \rho_* U_*^3$; Boltzmann number |
| B_u | $\rho_* \kappa_* L_*$; Bouguer number |
| \vec{B}_* | magnetic flux-density (dimensions: Webers/m ² in rationalized mks; emu (gauss) in Gaussian) |
| c | c_*/U_* ; speed of light |
| $c_{v\alpha}$ | $\left(\frac{\partial e_\alpha}{\partial T_\alpha} \right) \rho_\alpha$; specific heat at constant volume |
| c_* | dimensional speed of light |
| $d_{i,j}$ | distance along ray i from z axis to intersection of ray i and arc j |
| ϵ_α | $e_\alpha + \langle u_\alpha^2 / 2 \rangle$; mean energy per unit mass of species α |
| \vec{E} | \vec{E}_*/E_* ; electric field intensity |

- E_* $\frac{\rho_* q_* L_{D*}}{M_* \epsilon_{O*}}$; reference electric field intensity
- \vec{E}_* electric field intensity (dimensions: volt/meter in rationalized mks ; esu (statvolt/cm) in Gaussian)
- e_R $\frac{e_{R*}}{4\sigma_* T_*^4 / c_*}$; radiative energy density
- $e_{R\nu}$ $h_* \nu_* n_{R\nu*} / (4\sigma_* T_*^4 / c_* \nu_{R*})$; energy density of photons of frequency ν
- e_{R*} dimensional radiative energy density
- e_α $e_{\alpha*} / U_*^2$; internal energy per unit mass of species α
- e_{R*} dimensional radiative energy density
- \vec{F}_α $\vec{F}_{\alpha*} / (M_* U_*^2 / L_*)$; force per particle on species α in addition to pressure stress and electromagnetic forces
- $\vec{F}_{\alpha*}$ dimensional force per particle on species α
- $f_{R\nu*}$ $(\vec{r}_*, \vec{c}_*, t_*)$; distribution function for photons of frequency ν_*
- $f_\alpha(\vec{u}, \vec{r}, t)$ distribution function of species α
- $\mathcal{L}_\alpha(1)$ $K m_\alpha w_\alpha(1)$; mass source term for species α
- $\vec{\mathcal{L}}_\alpha(2)$ $\rho_\alpha \left[\frac{\vec{F}_\alpha}{m_\alpha} + \frac{1}{\mathcal{M}} \frac{q_\alpha}{m_\alpha} \left(\vec{E} + \frac{\langle \vec{u}_\alpha \rangle \times \vec{B}}{c} \right) \right] + K m_\alpha \vec{w}_\alpha(u)$
- momentum source term for species α

- $\mathcal{E}_\alpha^{(3)}$ $B_o B_u \int [e_{R\nu} \kappa_{R\nu} (1 - J_{\nu\alpha}) - j_{\nu\alpha}] d\nu + \frac{\rho_\alpha}{m_\alpha} \langle \vec{u}_\alpha \rangle \cdot$
 $\cdot \left(\vec{F}_\alpha + \frac{q_\alpha}{m} \vec{E} \right) + K m_\alpha w_\alpha (e + u^2/2) ;$
 energy source term for species α
- $\mathcal{E}_\nu^{(1)}$ $c B_u \sum_\alpha \rho_\alpha \left[\kappa_{\nu\alpha} e_{R\nu} (1 - J_{\nu\alpha}) - j_{\nu\alpha} \right] ;$
 energy source term for photons of frequency ν
- $\mathcal{E}_\nu^{(2)}$ $c B_u Q_{R\nu} \sum_\alpha \rho_\alpha \kappa_{\nu\alpha} (1 - J_{\nu\alpha} + S_{\nu\alpha}) ;$
 energy-flux source term for photons of frequency ν
- $g_{\alpha\beta}$ $|\vec{u}_\alpha - \vec{u}_\beta| ;$ relative velocities of particles of species α and β
- h_r distance across a cell in the radial direction
- I maximum number of rays in the mesh
- \vec{I} unit identity tensor ; $(\vec{a} \cdot \vec{I} = \vec{I} \cdot \vec{a} = \vec{a})$
- $J_{i+1/2}$ maximum number of arcs in column $(i+1/2)$
- $J_{\alpha\pm}$ $\langle u_{\alpha n} \rangle_\pm = \int^P_\alpha \frac{dP_\alpha}{\rho_\alpha a_\alpha} ;$ hydrodynamic characteristics
- $J_{\nu\pm}$ $e_{R\nu} \pm \sqrt{3} Q_{R\nu n} ;$ characteristics of the equations of radiation transport
- $J_{1\pm}$ $B_{S_1} \pm E_{S_2} ;$ electromagnetic characteristics
- $J_{2\pm}$ $B_{S_2} \pm E_{S_1} ;$ electromagnetic characteristics

| | |
|------------------|--|
| $J_{\nu\alpha}$ | $\frac{J_{\nu\alpha*}}{\kappa_{\nu\alpha*}}$ |
| $J_{\nu\alpha*}$ | cross section for induced emission at frequency ν by unit mass of species α ; dimensions are area/mass |
| \vec{j} | \vec{j}_*/j_* ; current density |
| $j_{\nu\alpha}$ | $\frac{j_{\nu\alpha*}}{4\kappa_*\sigma_*T_*^4/\nu R_*}$ |
| $j_{\nu\alpha*}$ | spontaneous emission coefficient for energy at frequency ν by unit mass of species α ; dimensions are energy/mass · frequency |
| j_* | $N_*q_{e*}U_*$; reference current density |
| \vec{j}_* | electric current density (dimensions: amp/m ² in rationalized mks; esu(statamp) 10 m ² in Gaussian) |
| κ | $\frac{N_*k_*T_*}{\rho_*U_*^2}$ |
| K | $M_*\omega_*L_*/\rho_*U_*$; nondimensional parameter indicating relative importance of chemical reactions and hydrodynamic convection in changing the mass at a point |
| k_* | Boltzmann constant |
| \mathcal{L} | L_*/L_{D*} |
| L_{D*} | $\left(\frac{3k_*T_*\epsilon_{o*}}{N_*q_{e*}^2}\right)^{1/2}$; Debye length |
| L_* | reference length |
| $l_{i+1/2,j}$ | length of arc j in column $i + 1/2$ |

| | |
|--------------------|---|
| \mathcal{M} | $\left(\frac{\rho_* U_*}{N_*}\right) / \left(\frac{q_{e*} E_* L_*}{U_*}\right)$ |
| M_* | reference particle mass |
| m_α | $m_{\alpha*} / M_*$; mass of a particle of species α |
| N | number of species under consideration |
| N_* | reference particle density |
| n | rectangular Cartesian coordinate normal to a cell surface |
| $n_{R\nu_*}$ | number density of photons of frequency ν_* |
| n_{R*} | number density of photons of all frequencies |
| n_α | $n_{\alpha*} / (\rho_* / M_*)$; number density of particles of species α |
| $\vec{P}_{R\nu_*}$ | $\frac{\vec{P}_{R\nu_*}}{4\sigma_* T_*^4 / c_* \nu_{R*}}$; radiative pressure tensor |
| $\vec{P}_{R\nu_*}$ | dimensional radiative pressure tensor |
| P_α | $\frac{1}{3} \vec{P}_\alpha ; \vec{I}$ |
| \vec{P}_α | $\vec{P}_{\alpha*} / (\rho_* U_*^2)$; partial pressure tensor of species α |
| \vec{Q}_R | $\vec{Q}_{R*} / 4\sigma_* T_*^4$; radiative heat flux vector |
| $\vec{Q}_{R\nu}$ | $\frac{\int h_* \nu_* \vec{c}_* f_{R\nu_*} d\vec{c}_*}{4\sigma_* T_*^4 / \nu_{R*}}$; heat flux vector for photons of frequency ν_* |
| $Q_{R\nu n}$ | component of $\vec{Q}_{R\nu}$ normal to a cell surface |

| | |
|--------------------|--|
| \vec{Q}_{R*} | dimensional radiative heat flux vector |
| \vec{Q}_{α} | $\vec{Q}_{\alpha*} / (\rho_* U_*^3)$; heat flux vector of species α |
| q | q_*/q_{R*} ; charge density |
| q_{e*} | magnitude of the charge on the electron (positive) |
| q_{R*} | $N_* q_{e*}$; reference charge density |
| q_* | charge density (dimensions: coulombs/m ³ in rationalized mks ; esu/cm ³ (statcoul/cm ³) in Gaussian) |
| R_{α} | $R_{\alpha*} / (w_* U_*^3)$; rate of generation of particles of species α in unit phase space volume at (\vec{u}, \vec{r}) |
| \bar{R}_{α} | $\bar{R}_{\alpha*} / (w_* U_*^3)$; rate of loss of particles of species α in unit phase space volume at (\vec{u}, \vec{r}) |
| \vec{r} | \vec{r}_*/L_* ; position vector |
| \vec{r}_* | dimensional position vector |
| S | S_*/L_*^2 ; surface area |
| $S_{\nu\alpha}$ | $\frac{S_{\nu\alpha*}}{\kappa_{\nu\alpha*}}$ |
| $S_{\nu\alpha*}$ | cross -section for scattering of a photon of frequency ν by unit mass of species α ; dimensions are area/mass |
| s_{α} | $\frac{s_{\alpha*}}{T_*/U_*^2}$; entropy per unit mass of species α |
| s_1 | rectangular Cartesian coordinate tangential to a cell surface |
| s_2 | rectangular Cartesian coordinate tangential to a cell surface and normal to s_1 |

| | |
|--------------------------------------|--|
| T_* | reference temperature |
| t | $t_*/(L_*/U_*)$; time (T) |
| t_* | dimensional time |
| \vec{u} | $\frac{1}{\rho} \sum_{\alpha=1}^N \rho_{\alpha} \langle \vec{u}_{\alpha} \rangle$; mass velocity of the mixture |
| \vec{u}_{α} | \vec{u}_{α^*}/U_* ; velocity of a particle of species α |
| U_* | reference velocity |
| $\langle \vec{u}_{\alpha} \rangle_n$ | $\langle \vec{u}_{\alpha} \rangle \cdot \hat{v}$ |
| V | V_*/L_*^3 ; volume |
| \vec{V}_{α} | $\langle \vec{u}_{\alpha} \rangle - \vec{u}$; diffusion velocity of particles of species α |
| \vec{v}_{α} | $\vec{u}_{\alpha} - \langle \vec{u}_{\alpha} \rangle$; thermal velocity of a particle of species α |
| $\langle \vec{v}_{\alpha} \rangle$ | $\vec{u}_{\alpha} - \vec{u}$; mean thermal velocity of a particle of species α |
| \vec{W} | \vec{W}_*/U_* ; velocity of cell surface |
| W_n | W_{n^*}/U_* ; $\vec{W} \cdot \hat{v}$ |
| $w_{\alpha}(1)$ | $w_{\alpha^*}(1)/w_*$; rate of generation of particles of species α per unit volume |
| $\vec{w}_{\alpha}(u)$ | $\vec{w}_{\alpha^*}(\vec{u})/(w_*U_*)$; rate of generation of particle momentum of species α per unit volume |
| $w_{\alpha}(e + u^2/2)$ | $w_{\alpha^*}(e + u^2/2)/(w_*U_*^2)$; rate of generation of particle energy per unit volume |
| w_* | reference source rate (particles generated per unit volume per unit time) |

| | |
|-----------------------|--|
| α_i | angle between ray i and the negative z direction |
| $\beta_{i+1/2, j}$ | angle between arc j in column $i + 1/2$ and the positive z direction |
| $\Delta r_{i+1/2, j}$ | radial increment of arc j in column $i + 1/2$ |
| Δt | $\Delta t_* U_* / L_*$; time step |
| Δt_r | stable time step for a one-dimensional calculation in the radial direction |
| Δt_z | stable time step for a one-dimensional calculation in the axial direction |
| $\Delta z_{i+1/2, j}$ | axial increment of arc j in column $i + 1/2$ |
| e^{ijk} | antisymmetric three-tensor |
| e^{ijk} | $\begin{cases} +1, & \text{if } i, j, k \text{ is an even permutation of } 1, 2, 3 \\ -1, & \text{if } i, j, k \text{ is an odd permutation of } 1, 2, 3 \\ 0, & \text{otherwise} \end{cases}$ |
| ϵ_{0*} | primary electric constant in rationalized mks units (8.854×10^{-12} coulomb/volt \cdot m) $1/(4\pi)$ in Gaussian units |
| η | cross-sectional area factor |
| η | $\begin{cases} 0, & \text{plane geometry} \\ \pi, & \text{cylindrical geometry} \\ 4, & \text{spherical geometry} \end{cases}$ |
| $\kappa_{\nu\alpha}$ | $\kappa_{\nu\alpha} / \kappa_*$ |
| $\kappa_{\nu\alpha*}$ | dimensional mass absorption cross section of species α for photons of frequency ν ; dimensions are area/mass |

| | |
|-------------------|--|
| κ_* | reference mass absorption cross section; dimensions are area/mass |
| μ_{0*} | primary magnetic constant in rationalized mks units ($4\pi \times 10^{-7}$ weber/amp · m); 4π in Gaussian units |
| ν_{R*} | reference photon frequency |
| ν_r | direction cosine between outward normal to cell surface and r (or x for plane geometry) direction |
| ν_z | direction cosine between outward normal to cell surface and z direction. $\nu_z = 0$ for spherical geometry |
| $\hat{\nu}$ | unit outward normal to the surface of a volume element |
| ν_* | photon frequency |
| ρ | $\sum_{\alpha=1}^N \rho_{\alpha}$; mass of mixture per unit volume |
| ρ_{α} | $\rho_{\alpha*}/\rho_*$; density of species α |
| ρ_* | reference mass density (mass per unit volume) |
| σ_* | Stefan-Boltzmann constant |
| $\langle \rangle$ | denotes the Boltzmann average: for any quantity φ , $\langle \varphi_{\alpha} \rangle \equiv \int \varphi_{\alpha}(\vec{u}) f_{\alpha}(\vec{u}) d\vec{u} / \int f_{\alpha}(\vec{u}) d\vec{u}$ |

This page intentionally left blank.

SECTION I INTRODUCTION

In recent years a great deal of effort has gone into the detailed computation of the structure of atmospheric nuclear bursts. The numerical procedures developed for these calculations assume the existence of conventional hydrodynamic collisional coupling of the explosion debris to the ambient atmosphere; thus, strong shock waves are assumed. This assumption certainly is valid for altitudes below about 80 kilometers or so, and the numerical results for low altitude explosions appear valid.

The assumption of strong collisional coupling of the debris to the ambient atmosphere is not necessarily valid at higher altitudes; however, as a result, present computational techniques do not give reliable information concerning the effects of high yield, high altitude explosions.

1. PROBLEM DEFINITION

The information which is required and which existing techniques do not give concerns high yield explosions at high altitudes. The means by which such explosions couple to the atmosphere and the gross effects of the explosions are to be determined. In particular, techniques capable of computing the transient structure of the expanding debris of an explosion in the megaton range at an altitude between 100 and 500 km are desired. The computed structure is to include late-time effects, including disturbances of the earth's magnetic field.

2. REVIEW OF EXISTING METHODS

Existing attempts to treat high-altitude explosions either assume conventional coupling and apply ordinary hydrodynamic computer codes with a more rarefied atmosphere, or assume there is no coupling until the debris has expanded to some "coupling length," after which conventional hydrodynamic coupling is invoked. The assumption that conventional collisional coupling always exists obviously breaks down at some point: at a sufficiently high altitude, the mean free path for ambient ions becomes greater than the debris radius, and the conventional momentum transfer process disappears. The range of altitudes in which this coupling breakdown occurs is not known; however, because the energy released by the explosion so disturbs the ambient temperature and ionization that estimates of the effective mean free path for momentum transfer are not reliable.

Existing methods of accounting for the coupling breakdown do so by attempting to estimate an effective mean free path or "coupling length." Various processes have been postulated as ultimate sources of the coupling: examples include the "Longmire Piston," in which the motion of the ionized debris generates a magnetic field that turns or "picks up" the ambient ions; two-stream instability, in which the electric field between the debris ions and the ambient ions grows in an unstable fashion until it becomes strong enough to pick up the ambient ions; and the collisional model, in which the mean free path for direct collisions is estimated on the basis of the relative velocities of the debris and ambient ions. All of these postulated coupling processes require rather involved mathematical formulations which are not usable in existing hydrodynamics codes. As a result, the only calculations which have been made with these processes are approximate analytical calculations solely intended to demonstrate the possibility that the process is

significant. No detailed calculations intended to show the actual effect of such processes have been made.

3. SUMMARY OF THE PRESENT APPROACH

Because of the potential significance of coupling processes of the type discussed above, a physics code is developed which can handle the mathematical formalism associated with these coupling processes. A suitable coding technique exists and has been used on transient interaction problems in the past; further, the code has been redeveloped to the point where it is useful for studying the detailed behavior of the proposed coupling models. This code, which is an Eulerian code with a floating mesh, employs the characteristic flux differencing technique: the changes in all properties during a time-step are caused by the fluxes of those properties across the surface of the cell during the time-step. Because surface fluxes in a rarefied gas do not involve thermodynamics or kinetic processes such as collisions, it is possible to construct the entire finite-difference code without such models. These models are added in subroutine form for the evaluation of properties such as partial pressures and sound speeds within each cell. This differencing procedure has the great versatility of permitting a complete change of the kinetic and thermodynamic models to be made merely by changing a few subroutines.

This code structure will be useful for carrying out detailed one-dimensional studies of the interaction of debris and ambient ions for each of the postulated coupling processes. The results of the more effective of these processes can be scaled into "coupling laws," which might be used in a two-dimensional calculation of the gross expansion. In addition, two-dimensional studies can be made for those coupling mechanisms which are inherently two-dimensional; the "Longmire Piston" with its streaming debris, perpendicular magnetic field, and

turning of the ambient ions is an example of a coupling process which must be treated as at least two-dimensional.

In addition, numerical studies for evaluating the several coupling mechanisms and calculating the gross expansion structure of high-altitude explosions can be carried out.

SECTION II

FORMULATION OF THE PROBLEM AND METHOD OF SOLUTION

The problem being treated here is that of developing a computer code which can be used for the dual purposes of (1) testing the efficacy of proposed mechanisms for coupling the debris from a high-altitude explosion to the ambient atmosphere, and (2) computing the overall features of explosions for which the coupling mechanisms have been determined. The method of treating this problem consists of using the governing equations in a form that is valid regardless of the coupling mechanism, selecting an appropriate numerical procedure for solving these equations, and developing (and coding as sub-routines) models of the proposed coupling mechanisms.

1. STATEMENT OF THE EQUATIONS AND BOUNDARY CONDITIONS

A mathematical description of explosion phenomenology must involve conservation of mass, momentum, and energy; probably must include radiative phenomena; and must account for electromagnetic effects. In addition, a set of constitutive equations is required, including equations of state and of electrical conductivity. Finally, appropriate boundary conditions must be prescribed.

The interacting explosion debris and ambient atmosphere may consist of molecular, atomic, and ionized species plus electrons. It is assumed that there are N such species present, including electrons; an individual species is denoted by subscript alpha. The symbols

used in the following equations are defined in the Glossary, and the normalization is discussed in Subsection II-2 below.

a. Hydrodynamic Conservation Equations

The equations expressing the conservation of mass, momentum, and energy of species α are obtained by taking moments of the Boltzmann equation for species α (Appendix I). The resulting conservation equations are

Mass:

$$\frac{\partial \rho_\alpha}{\partial t} + \vec{\nabla} \cdot (\rho_\alpha \langle \vec{u}_\alpha \rangle) = K m_\alpha w_\alpha \quad (1)$$

Momentum:

$$\begin{aligned} \frac{\partial}{\partial t} (\rho_\alpha \langle \vec{u}_\alpha \rangle) + \vec{\nabla} \cdot (\rho_\alpha \langle \vec{u}_\alpha \rangle \langle \vec{u}_\alpha \rangle + \vec{P}_\alpha) \\ = \rho_\alpha \langle \vec{F}_\alpha / m_\alpha \rangle + K m_\alpha \vec{w}_\alpha(u) \end{aligned} \quad (2)$$

Energy:

$$\begin{aligned} \frac{\partial}{\partial t} (\rho_\alpha e_\alpha) + \vec{\nabla} \cdot (\rho_\alpha e_\alpha \langle \vec{u}_\alpha \rangle + \vec{P}_\alpha \cdot \langle \vec{u}_\alpha \rangle) \\ = - \vec{\nabla} \cdot \vec{Q}_\alpha + \rho_\alpha \langle \vec{F}_\alpha / m_\alpha \rangle \cdot \langle \vec{u}_\alpha \rangle \\ + K m_\alpha w_\alpha (e + u^2/2) \end{aligned} \quad (3)$$

Equations 1 through 3 are valid for nonequilibrium flow as well as equilibrium flow. The w_α terms on the right-hand sides of these equations represent sources and sinks of mass, momentum, and energy resulting from particle collisions. In the event of equilibrium flow, these source terms, which derive from the collisional term in the Boltzmann equation, vanish, and the pressure tensor is given by the equilibrium equation of state. In the event of nonequilibrium or of chemically-reacting flow, these terms are

evaluated by approximating the collisional terms in the Boltzmann equation by experimentally determined cross sections for the collision in question (see Appendix I).

b. Radiation Transport Equations

Equations for the energy density and heat-flux vector of radiation of frequency ν are obtained by taking moments of the Boltzmann equation for the distribution function of photons of energy $h\nu$ (Appendix III). The resulting equations are

$$\frac{1}{c} \frac{\partial e_{R\nu}}{\partial t} + \vec{\nabla} \cdot \vec{Q}_{R\nu} = -Bu \sum_{\alpha} \rho_{\alpha} \left[\kappa_{\nu\alpha} e_{R\nu} (1 - J_{\nu\alpha}) - j_{\nu\alpha} \right] \quad (4)$$

$$\frac{1}{c} \frac{\partial \vec{Q}_{R\nu}}{\partial t} + \vec{\nabla} \cdot \vec{P}_{R\nu} = -Bu \vec{Q}_{R\nu} \sum_{\alpha} \rho_{\alpha} \kappa_{\nu\alpha} (1 - J_{\nu\alpha} + S_{\nu\alpha}) \quad (5)$$

Equations 4 and 5 are valid for any radiation condition. The terms on the right-hand sides of these equations represent sources and sinks of radiative energy and heat flux resulting from absorption, emission, and scattering.

c. Maxwell's Equations

Maxwell's equations must be normalized into a form which can be related to a wide variety of initial conditions in order to be convenient for general computational purposes. It is shown in Appendix IV that either the rationalized mks form or the Gaussian form of Maxwell's equations can be normalized into the following set:

$$\vec{\nabla} \cdot \vec{E} = \mathcal{E}q \quad (6)$$

$$\vec{\nabla} \cdot \vec{B} = 0 \quad (7)$$

$$\vec{\nabla} \times \vec{E} = -\frac{1}{c} \frac{\partial \vec{B}}{\partial t} \quad (8)$$

$$\vec{\nabla} \times \vec{B} = \frac{\mathcal{L} \vec{j}}{c} + \frac{1}{c} \frac{\partial \vec{E}}{\partial t} \quad (9)$$

Equations 6 through 9 are valid for the electromagnetic fields in any moving medium with no inaccessible charges or currents; that is, all charges and currents are assumed accounted for by the moving particles of the medium, and there are no polarization currents.

d. Constitutive Equations

The field equations listed above must be complemented by a set of constitutive equations which govern the transport properties of the fields in the medium of propagation. Thus, Equation 2 requires an equation for the partial pressure tensor of species α (or for the transport of momentum) and Equation 3 requires an equation for the heat-flux vector of species α (or for the transport of energy). Similarly, Equation 5 requires an equation for the radiative pressure tensor (or for the transport of radiative momentum), while Equation 9 requires an equation for the current (or for the transport of charge). These constitutives represent moments of the nonequilibrium distribution functions, and generally are not known. However, it is possible to postulate various models for these needed equations, and it will be shown (Subsection III-2c) that these constitutive equations do not affect or enter into the differencing technique for the numerical code. As a result, it is possible to change the constitutive equations used in the code merely by changing the corresponding subroutines.

A number of models for the hydrodynamic constitutive equations are available; these models usually are based either on the

Chapman and Enskog perturbation theory for the nonequilibrium distribution function (Reference 1), or on extensive experimental data. The simplest models having any physical reality for the hydrodynamic constitutive equations (and the ones which are being used for the initial numerical work with the code) are

$$\vec{P}_{\alpha*} = n_{\alpha*} k_* T_{\alpha*} \vec{I} \quad (10)$$

and

$$\vec{Q}_{\alpha*} = 0 \quad (11)$$

Equation 10 is a valid equation for nonequilibrium flow, but is an approximate model because shearing stresses have been ignored (see, for example, Section 2, Chapter IX of Reference 2). In normalized form, Equations 10 and 11 are

$$\vec{P}_{\alpha} = n_{\alpha} k T_{\alpha} \vec{I} \quad (12)$$

and

$$\vec{Q}_{\alpha} = 0 \quad (13)$$

A satisfactory constitutive equation for the radiative pressure tensor appears to be that given by the Milne-Eddington approximation (which has been used successfully in astrophysics):

$$\vec{P}_{R\nu} = \frac{eR_{\nu}}{3} \vec{I} \quad (14)$$

It can be shown that Equations 4 and 5 with Equation 14 lead to the correct radiation transport formulae in the optically thick and optically thin limits as well as in the limit of isotropic radiation. Equations 4 and 5 with Equation 14 are similar in form to the equations obtained in the first approximation in the spherical-harmonic method of neutron transport theory; in that theory it is

known that the odd approximations are more accurate than the succeeding even approximations (Reference 2). A final comment on the validity of Equation 14 is that it deals with the transport of radiative momentum, and that radiative momentum considerations only enter in a relativistic theory. Consequently, Equation 14 is expected to be a satisfactory constitutive equation in a nonrelativistic theory.

The necessary constitutive equation for the current density in Equation 9 is straightforward as long as all of the charges move by convective flow and no conduction currents exist; this equation is

$$\vec{j} = \sum_{\alpha} n_{\alpha} q_{\alpha} \langle \vec{u}_{\alpha} \rangle \quad (15)$$

If problems involving conduction currents are to be treated, it will be necessary to develop an expression for the conductivity of the flowing gas. The initial numerical work, however, will rely on Equation 15.

e. Coupled Equations

The momentum and heat transfer effects governed by the radiation transport equations and Maxwell's equations must be coupled into the hydrodynamic equations to provide a complete description of the physics of the problem.

As shown in Appendix IV, the electromagnetic component of the force term in Equation 2 has the normalized form

$$\vec{F}_{\alpha} = \frac{q_{\alpha}}{m} \left(\vec{E} + \frac{\vec{u}_{\alpha} \times \vec{B}}{c} \right) \quad (16)$$

Similarly, the electromagnetic component of the normalized work term in Equation 3 is shown to be

$$\vec{F}_\alpha \cdot \vec{u}_\alpha = \frac{q_\alpha}{m} \vec{E} \cdot \vec{u}_\alpha \quad (17)$$

The heat added to species α by absorption of radiative energy is given by Equation 273 of Appendix III as

$$\frac{\partial}{\partial t} (\rho e_\alpha)_R = B_o B_u \int [e_{R\nu} \kappa_{R\nu} (1 - J_{\nu\alpha}) - j_{\nu\alpha}] d\nu \quad (18)$$

Coupling Equations 16 through 18 into Equations 1 through 3 gives the coupled hydrodynamic equations:

$$\frac{\partial \rho_\alpha}{\partial t} + \vec{\nabla} \cdot (\rho_\alpha \langle \vec{u}_\alpha \rangle) = K m_\alpha w_\alpha (1) \quad (19)$$

$$\begin{aligned} \frac{\partial}{\partial t} (\rho_\alpha \langle \vec{u}_\alpha \rangle) + \vec{\nabla} \cdot (\rho_\alpha \langle \vec{u}_\alpha \rangle \langle \vec{u}_\alpha \rangle + \vec{P}_\alpha) \\ = \rho_\alpha \left[\frac{\vec{F}_\alpha}{m_\alpha} + \frac{1}{m} \frac{q_\alpha}{m_\alpha} \left(\vec{E} + \frac{\langle \vec{u}_\alpha \rangle \times \vec{B}}{c} \right) \right] + K m_\alpha \vec{w}_\alpha (u) \end{aligned} \quad (20)$$

$$\begin{aligned} \frac{\partial}{\partial t} (\rho_\alpha e_\alpha) + \vec{\nabla} \cdot (\rho_\alpha e_\alpha \langle \vec{u}_\alpha \rangle + \vec{P}_\alpha \cdot \langle \vec{u}_\alpha \rangle) \\ = -\vec{\nabla} \cdot \mathbf{Q}_\alpha + B_o B_u \int [e_{R\nu} \kappa_{R\nu} (1 - J_{\nu\alpha}) - j_{\nu\alpha}] d\nu \\ + \frac{\rho_\alpha}{m_\alpha} \langle \vec{u}_\alpha \rangle \cdot \left(\vec{F}_\alpha + \frac{q_\alpha \vec{E}}{m} \right) + K m_\alpha w_\alpha (e + u^2/2) \end{aligned} \quad (21)$$

The force \vec{F}_α in Equations 20 and 21 is included to provide an easy means of adding the gravitational acceleration at a future date.

f. Boundary Conditions

Appropriate boundary conditions must be provided on the boundary of the region of interest. In mathematical terms, the boundary requirement is that all characteristics crossing into the region of interest from the exterior region must be known. In the case of Maxwell's equations, this statement means that either there must be no charges or currents in the exterior region (in which case the boundary conditions are those of the fields at infinity) or the time-dependent fields on the boundary must be prescribed ahead of time. The boundary conditions for the radiation transport equations are similar to those for Maxwell's equations: either there must be no emission, absorption, or scattering in the exterior region (in which case the boundary condition is that of constant flux from infinity) or the time-dependent radiation fields on the boundary must be prescribed ahead of time.

The boundary conditions required for the hydrodynamic equations depend upon whether the flow within the boundary is supersonic or subsonic relative to the boundary. If the flow is supersonic relative to the boundary and crossing out of the region of interest, there can be no characteristics entering the region of interest (hydrodynamic characteristics propagate at the speed of sound) and no boundary conditions are needed. In any other case, however, the flow on the exterior of the boundary must be prescribed.

For all of the numerical calculations planned for the near future, these boundary conditions will be satisfied by assuming that the fields at the boundary are identical to the undisturbed fields at infinity.

2. NORMALIZATION

The normalization of the equations listed in Subsection II-1 is indicated in the notations; this normalization is intended to ensure that the only quantities in Equations 4 through 9 and 12 through 21 which are not of order unity are the parameters c , B_u , \mathcal{L} , \mathcal{K} , \mathcal{M} , B_0 , and K . These parameters are measures of the relative importances of the various physical processes represented in these equations. Thus, c is the ratio of the speed of light to the characteristic hydrodynamic velocity, and is a measure of the importance of transient radiative and electromagnetic effects. Large c implies that radiative energy transport occurs on a time scale which is short compared to the hydrodynamic time scale, and therefore, these effects become quasi-steady. Small c (c of order unity) implies that radiative and electromagnetic transient effects are important, and therefore, the radiative and electromagnetic energy densities in transit are important. B_u , the Bouguer number, is a measure of the relative opacity of the radiating gas. Large B_u implies there are many optical path lengths in a characteristic geometric length, and therefore, absorptive and emissive properties of the gas are important. Small B_u implies that a characteristic geometric is short compared to an optical path length, and therefore, the absorptive and emissive properties of the gas are unimportant. \mathcal{L} , the ratio of the geometric scale length to the Debye length, is a measure of the relative lengths of the hydrodynamic and electromagnetic fluctuations. Large \mathcal{L} implies that a geometric scale length contains many fluctuations of the electromagnetic fields, and therefore, the charge and current densities (the sources of the fluctuations) are important. Small \mathcal{L} implies that the electromagnetic fluctuations are not important over a geometric scale length, and therefore, the charge and

current densities are unimportant. κ , which is very nearly the square of the reciprocal of the Mach number, is a measure of the relative energies of random motion and directed motion in the gas. Large κ implies that the thermal energy of random motion is large compared to the directed energy of the streaming motion, and therefore, pressure effects are important. Small κ implies that the thermal energy of the random motion is small compared to the directed energy of the streaming motion, and therefore, pressure effects are unimportant. \mathcal{M} is a measure of the relative importance of the hydrodynamic momentum of a particle and of the impulse delivered to the particle in unit time by the local electric field. Thus, large \mathcal{M} implies that electromagnetic effects are not important, while small \mathcal{M} implies that such effects become dominant. B_0 , the Boltzmann number, is a measure of the relative importance of radiative energy transport and of convective energy transport. Large B_0 signifies that radiative transport is important, while small B_0 signifies that radiative transport is unimportant. K is a measure of the relative importance of the change in particle density of a species caused by chemical reactions and the change caused by hydrodynamic convection. Chemical reactions are important for large K and unimportant for small K .

3. CAPABILITIES OF AVAILABLE FINITE-DIFFERENCE METHODS

The problem outlined in Subsection II-1 is of such complexity that only a numerical solution appears possible. There are a number of finite-difference methods available, but nearly all of these methods have limitations which preclude the possibility of treating the above equations in their full generality. Such limiting techniques include the conventional Eulerian and Lagrangian procedures as well

as the Particle-in-Cell approach. By reviewing these procedures, however, it is possible to define the desirable features of a more general numerical approach, and then to outline such an approach.

a. Eulerian Methods

Eulerian finite-difference methods, which are frequently used for two-dimensional problems, proceed by applying the governing differential equations at a set of discrete points in space. The differentials in the equations are approximated by finite-differences between the fixed points. Because of the fixed geometry associated with these methods, Eulerian procedures are readily able to compute shearing stresses and to treat tangential forces. This capability is a necessity for the complex problems considered here because of the shearing stresses associated with magnetic field and the resulting nonequality of the diagonal components of the hydrodynamic pressure tensor.

One of the major disadvantages associated with Eulerian methods is that they are unable to maintain sharp contact discontinuities between two separate fluids. This inability arises because the fluid characteristics at a point represent the average characteristics of the fluid in a small volume surrounding the point; thus, when a contact discontinuity enters such a volume, the sharp discontinuity is represented by an average at the point at the center of the volume. In this fashion, the contact discontinuity becomes smeared out after a few computational cycles. A detailed study, including a numerical example, of this smearing of contact surfaces is given in Subsection 2 of Appendix F of Reference 3. Unfortunately, many of the problems considered here have interacting gas streams or colliding shock waves which produce contact surfaces; consequently, this inability of Eulerian methods to properly represent such contact surfaces is a strong disadvantage of these methods.

A second disadvantage associated with Eulerian methods is that they generally are unable to treat non-rectangular boundaries. This inability results from the finite-difference approach of representing differentials by differences taken between successive points of the computational net. It is straightforward to treat the problem of rectangular walls by imposing symmetry on the fixed points in the computational network, but similarly satisfying procedures for other geometries are lacking. In the problems considered here, however, the constraints imposed by the atmospheric variations and the earth's magnetic field may dictate a nonrectangular boundary for the numerical problem. As a result, this limitation of Eulerian methods is a disadvantage.

b. Lagrangian Methods

Lagrangian computational methods refer to a specific set of fluid particles rather than to a set of spatial points. Newton's laws are applied to these representative points to obtain the motion of the fluid as a whole. Because Lagrangian methods follow individual fluid particles, such techniques are able to represent contact surfaces between two gases; as discussed above, this ability is important for the problems to be treated.

The major disadvantage of Lagrangian methods is that they do not treat shearing stresses satisfactorily. This difficulty arises because the calculation of the stresses is based upon the geometric distances between the fluid particles, and the calculation of these distances becomes unacceptably tedious after the fluid has undergone some distortion because of the shearing stresses. As discussed in Subsection II-3a, however, shearing stresses are important in the present application, and the inability of Lagrangian methods to handle them is a serious disadvantage.

c. Particle-in-Cell Technique

The Particle-in-Cell (or PIC) technique represents an attempt to gain the advantage both of Eulerian and Lagrangian methods by superimposing a set of Lagrangian mass points on a set of Eulerian volume elements. The fluid stresses are computed on the basis of the average properties of all of the mass points in each of the volume elements, and the motion of the fluid is computed by using these stresses to determine the acceleration and velocity of each of the mass points. The use of volume elements permits this technique to treat shearing stresses, while the presence of mass points allows good representation of contact surfaces. As a result, the PIC technique has advantages over the Eulerian and Lagrangian methods described above.

The disadvantage of being unable to treat nonrectangular boundaries remains, however. The presence of this disadvantage is because of the use of Eulerian difference procedures for computing the stresses on the mass points, and results in exactly the same way as the rectangular boundary requirement discussed in Subsection II-3a.

A further disadvantage of the PIC technique is that the mass points are part of a Lagrangian net and there may be only a few points of each species in a given Eulerian cell. As a result, it is difficult to represent the smooth change in the density of a species because of chemical reactions by changing the number of mass points in the cell. Consequently, the PIC technique shares the Lagrangian disadvantage of not being well suited for chemical nonequilibrium.

d. Characteristic Flux Method

A method which uses moving Eulerian cell boundaries to follow contact discontinuities is able to overcome the disadvantages

of all of the above methods. Such a method is discussed in great detail in Reference 3. The basic concept of this method is that of choosing an Eulerian spatial mesh and applying the governing equations in integral form, rather than differential form, to the mesh. The resulting computational equations give the changes in fluid properties within a cell in terms of the fluxes of mass, momentum, and energy of the fluid crossing each face of the cell. Because the fluid properties are assumed constant within each cell, however, the properties on any face of the cell must be given in terms of a simple wave emanating from within the cell (Section 29, Reference 4). Thus, the fluxes crossing the cell surface are computed by the method of characteristics, and no distances to cell centroids are needed. Furthermore, the determination by the method of characteristics of the fluxes crossing each cell face is based upon velocities relative to the cell face; thus, the Eulerian grid can move through the gas.

A computational procedure based upon this characteristic flux method has all of the advantages of the above methods without any of the disadvantages. Thus, the use of integral equations replaces calculations of gradients with calculations of forces and fluxes on cell surfaces. Because the Eulerian cell surfaces do not become distorted by the shear flow, these force and flux calculations remain straightforward. At the same time, the movable cell boundaries permit good representation of contact discontinuities. For example, cell surfaces can be aligned with and allowed to move with material interfaces; thereby, preventing the usual smearing of the interfaces into adjacent cells. Such a technique was used successfully in Reference 5 in treating the contact surface formed by the colliding shock waves when a reentry vehicle penetrates a blast wave.

The characteristic flux technique also is able to treat chemical nonequilibrium without difficulty. Since the procedure is an Eulerian procedure, masses are computed by the use of continuous densities rather than by the use of discrete mass points. As a result, reaction rate equations can be coupled into the procedure directly.

Finally, the characteristic flux procedure can treat boundaries of any geometry. This ability results from the replacement of gradients in the differential equations by fluxes crossing cell walls in the integral equations. Thus, it only is necessary to align cell surfaces with the boundary to treat arbitrary geometries. For example, ellipsoidal as well as spherical bodies were treated in References 3 and 5.

4. METHOD OF SOLUTION

As discussed in Subsection II-3, the characteristic flux numerical method is the only available procedure which can treat with the required generality Equations 4 through 9 and 19 through 21 along with the associated boundary conditions. Consequently, these equations are integrated over a cell volume, and the method of characteristics is used to obtain the required fluxes crossing the cell surfaces.

The Eulerian cells are referred to a moving mesh. As discussed in Subsection II-3. d, such a mesh makes it possible to maintain internal interfaces in the gas; subroutines are provided for determining the mesh motion required for the following of the interfaces. In addition, the use of a moving mesh makes it possible to have the computational mesh expand with the flow (as in the case of the expanding debris from an explosion); thereby, permitting a constant

number of cells, with the resulting uniform accuracy, to cover the entire flow field. This type of motion obviates the need for rezoning the mesh periodically by adding or deleting cells.

Finally, all of the calculations involving the constitutive equations are carried out in subroutines; thereby, facilitating the changing of such equations as new models are developed.

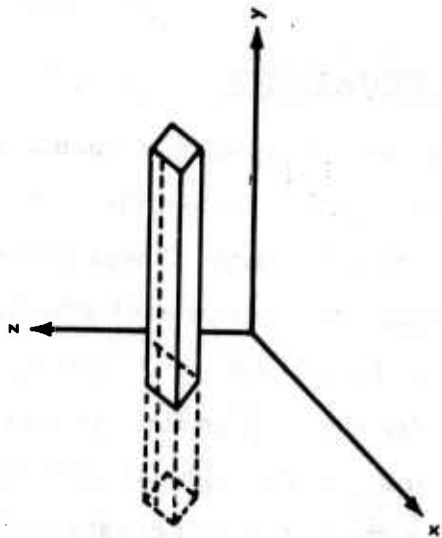
SECTION III

FORMULATION OF THE PHYSICS CODE

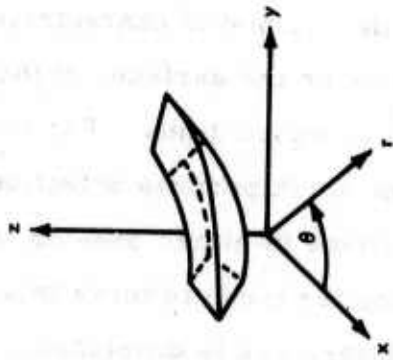
A general physics code is developed to treat the equations presented in Section II under a wide selection of boundary conditions. This code is developed by integrating the governing equations over the volume of a cell and then using the method of characteristics for the computation of the field properties on the surfaces of the cells. The constitutive equations are added as subroutines. The computational mesh is set up in a general form which permits selection of plane, cylindrical, or spherical geometries in either one- or two-dimensions as needed. A method for causing the mesh to move in such a way as to follow a set of prescribable interfaces is developed. A stability analysis of the resulting code is carried out, and detailed flow charts of the code are presented.

1. INTEGRATION OF THE EQUATIONS

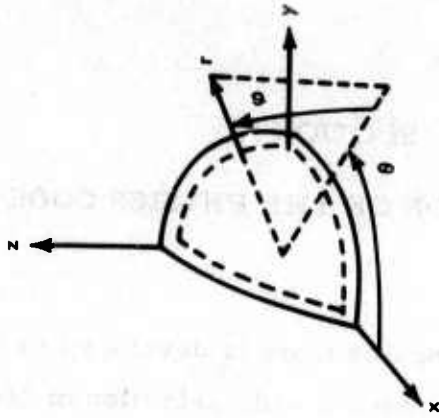
The equations are integrated in such a way as to be correctly represented in either one- or two-dimensions and in either plane, cylindrical, or spherical geometry. These three coordinate systems plus a typical computational cell in each system are illustrated in Figure 1. The geometrical definitions which specify a cell in any of these systems are shown in Figure 2. The field properties represented by Equations 4 through 9 and 19 through 21 are assumed to be constant within each cell during a time step and constant on each face of each cell during the time step. The equations are then integrated over the volume of a cell and over a time step.



(a) Plane Symmetry



(b) Cylindrical Symmetry



(c) Spherical Symmetry

Figure 1. Computational Cells for Plane, Cylindrical, and Spherical Symmetries

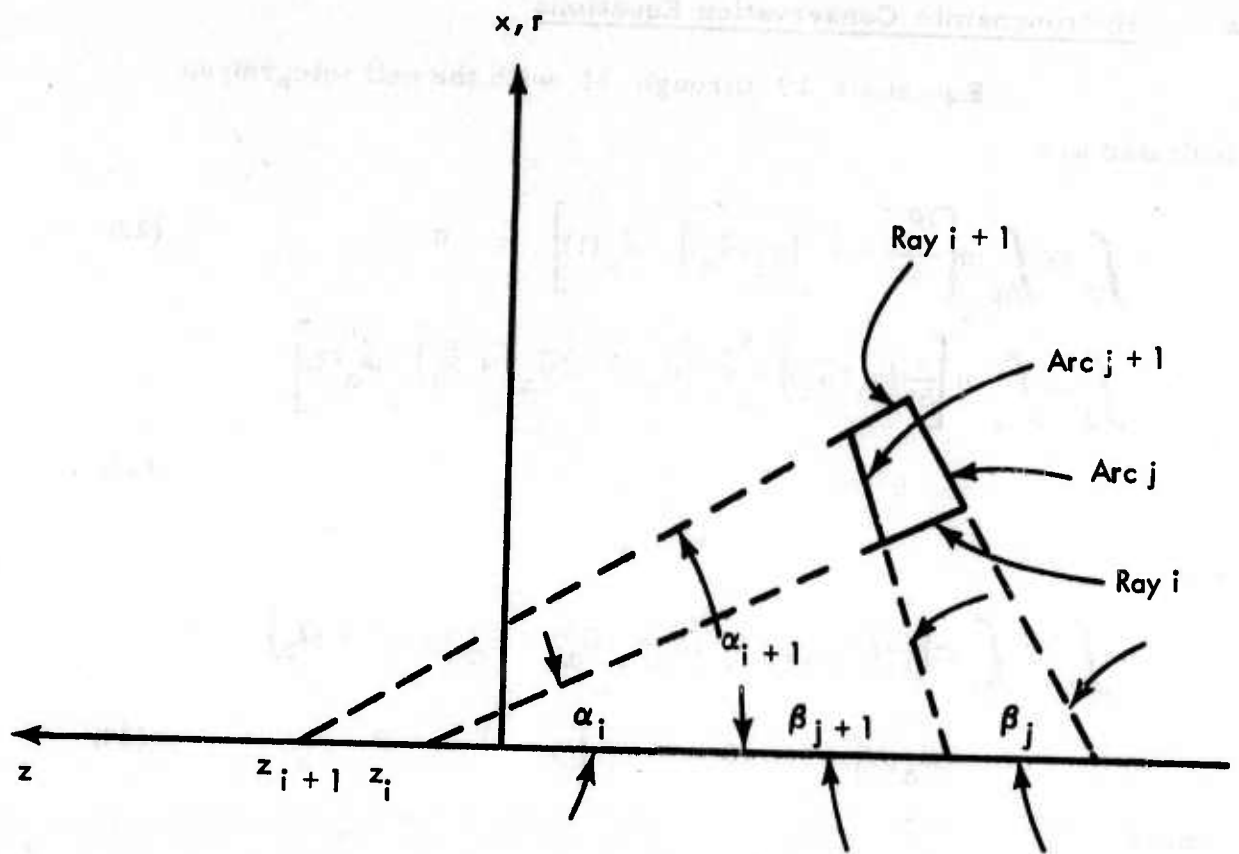


Figure 2. Cross-Sectional Geometry of a Cell

a. Hydrodynamic Conservation Equations

Equations 19 through 21 with the cell integration indicated are

$$\int_V dV \int_{\Delta t} dt \left[\frac{\partial \rho_\alpha}{\partial t} + \vec{\nabla} \cdot (\rho_\alpha \langle \vec{u}_\alpha \rangle) - \mathcal{L}_\alpha(1) \right] = 0 \quad (22)$$

$$\int_V dV \int_{\Delta t} dt \left[\frac{\partial}{\partial t} (\rho_\alpha \langle \vec{u}_\alpha \rangle) + \vec{\nabla} \cdot (\rho_\alpha \langle \vec{u}_\alpha \rangle \langle \vec{u}_\alpha \rangle + \vec{P}_\alpha^{\parallel}) - \mathcal{L}_\alpha(2) \right] = 0 \quad (23)$$

and

$$\int_V dV \int_{\Delta t} dt \left[\frac{\partial}{\partial t} (\rho_\alpha \epsilon_\alpha) + \vec{\nabla} \cdot (\rho_\alpha \epsilon_\alpha \langle \vec{u}_\alpha \rangle + \vec{P}_\alpha^{\parallel} \cdot \langle \vec{u}_\alpha \rangle + \vec{Q}_\alpha) - \mathcal{L}_\alpha(3) \right] = 0 \quad (24)$$

where

$$\mathcal{L}_\alpha(1) = K m_\alpha w_\alpha(1) \quad (25)$$

$$\mathcal{L}_\alpha(2) = \rho_\alpha \left[\frac{\vec{F}_\alpha}{m_\alpha} + \frac{1}{\mathcal{M}} \frac{q_\alpha}{m_\alpha} \left(\vec{E} + \frac{\langle \vec{u}_\alpha \rangle \times \vec{B}}{c} \right) \right] + K m_\alpha \vec{w}_\alpha(u) \quad (26)$$

and

$$\mathcal{L}_\alpha(3) = B_0 B_u \int \left[e_{R_V} \kappa_{R_V} (1 - J_{V\alpha}) - j_{V\alpha} \right] dV + \frac{\rho_\alpha}{m_\alpha} \langle \vec{u}_\alpha \rangle \cdot \left(\vec{F}_\alpha + \frac{q_\alpha}{\mathcal{M}} \vec{E} \right) + K m_\alpha w_\alpha(e + u^2/2) \quad (27)$$

The integrations in Equations 22 through 24 are carried out over the volume of a cell, V , and over a time step, Δt . In carrying out these integrations, it is assumed that the time rates of change and the source functions, \mathcal{L} , within each cell are constant during the time step. The

divergence term is converted to an integral over the cell surface by means of Green's theorem, and the resulting properties on the cell surfaces are assumed constant during the time step. In integrating the unsteady term in these equations, it must be remembered that the cell volume is a function of time because of the moving mesh; thus, this term is integrated by parts, and the resulting expression for the rate of change of cell volume is replaced by an integral over the surface of the cell of the normal component of the velocity of the surface. These integration procedures are carried out in Appendix V for representative scalar and vector equations.

Making use of the model integrals provided by Equations 319 and 331 and by Equations 320, 339, and 369 of Appendix V, the integrated forms of Equations 22 through 24 become

$$\begin{aligned}
 (\rho_\alpha v)^{i+1/2, j+1/2} &= (\rho_\alpha v)_{i+1/2, j+1/2} \\
 &+ \Delta t \left\{ \sum_{\text{cell faces}} \rho_\alpha (W_n - \langle u_\alpha \rangle_n) S + \right. \\
 &\left. + \mathcal{J}_\alpha^{(1)}{}_{i+1/2, j+1/2} \left(v_{i+1/2, j+1/2} + \frac{\Delta t}{2} \sum_{\text{cell faces}} W_n S \right) \right\} \quad (28)
 \end{aligned}$$

$$\begin{aligned}
 (\rho_\alpha v \langle u_{\alpha_r} \rangle)^{i+1/2, j+1/2} &= (\rho_\alpha v \langle u_{\alpha_r} \rangle)_{i+1/2, j+1/2} \\
 &+ \Delta t \left\{ \sum_{\text{cell faces}} \left[\rho_\alpha \langle u_{\alpha_r} \rangle (W_n - \langle u_{\alpha_n} \rangle) - P_{\alpha_{rr}} v_r - P_{\alpha_{rz}} v_z \right] S + \right. \\
 &\left. + 2A\eta P_{\theta\theta} + \mathcal{J}_{\alpha_r}^{(2)}{}_{i+1/2, j+1/2} \left(v_{i+1/2, j+1/2} + \frac{\Delta t}{2} \sum_{\text{cell faces}} W_n S \right) \right\} \quad (29)
 \end{aligned}$$

$$\begin{aligned}
(\rho_\alpha V \langle u_{\alpha z} \rangle)^{i+1/2, j+1/2} &= (\rho_\alpha V \langle u_{\alpha z} \rangle)_{i+1/2, j+1/2} \\
&+ \Delta t \left\{ \sum_{\text{cell faces}} \left[\rho_\alpha \langle u_{\alpha z} \rangle (W_n - \langle u_\alpha \rangle_n) - P_{\alpha zr} v_r - P_{\alpha zz} v_z \right] S \right. \\
&\left. + \mathcal{L}_{\alpha z}^{(2)} \right\}_{i+1/2, j+1/2} \left(v_{i+1/2, j+1/2} + \frac{\Delta t}{2} \sum_{\text{cell faces}} W_n S \right) \quad (30)
\end{aligned}$$

and

$$\begin{aligned}
(\rho_\alpha V \mathcal{E}_\alpha)^{i+1/2, j+1/2} &= (\rho_\alpha V \mathcal{E}_\alpha)_{i+1/2, j+1/2} \\
&+ \Delta t \left\{ \sum_{\text{cell faces}} \left[\rho_\alpha \mathcal{E}_\alpha (W_n - \langle u_\alpha \rangle_n) - (P_{\alpha rr} \langle u_{\alpha r} \rangle \right. \right. \\
&+ P_{\alpha rz} \langle u_{\alpha z} \rangle + Q_{\alpha r}) v_r - (P_{\alpha zr} \langle u_{\alpha r} \rangle \\
&+ P_{\alpha zz} \langle u_{\alpha z} \rangle + Q_{\alpha z}) v_z \left. \right] S \\
&\left. + \mathcal{L}_{\alpha}^{(3)} \right\}_{i+1/2, j+1/2} \left(v_{i+1/2, j+1/2} + \frac{\Delta t}{2} \sum_{\text{cell faces}} W_n S \right) \quad (31)
\end{aligned}$$

In Equations 28 through 31, W_n is the velocity of the cell surface along its outward normal, $\langle u_\alpha \rangle_n$ is the velocity along the outward normal of the cell surface of species α , and v_r and v_z are the direction cosines between the r and z axes and the outward normal to the cell surface. The index $(i+1/2, j+1/2)$ denotes properties evaluated within cell $(i+1/2, j+1/2)$; raised indices denote properties evaluated at the end of the time step, while lowered indices denote properties evaluated at the beginning of the time step.

b. Radiation Transport Equations

Equations 4 and 5 with the cell integration indicated are

$$\int_V dV \int_{\Delta t} dt \left[\frac{\partial e_{R_V}}{\partial t} + c \vec{\nabla} \cdot \vec{Q}_{R_V} + \mathcal{L}_V(1) \right] = 0 \quad (32)$$

and

$$\int_V dV \int_{\Delta t} dt \left[\frac{\partial \vec{Q}_{R_V}}{\partial t} + c \vec{\nabla} \cdot \vec{P}_{R_V} + \vec{\mathcal{L}}_V(2) \right] = 0 \quad (33)$$

where

$$\mathcal{L}_V(1) = c B_u \sum_{\alpha} \rho_{\alpha} \kappa_{V\alpha} e_{R_V} (1 - J_{V\alpha}) - j_{V\alpha} \quad (34)$$

and

$$\vec{\mathcal{L}}_V(2) = c B_u \vec{Q}_{R_V} \sum_{\alpha} \rho_{\alpha} \kappa_{V\alpha} (1 - J_{V\alpha} + S_{V\alpha}) \quad (35)$$

Equations 32 and 33 are integrated with the same assumptions and in the same manner as Equations 22 through 24. The resulting integrated forms are

$$\begin{aligned} (e_{R_V})^{i+1/2, j+1/2} &= (e_{R_V})_{i+1/2, j+1/2} \\ &+ \Delta t \left\{ \sum_{\text{cell faces}} [e_{R_V} W_n - c(Q_{R_V r} v_r + Q_{R_V z} v_z)] S - \right. \\ &\left. - \mathcal{L}_V(1)_{i+1/2, j+1/2} \left(v_{i+1/2, j+1/2} + \frac{\Delta t}{2} \sum_{\text{cell faces}} W_n S \right) \right\} \quad (36) \end{aligned}$$

$$\begin{aligned} (Q_{R_V r})^{i+1/2, j+1/2} &= (Q_{R_V r})_{i+1/2, j+1/2} \\ &+ \Delta t \left\{ \sum_{\text{cell faces}} [Q_{R_V r} W_n - c(P_{R_V rr} v_r + P_{R_V rz} v_z)] S \right. \\ &+ 2\eta A c P_{R_V \theta\theta} - \mathcal{L}_{Vr}(2)_{i+1/2, j+1/2} \left(v_{i+1/2, j+1/2} \right. \\ &\left. + \frac{\Delta t}{2} \sum_{\text{cell faces}} W_n S \right) \quad (37) \end{aligned}$$

and

$$\begin{aligned}
 (Q_{R_{\nu_z} V})^{i+1/2, j+1/2} &= (Q_{R_{\nu_z} V})_{i+1/2, j+1/2} \\
 &+ \Delta t \left\{ \sum_{\text{cell faces}} \left[Q_{R_{\nu_z}} W_n - c (P_{R_{\nu_z r}} \nu_r + P_{R_{\nu_z z}} \nu_z) \right] S \right. \\
 &\left. - \mathcal{L}_{\nu_z}^{(2)}{}_{i+1/2, j+1/2} \left(V_{i+1/2, j+1/2} + \frac{\Delta t}{2} \sum_{\text{cell faces}} W_n S \right) \right\} \quad (38)
 \end{aligned}$$

c. Maxwell's Equations

Equations 6 and 7 will always be satisfied if they are satisfied by the initial conditions; consequently, they need not be differenced. Equations 8 and 9 with the cell integration indicated are

$$\int_V dV \int_{\Delta t} dt \left[\frac{\partial \vec{B}}{\partial t} + c \vec{\nabla} \times \vec{E} \right] = 0 \quad (39)$$

and

$$\int_V dV \int_{\Delta t} dt \left[\frac{\partial \vec{E}}{\partial t} - c \vec{\nabla} \times \vec{B} + \mathcal{L} \vec{j} \right] = 0 \quad (40)$$

Equations 39 and 40 are integrated with the same assumptions and in the same manner as Equations 22 through 24.

The resulting integrated forms are

$$\begin{aligned}
 (B_r V)^{i+1/2, j+1/2} &= (B_r V)_{i+1/2, j+1/2} \\
 &+ \Delta t \sum_{\text{cell faces}} (B_r W_n + c E_\theta \nu_z) S \quad (41)
 \end{aligned}$$

$$\begin{aligned}
 (B_z V)^{i+1/2, j+1/2} &= (B_z V)_{i+1/2, j+1/2} \\
 &+ \Delta t \sum_{\text{cell faces}} (B_z W_n - c E_\theta \nu_r) S \quad (42)
 \end{aligned}$$

$$\begin{aligned}
(E_r V)^{i+1/2, j+1/2} &= (E_r V)_{i+1/2, j+1/2} \\
&+ \Delta t \left\{ \sum_{\text{cell faces}} (E_r W_n - c B_\theta v_z) S \right. \\
&\left. - \mathcal{L} j_{r_{i+1/2, j+1/2}} \left(v_{i+1/2, j+1/2} + \frac{\Delta t}{2} \sum_{\text{cell faces}} W_n S \right) \right\} \quad (43)
\end{aligned}$$

and

$$\begin{aligned}
(E_z V)^{i+1/2, j+1/2} &= (E_z V)_{i+1/2, j+1/2} \\
&+ \Delta t \left\{ \sum_{\text{cell faces}} (E_z W_n + c B_\theta v_r) S \right. \\
&\left. - \mathcal{L} j_{z_{i+1/2, j+1/2}} \left(v_{i+1/2, j+1/2} + \frac{\Delta t}{2} \sum_{\text{cell faces}} W_n S \right) \right\} \quad (44)
\end{aligned}$$

2. CHARACTERISTIC SOLUTIONS ON CELL BOUNDARIES

Equations 28 through 31, 36 through 38, and 41 through 44 all contain terms evaluated on the faces of the computational cells. These terms represent fluxes of the property in question across the cell faces, and are calculated by the method of characteristics.

a. General Theory

The various field properties governed by the above integrated equations are considered to be constant within each cell; thus, the cell faces constitute a region bounding a region of constant field. As shown in Section 29 of Reference 4, however, the field in a region adjacent to a region of constant state must be a simple wave emanating from the region of constant state. The leading edge of this simple wave propagates along the undisturbed characteristic of the constant state, and in the limit of small differences between the constant state and the cell

surface, the entire simple wave can be approximated by a single characteristic. In the same way, the flow on the cell surface must be given by a characteristic coming from the cell on the other side of the cell surface; thus, the fields on the cell surface are given by the solution of two characteristics.

b. Characteristic Equations

In the absence of nonuniformities in the fields, characteristic properties are properties which remain constant on specific space-time paths. These characteristic properties are to be referred to the cell surfaces; consequently, it is convenient to introduce a local rectangular Cartesian coordinate system on each cell surface as depicted in Figure 3.

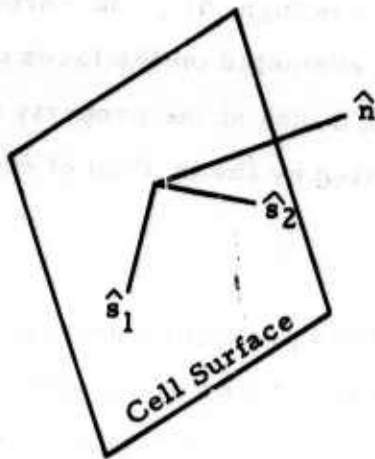


Figure 3. Cell-Surface Coordinate System

In terms of this coordinate system, it is shown in Subsection VI-1 of Appendix VI that the hydrodynamic characteristics are

$$J_{\alpha_{\pm}} = \langle u_{\alpha_n} \rangle \pm \int^{P_{\alpha}} \frac{dP_{\alpha}}{\rho_{\alpha} a_{\alpha}} \quad (45)$$

and that $J_{\alpha_{\pm}}$ is constant on the path

$$n = n_0 + a_{\alpha}(M_{\alpha} + 1)t \quad (46)$$

while $J_{\alpha_{-}}$ is constant on the path

$$n = n_0 + a_{\alpha}(M_{\alpha} - 1)t \quad (47)$$

where a_{α} is the speed of sound of species α and

$$M_{\alpha} = \langle u_{\alpha_n} \rangle / a_{\alpha} \quad (48)$$

Similarly, it is shown in Subsection VI-2 of Appendix VI that the radiation transport characteristics are

$$J_{\nu_{\pm}} = e_{R_{\nu}} \pm \sqrt{3} Q_{R_{\nu_n}} \quad (49)$$

and that $J_{\nu_{+}}$ is constant on the path

$$n = n_0 + ct/\sqrt{3} \quad (50)$$

while $J_{\nu_{-}}$ is constant on the path

$$n = n_0 - ct/\sqrt{3} \quad (51)$$

where $Q_{R_{\nu_n}}$ is the component of $\vec{Q}_{R_{\nu}}$ along \hat{n} .

Maxwell's equations are treated in Subsection VI-3 of Appendix VI. It is shown that Maxwell's equations have two sets of characteristics:

$$J_{1\pm} = B_{s1} \pm E_{s2} \quad (52)$$

and

$$J_{2\pm} = B_{s2} \pm E_{s1} \quad (53)$$

Further, J_{1+} and J_{2-} are constant along the path

$$n = n_0 - ct \quad (54)$$

while J_{1-} and J_{2+} are constant along the path

$$n = n_0 + ct \quad (55)$$

c. Characteristic Properties on Cell Boundaries

The characteristics listed in Subsection III-2b define the properties on the cell boundaries. Thus, let cell 1 lie on the negative n side of the cell surface and cell 2 on the positive n side. Then, if

$$-1 < M_\alpha < 1 \quad (56)$$

Equations 46 and 47 show that

$$\langle J_{\alpha+} \rangle_{\text{cell surface}} = \langle J_{\alpha+} \rangle_1 \quad (57)$$

and

$$\langle J_{\alpha-} \rangle_{\text{cell surface}} = \langle J_{\alpha-} \rangle_2 \quad (58)$$

Equations 45 and 57 give

$$\langle u_{\alpha n} \rangle_{\text{cell surface}} = \langle u_{\alpha n} \rangle_1 + \int_{P_{\alpha}}^{P_{\alpha 1}} dP_{\alpha} / \rho_{\alpha} a_{\alpha} \quad (59)$$

Assuming that the integrand in Equation 59 is nearly constant because of the assumed small difference between properties on the cell surface

and those in the adjacent cells,

$$\langle u_{\alpha n} \rangle_{\text{cell surface}} + \frac{P_{\alpha \text{ cell surface}}}{(\rho_{\alpha \alpha})_1} = \langle u_{\alpha n} \rangle_1 + \frac{P_{\alpha 1}}{(\rho_{\alpha \alpha})_1} \quad (60)$$

Similarly, Equations 45 and 58 lead to

$$\langle u_{\alpha n} \rangle_{\text{cell surface}} - \frac{P_{\alpha \text{ cell surface}}}{(\rho_{\alpha \alpha})_2} = \langle u_{\alpha n} \rangle_2 - \frac{P_{\alpha 2}}{(\rho_{\alpha \alpha})_2} \quad (61)$$

Solving Equations 60 and 61 for the cell surface properties,

$$\langle u_{\alpha n} \rangle_{\text{cell surface}} = \frac{(\rho_{\alpha \alpha})_1 \langle u_{\alpha n} \rangle_1 + (\rho_{\alpha \alpha})_2 \langle u_{\alpha n} \rangle_2 + P_{\alpha 1} - P_{\alpha 2}}{(\rho_{\alpha \alpha})_1 + (\rho_{\alpha \alpha})_2} \quad (62)$$

and

$$P_{\alpha \text{ cell surface}} = \frac{(\rho_{\alpha \alpha})_2 P_{\alpha 1} + (\rho_{\alpha \alpha})_1 P_{\alpha 2} + (\rho_{\alpha \alpha})_1 (\rho_{\alpha \alpha})_2 (\langle u_{\alpha n} \rangle_1 - \langle u_{\alpha n} \rangle_2)}{(\rho_{\alpha \alpha})_1 + (\rho_{\alpha \alpha})_2} \quad (63)$$

The density on the cell surface is obtained by use of Equation 397 of Appendix VI. Thus, if

$$\langle u_{\alpha n} \rangle_{\text{cell surface}} \geq 0 \quad (64)$$

the gas on the cell surface is deemed to have come from cell 1, and

$$\rho_{\alpha \text{ cell surface}} = \rho_{\alpha 1} + \frac{P_{\alpha \text{ cell surface}} - P_{\alpha 1}}{a_{\alpha 1}^2} \quad (65)$$

Similarly, if

$$\langle u_{\alpha n} \rangle_{\text{cell surface}} < 0 \quad (66)$$

the density is given by

$$\rho_{\alpha \text{ cell surface}} = \rho_{\alpha 2} + \frac{P_{\alpha \text{ cell surface}} - P_{\alpha 2}}{a_{\alpha 2}^2} \quad (67)$$

With P_α and ρ_α known on the cell surface, the remaining thermodynamic properties on the cell surface are found by application of the chosen model of the equation of state. The velocity tangential to the cell surface is taken equal to the tangential velocity in the cell from which the gas crosses the cell surface.

If Equation 46 is not satisfied, the flow is supersonic; such a condition means that the gas moves faster than either characteristic. In this case, the flowing gas drags its characteristics with it. Thus, if

$$M_\alpha \geq 1 \quad (68)$$

the flow is supersonic from cell 1 into cell 2, and both characteristics on the cell surface come from cell 1. In this case, the flow properties on the cell surface are identical to those in cell 1:

$$\langle u_{\alpha n} \rangle_{\text{cell surface}} = \langle u_{\alpha n} \rangle_1 \quad (69)$$

$$P_{\alpha \text{ cell surface}} = P_{\alpha 1} \quad (70)$$

$$\rho_{\alpha \text{ cell surface}} = \rho_{\alpha 1} \quad (71)$$

Similarly, if

$$M_\alpha \leq -1 \quad (72)$$

the flow is supersonic from cell 2 into cell 1 and

$$\langle u_{\alpha n} \rangle_{\text{cell surface}} = \langle u_{\alpha n} \rangle_2 \quad (73)$$

$$P_{\alpha \text{ cell surface}} = P_{\alpha 2} \quad (74)$$

$$\rho_{\alpha \text{ cell surface}} = \rho_{\alpha 2} \quad (75)$$

If the cell surface itself is moving, the selection of the appropriate set of cell surface properties is based upon the motion of the characteristics relative to the moving surface. Since the characteristics move at the local speed of sound, these choices may be summarized as follows:

1. If

$$\langle u_{0n} \rangle_1 - a_{01} - W_n \geq 0 \quad (76)$$

the flow is supersonic from cell 1 into cell 2 and Equations 69 through 71 are appropriate;

2. If

$$W_n - \langle u_{0n} \rangle_2 - a_{02} \geq 0 \quad (77)$$

the flow is supersonic from cell 2 into cell 1 and Equations 73 through 75 are appropriate;

3. If neither of inequalities 76 and 77 holds, the flow is subsonic relative to the cell surface, and Equations 62 through 67 are appropriate.

The characteristic surface properties are simpler for the equations of radiation transport because these characteristics propagate at a speed of $c/\sqrt{3}$; consequently, there is no practical case in which the cell surface can outrun a characteristic. Thus, Equations 50 and 51 show that

$$(J_{v+})_{\text{cell surface}} = (J_{v+})_1 \quad (78)$$

and

$$(J_{v-})_{\text{cell surface}} = (J_{v-})_2 \quad (79)$$

Inserting Equation 49 into Equations 78 and 79 and solving for the cell surface properties by the same method as used in Equations 60 through 63,

$$e_{Rv} \text{ cell surface} = \frac{e_{Rv_1} + e_{Rv_2} + \sqrt{3}(Q_{Rv_{n_1}} - Q_{Rv_{n_2}})}{2} \quad (80)$$

and

$$Q_{Rv} \text{ cell surface} = \frac{Q_{Rv_{n_1}} + Q_{Rv_{n_2}} + (e_{Rv_1} - e_{Rv_2})/\sqrt{3}}{2} \quad (81)$$

Similarly for Maxwell's equations, Equations 54 and 55 give

$$(J_{1+}) \text{ cell surface} = (J_{1+})_2 \quad (82)$$

$$(J_{1-}) \text{ cell surface} = (J_{1+})_1 \quad (83)$$

$$(J_{2+}) \text{ cell surface} = (J_{2+})_1 \quad (84)$$

and

$$(J_{2-}) \text{ cell surface} = (J_{2-})_2 \quad (85)$$

Using Equations 52, 82, and 83 and solving for the surface properties gives

$$(B_{s_1}) \text{ cell surface} = \frac{(B_{s_1})_1 + (B_{s_1})_2 + (E_{s_2})_2 - (E_{s_2})_1}{2} \quad (86)$$

and

$$(E_{s_2}) \text{ cell surface} = \frac{(E_{s_2})_1 + (E_{s_2})_2 + (B_{s_1})_2 - (B_{s_1})_1}{2} \quad (87)$$

Similarly, Equations 53, 84, and 85 give

$$(B_{s_2}) \text{ cell surface} = \frac{(B_{s_2})_1 + (B_{s_2})_2 + (E_{s_1})_1 - (E_{s_1})_2}{2} \quad (88)$$

and

$$(E_{s1})_{\text{cell surface}} = \frac{(E_{s1})_1 + (E_{s1})_2 + (B_{s2})_1 - (B_{s2})_2}{2} \quad (89)$$

3. CONSTITUTIVE EQUATIONS

As discussed in Subsection II-1d, the values of the collision cross sections and of the various reaction rates will be assumed known. The values initially selected will be obtained from a cursory check of the literature. Since the purpose of the initial one-dimensional calculations is the testing of the sensitivity of the numerical solution to the various parameters of the problem, such a choice of cross sections and reaction rates is a satisfactory method of gaining a starting point for a parametric study. A more thorough evaluation of these parameters will have to be undertaken for the two-dimensional overall-effects code, however.

The detailed study of initial conditions that may be required for predicting the debris behavior of specific bursts is being postponed, at least until the two-dimensional code is ready for running. If the parametric studies proposed for the one-dimensional code indicate a lack of sensitivity to the precise initial conditions, then such detailed studies may not be warranted.

a. Source Effects

The continuity equation for species α requires a knowledge of the volume production and/or loss rate of the species. We have begun to investigate the various cross sections and reaction mechanisms which contribute to the rates. Among these are ionization, charge transfer, dissociation, and recombination of free electrons with positive ions. The following summarizes the preliminary results of our survey to date.

(1) Capture and loss of electrons by fission fragments

Bell (Reference 6) and Bohr and Lindhard (Reference 7) have shown that the capture and loss cross sections, σ_c and σ_l , respectively, of a highly ionized particle of atomic number Z and ionic charge z moving with velocity v in a target gas of moderately high atomic number Z_t are given by

$$\sigma_c = Z_t^{1/3} z^2 (v_0/v)^3 \pi a_0^2 \quad (90)$$

$$\sigma_l = Z_t^{2/3} Z^{4/3} z^{-3} (v/v_0)^2 \pi a_0^2 \quad (91)$$

Here v_0 is $c/137$ and πa_0^2 is the area of the first Bohr orbit ($8.8 \times 10^{-17} \text{ cm}^2$).

When charge equilibrium is attained as the fission fragment moves through the gas, the capture and loss cross sections are equal. The common cross-section under equilibrium conditions is then approximately

$$\sigma \approx (ZZ_t)^{1/2} \left(\frac{v_0}{v}\right) \pi a_0^2 \quad (92)$$

and the average ionic charge is

$$z = Z^{4/15} Z_t^{1/15} \left(\frac{v}{v_0}\right) \quad (93)$$

(2) Ionization of air by debris ions

Perhaps the currently most useful estimate of the cross section σ_i for ionization of a gas by high-speed ions is that from Firsov (Reference 8). His result, derived for atomic systems, is

$$\sigma_i = \sigma_0 \left[\left(\frac{v}{v_0}\right)^{1/5} - 1 \right]^2 \text{ cm}^2 \quad (94)$$

where v is the relative speed of the colliding pair of particles and σ_0 and v_0 are determined by the relations

$$\sigma_0 = \frac{3.3 \times 10^{-15}}{(Z_1 + Z_2)^{2/3}} \text{ cm}^2; \quad v_0 = \frac{2.3 \times 10^7}{(Z_1 + Z_2)^{5/3}} \text{ cm sec}^{-1} \quad (95)$$

Here, Z_1 and Z_2 are the atomic numbers of the incident and target particles, respectively, and I_0 is the smaller of the ionization energy (ev) of the two colliding particles.

Recent measurements by Fite et al (Reference 9) on ionization in air, N_2 and Ar gases by incident beams of Al^+ ions have produced the data shown in Figure 4. Included in this figure are the theoretical cross sections, predicted from Equation 94 for Al^+ ions in argon and atomic nitrogen. It is seen that the experimental curves do not exhibit quite as strong a velocity dependence as does the Firsov cross section. In addition, the data for N_2 are higher than

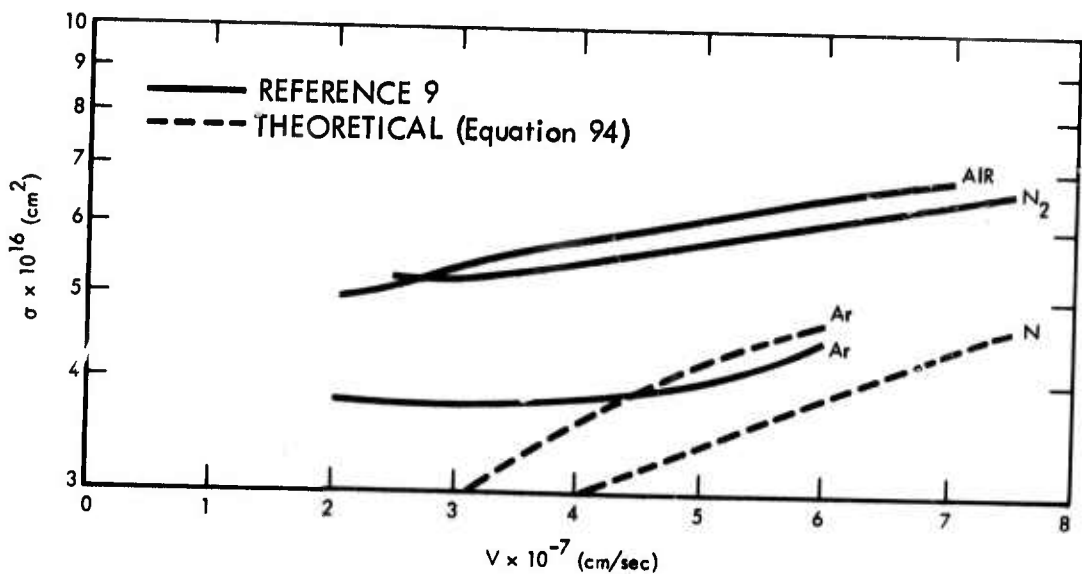


Figure 4. Ionization Cross Sections as a Function of Velocity for Al^+ in Ar, N_2 , and Air

that predicted for N. It seems reasonable, however, that in dealing with diatomic molecules, the value of σ_0 derived for atoms should be increased somewhat. This would then bring the theoretical and experimental curves more into line.

(3) Ionization of air by debris electrons

The available data on electron-induced ionization in various gases have recently been summarized by Kieffer and Dunn (Reference 10). In particular, the cross sections for ionization of N, O, N₂, O₂, NO, N⁺ and Li⁺ by electrons with energy between about 10 ev and 10 kev are available. If the electrons are in equilibrium at a temperature θ_e , then the rate coefficient α for production of ions M⁺ by the process



is given by

$$\alpha = \langle \sigma_i v \rangle_{\theta_e} \quad (97)$$

Here v is the electron speed, σ_i is the ionization cross section, and the brackets indicate an average over all speeds. If we use the data presented in Reference 10, together with an assumed velocity distribution for the electrons, α as a function of electron temperature can be obtained. This has been done (Reference 11) for ionization of atomic oxygen and nitrogen by assuming a Maxwell velocity distribution. The results are shown in Figure 5. Similar results can easily be obtained for the other species by numerical integration of the cross section data.

(4) Dissociative ionization of air molecules

Data have been obtained (Reference 10) on the dissociative ionization process

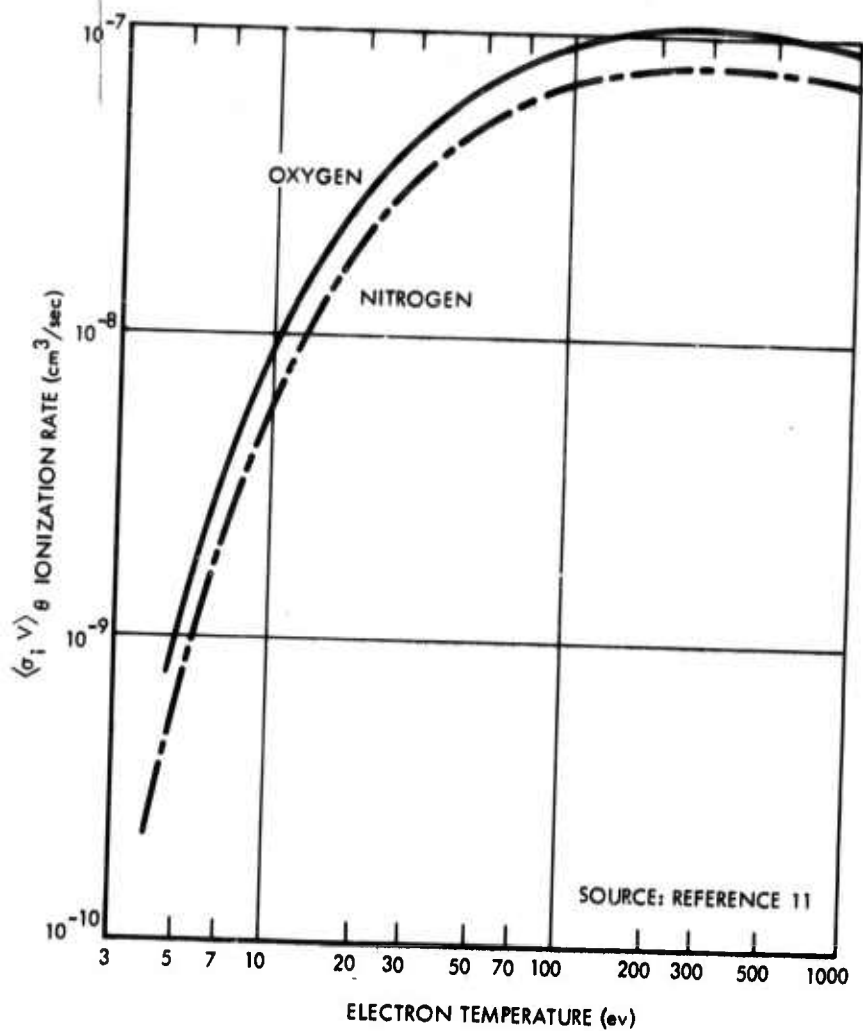


Figure 5. Ionization Rates for Atomic Oxygen and Nitrogen Versus Electron Temperatures.



for electron energies between about 10 ev and 1 kev and product ion (M^+) energies greater than 0.25 ev. Results for N_2 and O_2 are shown in Figures 6 and 7.

(5) Dissociation of air molecules by fast atoms

Gerasimenko and Oksyuk (Reference 12) have computed the cross section for dissociation of diatomic molecules in collision

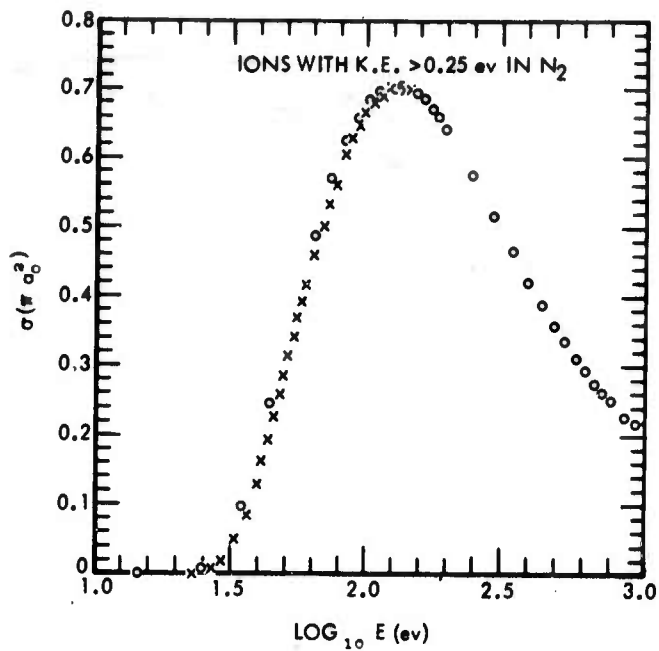


Figure 6. Cross Sections for the Dissociative Ionization of Molecular Nitrogen Yielding Product Ions with Kinetic Energies Greater than 0.25 ev.

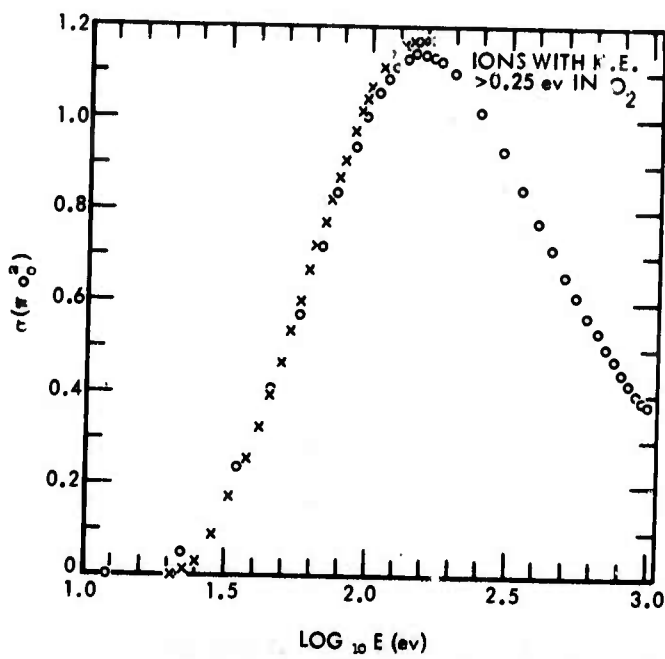


Figure 7. Cross Sections for the Dissociative Ionization of Molecular Oxygen Yielding Product Ions with Kinetic Energies Greater than 0.25 ev.

with atoms. It turns out that the quantum mechanical expression for the cross section which they derive gives results which differ at most by about 20 percent from the classical expression. We will, therefore, adopt the simpler classical expression for the dissociation cross section.

The dissociation cross section can be written as

$$\sigma_D = \sum_{j=1}^2 \int_D^{T_m} \sigma_j(T) w(T) dT \quad (99)$$

where $\sigma_j(T)$ is the cross section for elastic scattering by one of the atoms of the molecule, T is the energy transferred elastically to the atom, D is the dissociation energy and $w(T)$ is the probability that dissociation will occur. T_m , the maximum energy transferred elastically, is given in terms of the energy E of the incident atom and the masses M and M_j of the incident and target atoms, by

$$T_m = \gamma E \quad (100)$$

where

$$\gamma = \frac{4MM_j}{(M+M_j)^2} \quad (101)$$

The summation in Equation 99 is over the two atoms in the molecule.

Classically, $w = 1$, i. e., the molecule will definitely dissociate if the energy transferred elastically to one of the molecular atoms exceeds the dissociation energy. For a Coulomb interaction potential, we have (Reference 12),

$$\sigma_j(T) dT = \frac{2\pi e^4 Z^2 Z_j^2 \mu}{M_j^2 v^2} \frac{dT}{T^2} \quad (102)$$

where μ is the reduced molecular mass, v is the relative speed between incident and target atoms, and Z_e and Z_{je} are respectively the nuclear charges on incident and target atoms. If $T_m \gg D$, as will usually be the case, Equations 99 and 102 yield

$$\sigma_D = \frac{2\pi Z^2 e^4 \mu}{v^2 D} \left(\frac{Z_1^2}{M_1^2} + \frac{Z_2^2}{M_2^2} \right) \text{ cm}^2 \quad (103)$$

It is not difficult to use the more accurate screened-Coulomb interaction or the Thomas-Fermi function to obtain a slightly more accurate expression for the cross section.

In addition to the collisional effects discussed above, the decay rates from thermodynamic nonequilibrium to equilibrium are expected to be important at higher altitudes. These decay equations are generally given in the form

$$\frac{d\varphi_a}{dt} = \omega(\varphi_1, \varphi_2, \dots, \varphi_N, T) \quad (104)$$

where $\varphi_1, \varphi_2, \dots, \varphi_N$ are the N properties which are out of equilibrium and T is the temperature. The function ω in Equation 104 frequently is highly nonlinear, and recourse must be had to numerical means of integrating the equation. These rate equations frequently have very large time constants, however, and conventional Runge-Kutta techniques therefore do not work well. However, a modification of a method suggested by Certaine (Reference 13) has been developed; this modification appears accurate and efficient in terms of computer time.

The function ω in Equation 104 is approximated by

$$\omega_a = -D\varphi_a + \beta(t) \quad (105)$$

where

$$D = -\frac{1}{2} \left[\frac{\partial \omega_a}{\partial \varphi_a} (0) + \frac{\partial \omega_a}{\partial \varphi_a} (\Delta t) \right] \quad (106)$$

Equations 104 and 105 lead to

$$\frac{d}{dt} (\varphi_a e^{Dt}) = \beta e^{Dt} \quad (107)$$

If φ_{a*} represents the equilibrium value of property φ_a in a heat bath at temperature T , Equation 105 shows that

$$\beta(t) = \varphi_{a*} D \quad (108)$$

Equations 107 and 108 give

$$\begin{aligned} \varphi_a(\Delta t) e^{D\Delta t} - \varphi_a(0) &= \int_0^{\Delta t} \varphi_{a*}(t) D e^{Dt} dt \\ &= \int_0^{\Delta t} \left[\frac{d}{dt} (\varphi_{a*} e^{Dt}) - e^{Dt} \frac{d\varphi_{a*}}{dt} \right] dt \end{aligned} \quad (109)$$

Using the approximation

$$\frac{d\varphi_{a*}}{dt} = \frac{\varphi_{a*}(\Delta t) - \varphi_{a*}(0)}{\Delta t} \quad (110)$$

Equation 109 gives

$$\begin{aligned} \varphi_a(\Delta t) - \varphi_{a*}(\Delta t) &= \left[\varphi_a(0) - \varphi_{a*}(0) \right] e^{-D\Delta t} - \\ &\quad - \frac{\left[\varphi_{a*}(\Delta t) - \varphi_{a*}(0) \right]}{D \cdot \Delta t} (1 - e^{-D\Delta t}) \end{aligned} \quad (111)$$

Equation 111 is computed in three steps:

(1) The approximations

$$D = - \frac{\partial \omega_a}{\partial \varphi_a} (0) \quad (112)$$

and

$$\varphi_{a*}(\Delta t) = \varphi_{a*}(0) \quad (113)$$

are used, and a preliminary value of $\varphi_a(\Delta t)$ is computed;

(2) Using the preliminary value of $\varphi_a(\Delta t)$, final values of D and $\varphi_{a*}(\Delta t)$ are computed;

(3) The final values of D and $\varphi_{a*}(\Delta t)$ are used in Equation 111 to obtain the final value of $\varphi_a(\Delta t)$.

Equation 111 has been coded and tested by being employed to calculate the relaxation to equilibrium of a mixture of O_2 , O_2^+ , O , and O^+ with initial conditions of 10,000 °K and 100 percent O^+ . The computed relaxation was checked against results obtained by Runge-Kutta techniques and found satisfactory.

c. Correctness of Treatment

The treatment of the constitutive equations as discussed in Subsection III-3a is decoupled from the computation of the fluxes crossing the cell surfaces as discussed in Subsection III-2. The correctness of this decoupling is seen by recalling that the surface fluxes have to do with the transport of mass, momentum, and energy across the cell surfaces. As pointed out by Chapman and Cowling (Reference 1), however, the transport of molecular properties in a rarefied gas is caused almost entirely by the free motion of the particles between collisions and only negligibly to the transfer at collisions over the distance separating the two colliding particles.

Thus, for the rarefied gases considered here, particle collisions and molecular relaxations can have no effect upon the surface fluxes. Consequently, the decoupling of the collisional effects from the surface flux calculations is valid.

4. BOUNDARY CONDITIONS

The appropriate types of boundary conditions and the means by which they may be computed follow directly from the cell surface properties given in Subsection III-2c. The boundary conditions must be such that these surface properties can be computed; generally, this requirement means that all of the fields outside of the boundary must be prescribed.

In the case of the hydrodynamic equations, however, an additional type of boundary condition arises if the flow is supersonic out across the boundary. In this case, Equations 69 through 71 show that the surface properties on the cell boundary are given by the properties in the last cell within the boundary. Thus, the external fields need not be prescribed for this case.

In addition, it is possible to replace the surface property calculations of Subsection III-2c by specified surface properties. For example, if a cell surface is known to coincide with a hydrodynamic shock wave, a subroutine containing the Rankine-Hugoniot relations can be used for the calculation of the cell surface properties.

5. MESH GEOMETRY

The finite difference equations of Subsection III-1 have been written in a generalized geometry which facilitates the

aligning of the cell sides with any discontinuities in the flow. This generalized cell geometry coupled with the motion of the mesh implies that the cross sections of the cells are quadrilaterals, but not necessarily rectangles.

a. One or Two Dimensions

Three coordinate systems are used: plane, cylindrical, and spherical. In the first two of these, computations may be chosen to be either one- or two-dimensional; calculations in the spherical system must be one-dimensional. The ability to choose between one- and two-dimensional calculations results from the surface flux technique of differencing the equations: a one-dimensional calculation is achieved if two of the cell sides are dropped from the summations in Equations 28 through 30, 36 through 38, and 41 through 44. This dropping is achieved by setting the flag `NDIMEN` equal to unity. In addition, the z-component equations may be neglected in some of these calculations (but need not be). The resulting calculations will be executed as quickly as if the code had been written specifically for one-dimensional calculations.

b. General Quadrilateral Shapes

The general quadrilateral cross section of a cell is depicted in Figure 2. In the case of cylindrical geometry, this cross-sectional area is revolved around the z axis (Figure 1) to generate the computational cell. In the case of spherical geometry, the cell is a spherical shell, as illustrated in Figure 1. The choice between these three geometries is made by setting the geometry option word, `IGEOM`, equal to one for plane geometry, two for cylindrical geometry, and three for spherical geometry.

c. Method of Specification

The parameters needed to specify the cells are depicted in Figure 2. Each cell is bounded by two rays and two arcs; cell $(i+1/2, j+1/2)$ is bounded by rays i and $i+1$, and by arcs j and $j+1$. These rays and arcs intersect to form the four corner points of the cell: (i, j) , $(i+1, j)$, $(i, j+1)$, and $(i+1, j+1)$. The totality of cells between any two rays is referred to as a column of cells.

The arcs constitute the moving portion of the mesh. As a result of this motion, the arcs may become discontinuous as shown in Figure 8.

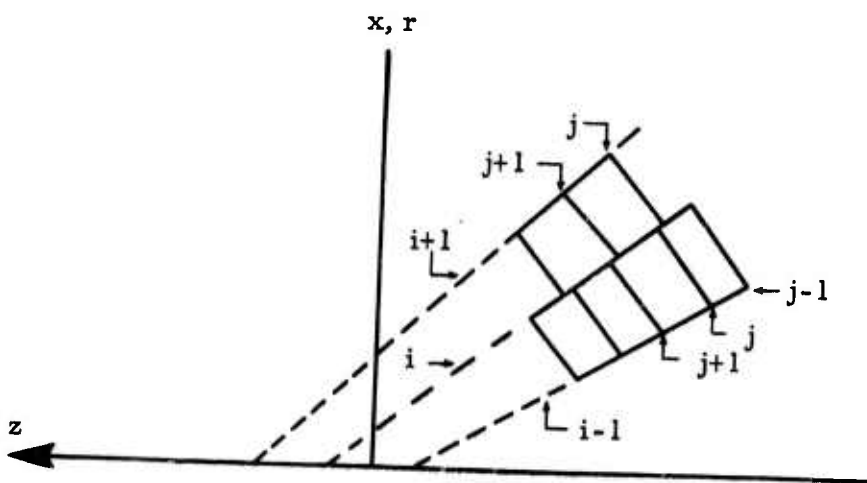


Figure 8. Discontinuous Arcs

The rays, however, are fixed straight lines during any one calculation. Thus, cell $(i+1/2, j+1/2)$ is completely specified if the angles α_i and α_{i+1} of the adjacent rays are given, if the intercepts z_i and z_{i+1} of the rays on the z axis are given, and if the distances $d_{i,j}$, $d_{i,j+1}$, $d_{i+1,j}$ and $d_{i+1,j+1}$ along rays i and $i+1$ from the z axis to the corners of the cell are given.

As can be seen from Figure 2, all of the areas and volumes associated with a cell are computable in terms of triangles and triangles of revolution about the z axis. Thus, the development of the formulae for the cell geometry is straightforward. The results are summarized in Appendix VII.

The first ray ($i=1$) and the last ray ($i=I$) are considered to be external boundaries, and have their surface fluxes prescribed in subroutines. In this fashion, the changing of boundary conditions is reduced to the changing of a few subroutines.

In the same way, the first arc ($j=1$) and the last arc ($j=J_{i+1/2}$) are considered to be external boundaries. In addition, the moving mesh can accommodate itself to moving boundaries; thus, any number of internal arcs may be aligned with discontinuities in the internal flow. For example, a contact surface might be represented by arc $j=5$ in column $(i+1/2)$, arc $j=6$ in column $(i+3/2)$, and so forth. All of these arc boundaries, both external and internal, have their surface fluxes prescribed in subroutines; thus, external conditions and internal discontinuities are easily changed.

In any given column, the arcs which are not associated with either external boundaries or internal discontinuities are positioned along the rays in such a way as to provide equal spacing between the discontinuities. Thus, the location of the points of intersection of all non-boundary arcs with the rays can be computed if the points of intersection of the boundary arcs are given. For example, if arc $j=J_{i+1/2}$ has intersections with rays i and $i+1$ located at $d_{i,J}$ and $d_{i+1,J}$; and if the next boundary arc is an internal boundary on arc $j=N$ with points of intersection at $d_{i,N}$ and $d_{i+1,N}$; then the intermediate points of intersection are located at

$$d_{i,j} = d_{i,j+1} + \frac{d_{i,N} - d_{i,J}}{J - N} \quad (114)$$

and

$$d_{i+1,j} = d_{i+1,j+1} + \frac{d_{i+1,N} - d_{i+1,J}}{J - N} \quad (115)$$

d. Multiple Boundaries

As can be seen by an examination of Figure 8, the moving mesh may cause the face on ray i of cell $(i+1/2, j+1/2)$ to share ray areas with the faces of several cells in the next column. In such a case, the characteristic property calculations of Subsection III-2c are carried out on each portion of the face, and the summations in the integrated equations of Subsection III-1 are taken over all portions of the cell face. The ray area formulae in Appendix VII can be used for the computation of each of these partial cell-face areas.

This technique of summing the fluxes on multiple boundaries has been used successfully in References 3 and 5. The method ensures the conservation of mass, momentum, and energy.

6. MESH MOTION

To follow the motion of the external and internal boundary arcs (if they move), it is necessary to allow all of the arcs to move. Thus, the motion of the boundary arcs is determined by the kinematics of the boundary, and the motion of the remaining arcs is scaled to maintain equal arc spacing between boundaries.

a. Node Velocities

The nodes are the points of intersection between the arcs and the rays. Those nodes which lie on arcs corresponding to internal

or external boundaries have their velocities determined by the velocity of the arc normal to itself. The means of computing these node velocities can be explained with the aid of the geometry depicted in Figure 9:

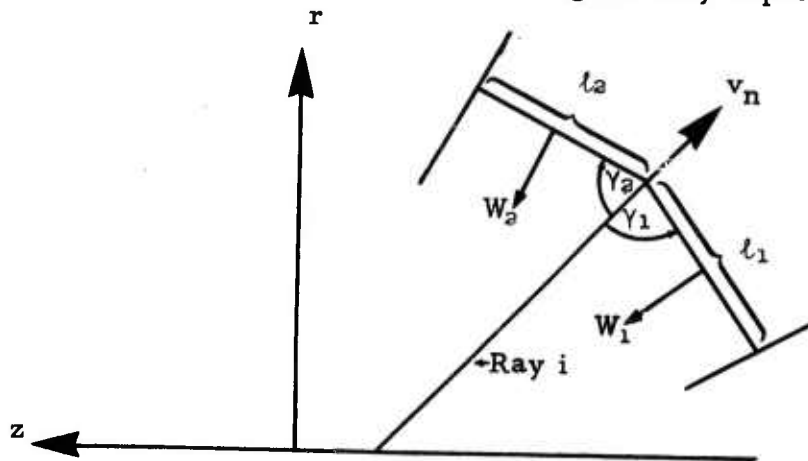


Figure 9. Node Velocity Geometry

The geometry illustrated in Figure 9 is easily calculated from the formulae of Appendix VII. The arc velocities, W_1 and W_2 , are given by the kinematics of the boundary; for example, a contact surface moves at the local material velocity and a shock wave moves at that velocity which renders the pressure, density, and velocity jumps across the discontinuity compatible with the Rankine-Hugoniot equations. These kinematic velocity calculations are included in the internal or external boundary subroutines appropriate to the arc in question.

In terms of the definitions illustrated in Figure 9, the node velocity is

$$v_n = \frac{l_1 W_2 / \sin \gamma_2 + l_2 W_1 / \sin \gamma_1}{l_1 + l_2} \quad (116)$$

The velocities of the nonboundary nodes along a ray are scaled to maintain equal node spacings between boundary nodes. For this purpose, Equations 114 and 115 are used with the distances replaced by the node velocities.

b. Cell Surfaces

The surface faces of the cells on the fixed rays do not move, but the faces on the arcs do move. The velocity of an arc face normal to itself is evaluated by calculating the volume swept out by the arc face during the time step and dividing this volume by the product of the face area and the time step. This procedure is used to ensure that volume is conserved by the floating mesh. Thus, if the position of node (i, j) at the start of the time step is $d_{i,j}(0)$, the position at the end of the time step is

$$d_{i,j}(\Delta t) = d_{i,j}(0) + v_{i,j} \cdot \Delta t \quad (117)$$

where $v_{i,j}$ is the velocity of the node along ray i as given by Equation 114 or Equation 116. The node positions before and after the time step are used in the cell volume formulae of Appendix VII to obtain the volume swept out by the cell face during the time step, ΔV . The velocity of face $(i+1/2, j)$ is then found from

$$W_{i+1/2,j} = -\Delta V / (S_{i+1/2,j} \cdot \Delta t) \quad (118)$$

In previous calculations with this type of moving mesh (Reference 5), it has been found necessary to recompute the velocity of any internal boundary arcs according to Equation 118 for the surface flux calculations; the velocity so computed differs only slightly from the velocity given by the kinematic subroutine corresponding to the arc, but this slight difference is sufficient to cause inaccuracies because of lack of conservation of volume.

7. STABILITY ANALYSIS AND TIME-STEP CALCULATION

The stability analyses used on these equations is based upon the von Neumann necessary condition as presented by Richtmyer

(Reference 14). The equations are linearized, the amplification matrix is found, and the eigenvalues of the amplification matrix are determined. Stability requires that these eigenvalues be less than unity.

a. Two-Dimensional Stability

It is shown in Subsection B. 3 of Appendix B of Reference 3 that the two-dimensional code will be stable if the time step is chosen to satisfy the inequality

$$\Delta t \leq \frac{\Delta t_r \Delta t_z}{\Delta t_r + \Delta t_z} \quad (119)$$

where Δt_r and Δt_z are the time steps for which the one-dimensional calculations in the radial and axial directions, respectively, are stable.

b. One-Dimensional Stability

For the hydrodynamic equations, it is shown in Appendix G of Reference 3 that the numerical method given here is stable in the radial direction if the time-step Δt_r satisfies the inequality

$$\Delta t_r \leq \frac{h_r}{|u_r| + a} \quad (120)$$

in every cell of the mesh and for each species. Here, h_r is the distance across the cell in the radial direction, u_r is the velocity in the radial direction, and a is the speed of sound within the cell. A similar expression holds for the axial time step, Δt_z . Equation 119 is valid if the cell surface properties of Subsection 3. 2. 3 are evaluated at the start of the time step. It is found in Reference 3 that the time step permitted by Equations 119 and 120 is sufficiently long to allow large percentage changes (as much as 50 percent) of the flow properties

within a cell. Since larger percentage changes would raise the question of accuracy, this time-step limit is considered satisfactory.

For Maxwell's equations and the equations of radiation transport, however, the situation is somewhat different. If the cell surface properties are evaluated at the start of the time step, it can be shown that the stable time step must satisfy the inequality

$$\Delta t_r \leq h_r/c \quad (121)$$

where c is the speed of light. Obviously, Equation 121 presents far too stringent a limitation on the time step for a practical numerical procedure. However, if the cell surface properties are evaluated at the end of the time step, it can be shown (Appendix VIII) that the numerical procedure is stable for any time step. Consequently, this option of evaluating the surface properties at the end of the time step is chosen for Maxwell's equations and the equations of radiation transport. In the case of one-dimensional calculations, the resulting numerical equations are easily inverted and solved directly, but in the case of two-dimensional calculations, an implicit set of equations results. Although there exists a number of relaxation methods for solving implicit equations, no method has been selected yet.

8. ORDER OF COMPUTATIONS IN THE CODE

The general flow of logic in the code is indicated in detail in the flow charts in Appendix II. The various formulae presented in this section are coded into subroutines and called as needed. The flow charts not only show the flow logic, but also give the FORTRAN II coding used.

The code does not yet contain Maxwell's equations or the equations of radiation transport. Furthermore, the code has not yet

been completely checked out, although some test calculations have been run successfully.

A few minor subroutines are not shown in the flow charts.

SECTION IV DISCUSSION

A numerical technique has been developed, but not yet fully tested, for the study of the dynamics of high altitude nuclear bursts.

1. METHOD OF USE

The numerical technique developed here can be used for both one-dimensional and two-dimensional studies.

a. One-Dimensional Coupling Studies

It is proposed to use the physics code described above in a series of one-dimensional calculations to study the coupling to the atmosphere of the debris from a high altitude explosion. Separate studies are proposed for collisional coupling, electromagnetic pickup, and pickup by scattering off of magnetic turbulence.

The collisional coupling studies will be carried out by use of expressions for the rate of change of momentum caused from collisions. These expressions are functions of the collision cross sections; it is proposed to vary the densities, energy of the debris, and cross sections within their range of uncertainty to observe the transition from collisionless flow to fully coupled flow. Scaling laws for this transitional region can then be developed.

The two-stream instability also can be studied with the one-dimensional physics code. Two neutral streams of ions and electrons

are allowed to approach one another in the absence of collisional terms. The presence of the complete Maxwell's equations in the code ensures that any electric field generated by density perturbations will be computed. This type of computation should give information as to the effective role of the two-stream instability in the coupling process. Here again, scaling laws giving the magnitude of the perturbation and the degree of pickup can be developed.

The one-dimensional code also can be used for studies of coupling by scattering of ions off of magnetic irregularities. The magnetic field is assumed to be trapped in the hydrodynamic turbulence in accordance with the model of Reference 15. The turbulence itself is computed by introducing a turbulent viscosity coefficient into the code, and using the scaling laws of Kolmogorov's theory (Section 32, Reference 16). The cross-section for scattering is given in Reference 15. By coupling the scattering off of the magnetic irregularities to the general flow by means of the physics code, it will be possible to deduce whether or not such a phenomenon can cause coupling.

b. Two-Dimensional Studies

The physics code discussed above also has been developed in a two-dimensional form (both plane and cylindrical symmetries). It is proposed to use this form of the code to study "Longmire" coupling and to compute the gross structure of the expanding debris.

The concept of "Longmire" coupling is fundamentally two-dimensional, because it involves the generation of a magnetic field by a stream of ions and a turning of additional ions by the magnetic field. The ability to remove the collisional terms from the code plus the presence of Maxwell's equations in the code permits the simulation

of this coupling. The computation is set up in cylindrical coordinates. A small region of ionized particles in the center of the computational mesh is given an initial outward velocity, and the ambient conditions outside this expanding region are taken as those of an ionized gas at rest in a magnetic field. The initial expansion energy, degree of ionization, and initial density can be varied in a parametric study of this form of coupling. If coupling does occur, appropriate scaling laws can be deduced.

Once scaling laws for the various types of coupling have been deduced, it will be possible to use the two-dimensional code for studies of the overall expansion of the debris from high altitude explosions. These scaling laws can be introduced at the expanding outer boundary of the debris in the same fashion as the Rankine-Hugoniot equations are introduced at the outer boundary of conventional hydrodynamics codes.

It is worth noting that the numerical procedure developed here can be used either as an Eulerian procedure or as a Lagrangian procedure. In a one-dimensional calculation, for example, the code will be Eulerian if the mesh is fixed in space; on the other hand, the code will be Lagrangian if each cell surface is caused to move at the local fluid velocity.

2. FURTHER DEVELOPMENT

The proposed physics code is capable of yielding detailed numerical information on the problem of the coupling of the debris of high altitude nuclear explosions to the ambient atmosphere. The code is also capable of incorporating this information in a manner suitable for the computation of the late-time debris structure. Most of the code as described in the foregoing section has been written but not debugged. Maxwell's equations have not yet been coupled into the code,

and the theory for the treatment of Maxwell's equations in two dimensions is not yet complete.

For the one-dimensional code, therefore, it is proposed that the first task be the debugging of the existing code. There are many solutions of channel flows which may be used to demonstrate the accuracy of the code. The second proposed task is the development of subroutines for the various thermodynamic and kinetic models. It is suggested that an equilibrium air equation of state be coded into a subroutine, and that a set of reaction rate equations for the decay from a nonequilibrium state to the equilibrium state be developed and coded. In addition, it is suggested that this second task include the development of subroutines which give the source of momentum due to particle collisions and due to scattering off of magnetic irregularities. These last two subtasks will involve finding or developing mathematical expressions for the cross-sections for the proposed reactions.

The third task proposed for the one-dimensional code is the adding of Maxwell's equations to the code and the subsequent debugging. The theory of the characteristic flux method as applied to Maxwell's equations in one dimension is completely developed, and the relevant stability analyses have been made. These equations can be coded in a fashion which is stable for any time step.

For the two-dimensional code, it is proposed that the first task be the debugging of the existing code. The blast penetration calculations of Reference 3 can be used as one standard during the debugging, and the point explosion results given in Sections 11 and 12 of Chapter IV of Reference 17 can be used as a second standard. These proposed standards cover the cases of strong interactions of high energy

streams with associated material interfaces and of high energy release in a small region.

The second task proposed for the two-dimensional code is the development and introduction of the appropriate thermodynamic routines. These routines would include all of those developed for the one-dimensional code, plus all of the scaling laws for coupling developed by use of the one-dimensional code. The latter class of thermodynamic routines would serve as proven coupling laws which can be used in the computation of the overall structure of the expanding debris.

Finally, it is proposed that a method be developed for coupling Maxwell's equations into the two-dimensional code. The characteristic flux technique has been applied to these equations, but the resulting stability matrix is not explicitly solvable and has not been evaluated numerically. It is suggested that evaluation of the stability matrix be undertaken, and that the equations be added to the code if proven stable. If the equations are not stable, it is suggested that attempts to generate a stable technique be undertaken.

(This Page Intentionally Left Blank)

APPENDIX I

CONSERVATION EQUATIONS FOR A REACTING NONEQUILIBRIUM MIXTURE OF GASES

The derivation of the usual hydrodynamic conservation equations for a nonreacting mixture of gases from Boltzmann's equations is given in many texts on physical gas dynamics. A similar derivation is presented here in order to demonstrate and document the consistence of the definitions used in Sections II and III of this report.

1. DEFINITION OF KINETIC PARAMETERS

Assume a chemically-reacting mixture of gases, and assume that all interactions are weak; i. e., no electromagnetic or radiative collision effects. Assume N species, including electrons (the species may be ionized).

Let ρ_α denote the mass per unit volume of species α , and let ρ denote the mass of mixture per unit volume:

$$\rho = \sum_{\alpha=1}^N \rho_\alpha \quad (122)$$

Let $f_\alpha(\vec{u}, \vec{r}, t)$ be the single-particle distribution function for species α and let

n_α = number density of particles of species α

m_α = mass of a particle of special α

Then

$$n_{\alpha}(\vec{r}, t) = \int f_{\alpha} d\vec{u}_{\alpha} \quad (123)$$

and

$$\rho_{\alpha}(\vec{r}, t) = m_{\alpha} n_{\alpha}(\vec{r}, t) \quad (124)$$

The mean velocity of particles of species α is defined as

$$\begin{aligned} \langle \vec{u}_{\alpha} \rangle &= \frac{\int \vec{u}_{\alpha} f_{\alpha} d\vec{u}_{\alpha}}{\int f_{\alpha} d\vec{u}_{\alpha}} \\ &= \frac{1}{n_{\alpha}} \int \vec{u}_{\alpha} f_{\alpha} d\vec{u}_{\alpha} \end{aligned} \quad (125)$$

The mass velocity of the mixture, \vec{u} , is defined as

$$\vec{u} = \frac{1}{\rho} \sum_{\alpha=1}^N \rho_{\alpha} \langle \vec{u}_{\alpha} \rangle \quad (126)$$

The thermal velocity of a particle of species α , \vec{v}_{α} , is defined as

$$\vec{v}_{\alpha} = \vec{u}_{\alpha} - \langle \vec{u}_{\alpha} \rangle \quad (127)$$

Note that Equation 127 is not the conventional definition of thermal velocity, which is expressed in terms of the mass velocity of the mixture. It is felt that for the situations considered here, which are nowhere near being equilibrium mixtures, species temperatures are better based on the motion of the individual species than on the motion of the mixture. The latter motion is given by the mean thermal velocity of a particle of species α , $\langle \vec{v}_{\alpha} \rangle$, defined as

$$\langle \vec{v}_{\alpha} \rangle = \vec{u}_{\alpha} - \vec{u} \quad (128)$$

obviously,

$$\vec{v}_\alpha - \langle \vec{v}_\alpha \rangle = \vec{u} - \langle \vec{u}_\alpha \rangle \quad (129)$$

The diffusion velocity of particles of species α , \vec{V}_α , is usually defined as

$$\vec{V}_\alpha = \langle \vec{u}_\alpha \rangle - \vec{u} \quad (130)$$

Thus, Equation 129 becomes

$$\vec{v}_\alpha - \langle \vec{v}_\alpha \rangle = -\vec{V}_\alpha \quad (131)$$

2. BOLTZMANN EQUATION FOR SPECIES α

Using tensor notation, the time-rate-of-change of species α within a fixed volume in (\vec{u}, \vec{r}) space is

$$\begin{aligned} \frac{d}{dt}(n_\alpha V) &= \frac{d}{dt} \iint f_\alpha d\vec{u} d\vec{r} \\ &= \iint \frac{\partial f_\alpha}{\partial t} d\vec{u} d\vec{r} \end{aligned} \quad (132)$$

This change results from two physical phenomena: 1) particle flux across the surface of V ; and 2) particle sources within V . The change arising from particle fluxes is

$$\frac{d}{dt}(n_\alpha V)_{\text{flux}} = - \int_S f_\alpha \varphi^i v_i ds \quad (133)$$

where

φ_i = generalized velocity of α particles in $(\vec{u}_\alpha, \vec{r}_\alpha)$ space,

v_i = unit outward normal to S ,

and

$S =$ bounding surface of V .

Using Green's theorem on Equation 133

$$\frac{d}{dt} (n_{\alpha} V)_{\text{flux}} = - \int_V (f_{\alpha} \varphi^i)_{,i} dV \quad (134)$$

For the three position variables,

$$\varphi^i = u^i \quad (135)$$

and for the three velocity variables,

$$\begin{aligned} \varphi^i &= \frac{du^i}{dt} \\ &= F_{\alpha}^i / m_{\alpha} \end{aligned} \quad (136)$$

where F_{α}^i is the force on a particle of species α . Note that u^i is not a function of r^i within the integral, so

$$u^i_{,i} = 0 \quad (137)$$

Also, note that the only velocity-dependent forces on particles are the Lorentz forces:

$$\begin{aligned} F_{\alpha}^i &\propto e^{ijk} B_k u_j \\ \frac{\partial F_{\alpha}^i}{\partial u^i} &\propto \frac{\partial}{\partial u^i} e^{ijk} B_k u_j \\ &\propto e^{ijk} \delta_{ij} B_k \\ &= 0 \end{aligned} \quad (138)$$

Using Equations 136 and 137 in Equation 134 gives

$$\frac{d}{dt}(n_{\alpha}V)_{\text{flux}} = - \int_V \varphi^i f_{\alpha,i} dV \quad (139)$$

a. Source Terms

The particle sources within the six-dimensional volume V are (1) creation of particles within physical space by chemical or nuclear processes; and (2) creation of particles within velocity space by scattering from another element of velocity space. Note that the nuclear processes involved here may emit or absorb photons, and the numerical processes being developed for these equations can treat photons as well as other species. Let the particle sources be defined as follows:

R_{α} = number of particles of species α generated per unit time in unit phase space volume around point (\vec{u}, \vec{r}) by all processes;

\bar{R}_{α} = number of particles of species α lost per unit time in unit phase space volume around point (\vec{u}, \vec{r}) by all processes.

Then

$$\frac{d}{dt}(n_{\alpha}V)_{\text{sources}} = \int_V (R_{\alpha} - \bar{R}_{\alpha}) dV \quad (140)$$

But

$$\frac{d}{dt}(n_{\alpha}V) = \frac{d}{dt}(n_{\alpha}V)_{\text{flux}} + \frac{d}{dt}(n_{\alpha}V)_{\text{sources}} \quad (141)$$

Combining Equations 132, 139, 140 and 141,

$$\int_V \frac{\partial f_{\alpha}}{\partial t} dV = - \int_V \varphi^i f_{\alpha,i} dV + \int_V (R_{\alpha} - \bar{R}_{\alpha}) dV \quad (142)$$

Noting that the volume of integration in Equation 142 is arbitrary, the Boltzmann equation results:

$$\frac{\partial f_{\alpha}}{\partial t} + \vec{u} \cdot \frac{\partial f_{\alpha}}{\partial \vec{r}} + \frac{\vec{F}_{\alpha}}{m_{\alpha}} \cdot \frac{\partial f_{\alpha}}{\partial \vec{u}} = R_{\alpha} - \bar{R}_{\alpha} \quad (143)$$

The source rates in Equation 143 are net rates resulting from all possible reactions; thus,

$$R_{\alpha} = \sum_{\beta\gamma}^{(2)} R_{\alpha, \beta\gamma} + \sum_{\beta\gamma, \delta}^{(3)} R_{\alpha, \beta\gamma; \delta} \quad (144)$$

where

$R_{\alpha, \beta\gamma}^{(2)}$ = rate at which particles of species β and γ react in two-body collisions to form particles of species α , and

$R_{\alpha, \beta\gamma; \delta}^{(3)}$ = rate at which particles of species β and γ react in three-body collisions (in the presence of species δ) to form particles of species α

Equation 144 obviously can be generalized to include higher than three-body collisions, but such effects seem unimportant.

There is a similar equation for \bar{R}_{α} :

$$\bar{R}_{\alpha} = \sum_{\beta} \bar{R}_{\alpha\beta}^{(2)} + \sum_{\beta, \gamma} \bar{R}_{\alpha\beta, \gamma}^{(3)} \quad (145)$$

where

$\bar{R}_{\alpha\beta}^{(2)}$ = rate at which particles of species α and β react in two-body collisions to annihilate particles of species α , and

and

$$\bar{R}_{\alpha\beta,\gamma}^{(3)} = \text{rate at which particles of species } \alpha \text{ and } \beta \text{ react in three-body collisions (in the presence of species } \gamma) \text{ to annihilate particles of species } \alpha.$$

It should be remembered that the terms "form" and "annihilate" as used in the above definitions refer to an element of six-dimensional phase space, and include scattering from one element of velocity space to another element of velocity space.

The above source rates can be expressed in terms of cross sections as follows. Suppose that a particle of species α and a particle of species β traveling with relative velocity

$$g_{\alpha\beta} = |\vec{u}_\alpha - \vec{u}_\beta| \quad (146)$$

have a cross section for the reaction

$$\alpha, \beta \rightarrow \gamma, \delta, \epsilon \quad (147)$$

of

$$\Omega(\vec{u}_\gamma, \vec{u}_\delta, \vec{u}_\epsilon; g_{\alpha\beta}) \quad (148)$$

where the cross section depends upon the velocities of the product particles. Then the rate of formation of particles γ, δ, ϵ because of this particular two-body interaction, $\Gamma_{\gamma\delta\epsilon, \alpha\beta}$ is

$$\Gamma_{\gamma\delta\epsilon, \alpha\beta}(\vec{u}_\gamma, \vec{u}_\delta, \vec{u}_\epsilon, \vec{r}, t) = \iint f_\alpha(\vec{u}_\alpha, \vec{r}, t) \cdot f_\beta(\vec{u}_\beta, \vec{r}, t) \cdot g_{\alpha\beta} \cdot \Omega(\vec{u}_\gamma, \vec{u}_\delta, \vec{u}_\epsilon; g_{\alpha\beta}) d\vec{u}_\alpha d\vec{u}_\beta \quad (149)$$

The rate of formation of any one species by two-body collisions is

$$R_{\gamma, \alpha\beta}^{(2)}(\vec{u}_\gamma, \vec{r}, t) = \iint \Gamma_{\gamma\delta\epsilon, \alpha\beta}(\vec{u}_\gamma, \vec{u}_\delta, \vec{u}_\epsilon, \vec{r}, t) d\vec{u}_\delta d\vec{u}_\epsilon \quad (150)$$

It is clear that if a standard form (such as the Maxwellian) for the distribution functions f_α and f_β can be assumed, and if the cross sections, Ω , are known, the integrals in Equations 149 and 150 can be evaluated, at least numerically, ahead of time.

The rate of loss of species α because of this two-body collision is

$$\begin{aligned} \bar{R}_{\alpha\beta}^{(2)}(\vec{u}_\alpha, \vec{r}, t) &= \iiint f_\alpha(\vec{u}_\alpha, \vec{r}, t) f_\beta(\vec{u}_\beta, \vec{r}, t) g_{\alpha\beta} \\ &\cdot \Omega(\vec{u}_\gamma, \vec{u}_\delta, \vec{u}_\epsilon; g_{\alpha\beta}) d\vec{u}_\gamma d\vec{u}_\delta d\vec{u}_\epsilon d\vec{u}_\beta \end{aligned} \quad (151)$$

Consideration of the integrals in Equations 149 through 151 makes it clear that the two-body source rates must satisfy the following "Compatibility Relation"

$$\begin{aligned} \int \bar{R}_{\alpha\beta}^{(2)} d\vec{u}_\alpha &= \int \bar{R}_{\beta\gamma}^{(2)} d\vec{u}_\beta = \int R_{\gamma, \alpha\beta}^{(2)} d\vec{u}_\gamma \\ &= \int \bar{R}_{\delta, \alpha\beta}^{(2)} d\vec{u}_\delta = \int R_{\epsilon, \alpha\beta}^{(2)} d\vec{u}_\epsilon \end{aligned} \quad (152)$$

b. Reduction to Spherically Symmetric Intermolecular Potential

That the above definition of two-body source rates is a satisfactory generalization of the definition given in standard texts on nonequilibrium kinetic theory may be seen as follows. Suppose that no nuclear or chemical process takes place during the two-body interaction: then particle γ is the same particle as particle α , particle δ is the same particle as particle β , particle ϵ does not exist, and the interaction degenerates into a two-body scattering. Because the integration over $d\vec{u}_\epsilon$ reduces to a delta function at $\vec{u}_\epsilon = 0$, Equations 149 and 150 give

$$R_Y^{(2)}(\vec{u}_Y, \vec{r}, t) = \iiint f_\alpha(\vec{u}_\alpha, \vec{r}, t) f_\beta(\vec{u}_\beta, \vec{r}, t) \cdot g_{\alpha\beta} \cdot \Omega(\vec{u}_\gamma, \vec{u}_\delta; g_{\alpha\beta}) d\vec{u}_\alpha d\vec{u}_\beta d\vec{u}_\delta \quad (153)$$

If the intermolecular potential is spherically symmetric,

$$\Omega(\vec{u}_\gamma, \vec{u}_\delta; g_{\alpha\beta}) d\vec{u}_\delta = \Omega(\omega, g_{\alpha\beta}) d\omega \quad (154)$$

where ω is the angle of scattering (this expression is merely the statement that conservation of angular momentum in an elastic two-body collision shows that the scattering cross section can only depend upon the relative velocity of the two approaching particles and upon the angle of scattering (see, for example, Section 3.2 of Reference 18). Furthermore, if ω and \vec{u}_β are specified, the conservation of momentum allows calculation of \vec{u}_α (mathematically, $\Omega = 0$ except for the curve $\vec{u}_\alpha = \vec{u}_\alpha(\omega, \vec{u}_\beta)$). Thus, Equations 153 and 154 become

$$R_Y^{(2)}(\vec{u}_Y, \vec{r}, t) = \iint f_\alpha[\vec{u}_\alpha(\omega, \vec{u}_\beta), \vec{r}, t] f_\beta(\vec{u}_\beta, \vec{r}, t) \cdot g_{\alpha\beta} \Omega(\omega, g_{\alpha\beta}) d\omega d\vec{u}_\beta \quad (155)$$

In a similar fashion,

$$\Omega(\vec{u}_\gamma, \vec{u}_\delta, \vec{u}_e; g_{\alpha\beta}) d\vec{u}_\gamma d\vec{u}_\delta d\vec{u}_e d\vec{u}_\beta = \Omega(\omega, g_{\alpha\beta}) d\omega d\vec{u}_\beta \quad (156)$$

Thus, Equation 151 becomes

$$\bar{R}_\alpha^{(2)} = \iint f_\alpha(\vec{u}_\alpha, \vec{r}, t) \cdot f_\beta(\vec{u}_\beta, \vec{r}, t) g_{\alpha\beta} \cdot \Omega(\omega, g_{\alpha\beta}) d\omega d\vec{u}_\beta \quad (157)$$

For an elastic two-body collision, specification of \vec{u}_γ causes \vec{u}_α and \vec{u}_β to become definite functions of \vec{u}_δ . Thus, Equation 155 can be written

$$R_{\gamma}^{(2)}(\vec{u}_{\gamma}, \vec{r}, t) = \iint f_{\alpha}[\vec{u}_{\alpha}(\vec{u}_{\gamma}, \vec{u}_{\delta}, \omega), \vec{r}, t] \cdot g_{\alpha\beta} \cdot \Omega(\omega, g_{\alpha\beta}) \cdot f_{\beta}[\vec{u}_{\beta}(\vec{u}_{\gamma}, \vec{u}_{\delta}, \omega), \vec{r}, t] d\vec{u}_{\delta} d\omega \quad (158)$$

Now interchange the indices in Equation 158 and note that conservation of momentum requires that $g_{\alpha\beta} = g_{\gamma\delta}$

$$R_{\alpha}^{(2)}(\vec{u}_{\alpha}, \vec{r}, t) = \iint f_{\alpha}[\vec{u}_{\gamma}(\vec{u}_{\alpha}, \vec{u}_{\beta}, \omega), \vec{r}, t] \cdot g_{\alpha\beta} \cdot \Omega(\omega, g_{\alpha\beta}) \cdot f_{\delta}[\vec{u}_{\delta}(\vec{u}_{\alpha}, \vec{u}_{\beta}, \omega), \vec{r}, t] d\vec{u}_{\beta} d\omega \quad (159)$$

Now let $\gamma \rightarrow \alpha'$ to represent particle α after the collision, and $\delta \rightarrow \beta'$; Equations 157 and 159 give

$$R_{\alpha}^{(2)} - \bar{R}_{\alpha}^{(2)} = \iint (f_{\alpha'} f_{\beta'} - f_{\alpha} f_{\beta}) g_{\alpha\beta} \Omega(\omega, g_{\alpha\beta}) d\omega d\vec{u}_{\beta} \quad (160)$$

Equation 160, except for minor differences of notation, is identical with the source rate equations usually given in texts on nonequilibrium kinetic theory (see, for example, Equation 3.34 of Reference 18). Thus, Equations 150 and 151 are satisfactory generalizations of the source rate terms in the Boltzmann equation.

c. Source Rates for Three-Body Collisions

The three-body source rates can be treated in a similar fashion. Thus, assume that particles α , β , and γ approach a collision region with velocities \vec{u}_{α} , \vec{u}_{β} , and \vec{u}_{γ} , and define

$$\vec{u}_3 \equiv \frac{m_{\alpha} \vec{u}_{\alpha} + m_{\beta} \vec{u}_{\beta} + m_{\gamma} \vec{u}_{\gamma}}{m_{\alpha} + m_{\beta} + m_{\gamma}} \quad (161)$$

Let the cross section for the reaction

$$\alpha, \beta; \gamma \rightarrow \delta, \epsilon \quad (162)$$

be

$$\Omega(\vec{u}_\delta, \vec{u}_\epsilon | \vec{u}_\alpha, \vec{u}_\beta; \vec{u}_\gamma) \quad (163)$$

where the notation denotes that particle γ may not enter into a chemical or nuclear reaction, but serves only to carry off excess energy. It should also be noted that particle ϵ need not be present ($\vec{u}_\epsilon = \delta(0)$); for example, in the case of molecular recombination, atoms α and β recombine into molecule δ with particle γ serving to conserve energy. The flux of particles of species α towards the collision area is $f_\alpha(\vec{u}_\alpha, \vec{r}, t) |\vec{u}_\alpha - \vec{u}_3|$, with similar expressions for the fluxes of particles of species β and γ . Then the rate of formation of particles δ and ϵ due to this particular three-body interaction, $\Gamma_{\delta\epsilon, \alpha\beta\gamma}$ is

$$\begin{aligned} \Gamma_{\delta\epsilon, \alpha\beta\gamma}(\vec{u}_\delta, \vec{u}_\epsilon, \vec{r}, t) &= \iiint |\vec{u}_\alpha - \vec{u}_3| \cdot |\vec{u}_\beta - \vec{u}_3| \cdot |\vec{u}_\gamma - \vec{u}_3| \\ &\quad \cdot f_\alpha(\vec{u}_\alpha, \vec{r}, t) \cdot f_\beta(\vec{u}_\beta, \vec{r}, t) \cdot f_\gamma(\vec{u}_\gamma, \vec{r}, t) \\ &\quad \cdot \Omega(\vec{u}_\delta, \vec{u}_\epsilon | \vec{u}_\alpha, \vec{u}_\beta; \vec{u}_\gamma) d\vec{u}_\alpha d\vec{u}_\beta d\vec{u}_\gamma \quad (164) \end{aligned}$$

The rate of formation of any one species, δ , by three-body processes is then

$$R_{\delta, \alpha\beta\gamma}^{(3)}(\vec{u}_\delta, \vec{r}, t) = \int \Gamma_{\delta\epsilon, \alpha\beta\gamma}(\vec{u}_\delta, \vec{u}_\epsilon, \vec{r}, t) d\vec{u}_\epsilon \quad (165)$$

The rate of loss of particles of species α due to this three-body process is

$$\begin{aligned} \bar{R}_{\alpha\beta, \gamma}^{(3)}(\vec{u}_\alpha, \vec{r}, t) &= \iiint |\vec{u}_\alpha - \vec{u}_3| \cdot |\vec{u}_\beta - \vec{u}_3| \cdot |\vec{u}_\gamma - \vec{u}_3| \\ &\quad \cdot f_\alpha(\vec{u}_\alpha, \vec{r}, t) \cdot f_\beta(\vec{u}_\beta, \vec{r}, t) \cdot f_\gamma(\vec{u}_\gamma, \vec{r}, t) \\ &\quad \cdot \Omega(\vec{u}_\delta, \vec{u}_\epsilon | \vec{u}_\alpha, \vec{u}_\beta; \vec{u}_\gamma) d\vec{u}_\gamma d\vec{u}_\delta d\vec{u}_\epsilon d\vec{u}_\beta \quad (166) \end{aligned}$$

It is clear from Equations 164 through 166 that the three-body source rates must satisfy the following "Compatibility Relation:"

$$\begin{aligned}
 \int \bar{R}_{\alpha\beta,\gamma}^{(3)} d\bar{u}_\alpha &= \int \bar{R}_{\beta\alpha,\gamma}^{(3)} d\bar{u}_\beta = \int R_{\delta,\alpha\beta;\gamma}^{(3)} d\bar{u}_\delta \\
 &= \int R_{\epsilon,\alpha\beta;\gamma}^{(3)} d\bar{u}_\epsilon \quad (167)
 \end{aligned}$$

With the source rates in Equation 144 defined, Equation 143 can be used to generate the conservation relations needed for the numerical study of high-altitude coupling effects.

d. Equation of Change

Let $\chi_\alpha(\bar{u})$ represent some parameter associated with species α . Then the equation of change is

$$\int \chi_\alpha \left\{ \frac{\partial f_\alpha}{\partial t} + \bar{u} \cdot \frac{\partial f_\alpha}{\partial \bar{r}} + \frac{\vec{F}_\alpha}{m_\alpha} \cdot \frac{\partial f_\alpha}{\partial \bar{u}} \right\} d\bar{u} = \int \chi_\alpha (R_\alpha - \bar{R}_\alpha) d\bar{u} \quad (168)$$

Now

$$\begin{aligned}
 \int \chi_\alpha \frac{\partial f_\alpha}{\partial t} d\bar{u} &= \int \frac{\partial}{\partial t} (f_\alpha \chi_\alpha) d\bar{u} = \frac{\partial}{\partial t} \int f_\alpha \chi_\alpha d\bar{u} \\
 &= \frac{\partial}{\partial t} (n_\alpha \langle \chi_\alpha \rangle) \quad (169)
 \end{aligned}$$

Similarly

$$\int \chi_\alpha \bar{u} \cdot \frac{\partial f_\alpha}{\partial \bar{r}} d\bar{u} = \int \frac{\partial}{\partial \bar{r}} \cdot (f_\alpha \chi_\alpha \bar{u}) d\bar{u} = \vec{v} \cdot (n_\alpha \langle \chi_\alpha \bar{u}_\alpha \rangle) \quad (170)$$

Also

$$\int \chi_\alpha \frac{\vec{F}_\alpha}{m_\alpha} \cdot \frac{\partial f_\alpha}{\partial \bar{u}} d\bar{u} = \int \frac{\partial}{\partial \bar{u}} \cdot \left(\chi_\alpha \frac{\vec{F}_\alpha}{m_\alpha} f_\alpha \right) d\bar{u} - \int f_\alpha \frac{\partial}{\partial \bar{u}} \cdot \left(\chi_\alpha \frac{\vec{F}_\alpha}{m_\alpha} \right) d\bar{u} \quad (171)$$

Now

$$\int \frac{\partial}{\partial \bar{u}} \cdot \left(\chi_\alpha \frac{\vec{F}_\alpha}{m_\alpha} f_\alpha \right) d\bar{u} = \left[\chi_\alpha \frac{\vec{F}_\alpha}{m_\alpha} f_\alpha \right]_{\bar{u}_{\alpha \min}}^{\bar{u}_{\alpha \max}} = 0 \quad (172)$$

because

$$f_{\alpha}(\vec{u}_{\alpha\max}) = f_{\alpha}(\vec{u}_{\alpha\min}) = 0 \quad (173)$$

Also, as indicated in Equation 138

$$\frac{\partial}{\partial \vec{u}} \cdot \vec{F}_{\alpha} = 0 \quad (174)$$

thus, Equation 171 becomes

$$\begin{aligned} \int \chi_{\alpha} \frac{\vec{F}_{\alpha}}{m_{\alpha}} \cdot \frac{\partial f_{\alpha}}{\partial \vec{u}} d\vec{u} &= - \int f_{\alpha} \frac{\vec{F}_{\alpha}}{m_{\alpha}} \cdot \vec{\nabla}_{\vec{u}} \chi_{\alpha} d\vec{u} \\ &= - \frac{n_{\alpha}}{m_{\alpha}} \langle \vec{F}_{\alpha} \cdot \vec{\nabla}_{\vec{u}} \chi_{\alpha} \rangle \end{aligned} \quad (175)$$

Finally

$$\int \chi_{\alpha} (R_{\alpha} - \bar{R}_{\alpha}) d\vec{u} = \Delta [\chi_{\alpha}] \quad (176)$$

where $\nabla[\chi_{\alpha}]$ denotes the time rate of change of χ_{α} per unit volume at (\vec{r}, t) because of chemical, molecular, and nuclear interactions.

Using Equations 168, 170, 175, and 176,

$$\frac{\partial}{\partial t} (n_{\alpha} \langle \chi_{\alpha} \rangle) + \vec{\nabla} \cdot (n_{\alpha} \langle \chi_{\alpha} \vec{u}_{\alpha} \rangle) = \frac{n_{\alpha}}{m_{\alpha}} \langle \vec{F}_{\alpha} \cdot \vec{\nabla}_{\vec{u}} \chi_{\alpha} \rangle + \nabla [\chi_{\alpha}] \quad (177)$$

3. CONSERVATION EQUATIONS

The "Conservation" equations required for the numerical work are obtained by choosing χ_{α} as the mass, momentum, and energy of a particle of species α . To handle the excited states of the atomic and molecular species, it is convenient to enumerate the possible internal energy states of species α ; thus, if state α_{β} ($\beta = 1, 2, \dots, N_{\alpha}$) denotes one of the possible internal energy states

of species β , the corresponding internal energy is denoted by $\epsilon_{\alpha\beta}$ (internal energy per particle). Furthermore, state α_β itself will have a distribution function, $f_{\alpha\beta}(\vec{u}, \vec{r}, t)$, which gives the number of particles of species α in internal energy state $\epsilon_{\alpha\beta}$ per unit velocity volume and unit physical volume at time t . It is clear that the overall distribution function for species α is given by

$$f_\alpha(\vec{u}, \vec{r}, t) = \sum_{\beta=1}^{N_\alpha} f_{\alpha\beta}(\vec{u}, \vec{r}, t) \quad (178)$$

Let $\psi(\vec{u})$ be an arbitrary function of velocity only.

Then, as in Equation 125

$$\langle \psi_\alpha \rangle = \frac{\int \psi(\vec{u}) f_\alpha d\vec{u}}{\int f_\alpha d\vec{u}} = \frac{1}{n_\alpha} \int \psi f_\alpha d\vec{u} \quad (179)$$

Similarly

$$\langle \psi_{\alpha\beta} \rangle = \frac{1}{n_{\alpha\beta}} \int \psi f_{\alpha\beta} d\vec{u} \quad (180)$$

where

$$n_{\alpha\beta} = \int f_{\alpha\beta} d\vec{u} \quad (181)$$

Substituting Equation 178 into Equation 179

$$\begin{aligned} n_\alpha \langle \psi_\alpha \rangle &= \int \psi \sum_{\beta=1}^{N_\alpha} f_{\alpha\beta} d\vec{u} \\ &= \sum_{\beta=1}^{N_\alpha} \int \psi f_{\alpha\beta} d\vec{u} \\ &= \sum_{\beta=1}^{N_\alpha} n_{\alpha\beta} \langle \psi_{\alpha\beta} \rangle \end{aligned} \quad (182)$$

by use of Equation 180

By use of

$$m_{\alpha} = m_{\alpha\beta} = \psi_{\alpha} \quad (183)$$

Equation 182 gives

$$\rho_{\alpha} = \sum_{\beta=1}^{N_{\alpha}} \rho_{\alpha\beta} \quad (184)$$

where

$$\rho_{\alpha\beta} = n_{\alpha\beta} m_{\alpha\beta} \quad (185)$$

a. Conservation of Mass

Let

$$\chi_{\alpha} = m_{\alpha} = m_{\alpha\beta} \quad (186)$$

Then

$$\vec{\nabla}_{\vec{u}} \chi_{\alpha} = 0 \quad (187)$$

and Equation 177 gives

$$\frac{\partial}{\partial t} (n_{\alpha\beta} m_{\alpha}) + \vec{\nabla} \cdot (n_{\alpha\beta} m_{\alpha} \langle \vec{u}_{\alpha\beta} \rangle) = \Delta [m_{\alpha\beta}] \quad (188)$$

Summing Equation 188 over all α_{β}

$$\sum_{\beta=1}^{N_{\alpha}} \left\{ \frac{\partial \rho_{\alpha\beta}}{\partial t} + \vec{\nabla} \cdot (\rho_{\alpha\beta} \langle \vec{u}_{\alpha\beta} \rangle) - \Delta [m_{\alpha\beta}] \right\} = 0 \quad (189)$$

Multiply Equation 182 by $m_{\alpha} = m_{\alpha\beta}$:

$$\rho_{\alpha} \langle \psi_{\alpha} \rangle = \sum_{\beta=1}^{N_{\alpha}} \rho_{\alpha\beta} \langle \psi_{\alpha\beta} \rangle \quad (190)$$

Equations 189 and 190 show that

$$\frac{\partial \rho_\alpha}{\partial t} + \vec{\nabla} \cdot (\rho_\alpha \langle \vec{u}_\alpha \rangle) = \Delta [m_\alpha] \quad (191)$$

where $\Delta [m_\alpha]$ is the time rate of change of mass of species α per unit volume at (\vec{r}, t) because of chemical, molecular, and nuclear processes.

b. Conservation of Momentum

Let

$$\chi_{\alpha\beta} = m_\alpha u^j \quad (192)$$

where u^j is the x^j component of \vec{u} . Now,

$$\begin{aligned} \langle \vec{F}_\alpha \cdot \vec{\nabla}_{\vec{u}} \chi_\alpha \rangle &= m_\alpha \langle F_\alpha^i \frac{\partial}{\partial u^i} u^j \rangle \\ &= m_\alpha \langle F_\alpha^i \delta_i^j \rangle \\ &= m_\alpha \langle F_\alpha^j \rangle \end{aligned} \quad (193)$$

Using Equation 193 in Equation 177

$$\frac{\partial}{\partial t} (\rho_{\alpha\beta} \langle \vec{u}_{\alpha\beta} \rangle) + \vec{\nabla} \cdot (\rho_{\alpha\beta} \langle \vec{u}_{\alpha\beta} \vec{u}_{\alpha\beta} \rangle) = \frac{\rho_{\alpha\beta}}{m_\alpha} \langle \vec{F}_\alpha \rangle + \Delta [m_\alpha \vec{u}_{\alpha\beta}] \quad (194)$$

Summing Equation 194 over all β and using Equation 190

$$\frac{\partial}{\partial t} (\rho_\alpha \langle \vec{u}_\alpha \rangle) + \vec{\nabla} \cdot (\rho_\alpha \langle \vec{u}_\alpha \vec{u}_\alpha \rangle) = \frac{\rho_\alpha}{m_\alpha} \langle \vec{F}_\alpha \rangle + \Delta [m_\alpha \vec{u}_\alpha] \quad (195)$$

where $\Delta [m_\alpha \vec{u}_\alpha]$ is the time rate of change of momentum of species α per unit volume by chemical, molecular, and nuclear processes.

c. Conservation of Energy

Let

$$\chi_{\alpha\beta} = \epsilon_{\alpha\beta} + \frac{m_{\alpha} u^2}{2} \quad (196)$$

Here

$$\begin{aligned} \langle \vec{F}_{\alpha}^i \cdot \vec{\nabla}_{\vec{u}} \chi_{\beta} \rangle &= \left\langle F_{\alpha}^i \frac{\partial}{\partial u^i} \left(\epsilon_{\alpha\beta} + \frac{m_{\alpha}}{2} u^j u_j \right) \right\rangle \\ &= m_{\alpha} \left\langle F_{\alpha}^i u_j \frac{\partial u^j}{\partial u^i} \right\rangle \\ &= m_{\alpha} \left\langle F_{\alpha}^i u_j \delta_i^j \right\rangle \\ &= m_{\alpha} \langle \vec{F}_{\alpha} \cdot \vec{u}_{\alpha\beta} \rangle \end{aligned} \quad (197)$$

Using Equations 196 and 197 in Equation 177

$$\begin{aligned} \frac{\partial}{\partial t} \left(n_{\alpha\beta} \left\langle \epsilon_{\alpha\beta} + \frac{m_{\alpha} u_{\alpha\beta}^2}{2} \right\rangle \right) + \vec{\nabla} \cdot \left[n_{\alpha\beta} \left\langle \vec{u}_{\alpha\beta} \left(\epsilon_{\alpha\beta} + \frac{m_{\alpha} u_{\alpha\beta}^2}{2} \right) \right\rangle \right] \\ = \frac{\rho_{\alpha\beta}}{m_{\alpha}} \langle \vec{F}_{\alpha} \cdot \vec{u}_{\alpha\beta} \rangle + \Delta \left[\epsilon_{\alpha\beta} + \frac{m_{\alpha}}{2} u_{\alpha\beta}^2 \right] \end{aligned} \quad (198)$$

Defining

$$e_{\alpha\beta} = \epsilon_{\alpha\beta} / m_{\alpha} \quad (199)$$

= internal energy per unit mass of
species α in state β

Equation 199 becomes

$$\begin{aligned} \frac{\partial}{\partial t} \left(\rho_{\alpha\beta} \left\langle e_{\alpha\beta} + \frac{u_{\alpha\beta}^2}{2} \right\rangle \right) + \vec{\nabla} \cdot \left[\rho_{\alpha\beta} \langle \vec{u}_{\alpha\beta} (e_{\alpha\beta} + \frac{u_{\alpha\beta}^2}{2}) \rangle \right] \\ = \frac{\rho_{\alpha\beta}}{m_{\alpha}} \langle \vec{F}_{\alpha}^i \cdot \vec{u}_{\alpha\beta} \rangle + \Delta \left[m_{\alpha} \left(e_{\alpha\beta} + \frac{u_{\alpha\beta}^2}{2} \right) \right] \end{aligned} \quad (200)$$

Summing over all β and using Equation 190 to effect

$$\rho_{\alpha} \langle u_{\alpha}^2 \rangle = \sum_{\beta=1}^{N_{\alpha}} \rho_{\alpha\beta} \langle u_{\alpha\beta}^2 \rangle, \quad \text{Equation 200 gives}$$

$$\begin{aligned} \frac{\partial}{\partial t} \left[\rho_{\alpha} \left(e_{\alpha} + \left\langle \frac{u_{\alpha}^2}{2} \right\rangle \right) \right] + \vec{\nabla} \cdot \left(\frac{\rho_{\alpha}}{2} \langle \vec{u}_{\alpha} u_{\alpha}^2 \rangle \right) + \vec{\nabla} \cdot \sum_{\beta=1}^{N_{\alpha}} \rho_{\alpha\beta} e_{\alpha\beta} \langle \vec{u}_{\alpha\beta} \rangle \\ = \frac{\rho_{\alpha}}{m_{\alpha}} \langle \vec{F}_{\alpha}^i \cdot \vec{u}_{\alpha} \rangle + \sum_{\beta=1}^{N_{\alpha}} \Delta \left[m_{\alpha} \left(e_{\alpha\beta} + \frac{u_{\alpha\beta}^2}{2} \right) \right] \end{aligned} \quad (201)$$

where

$$\rho_{\alpha} e_{\alpha} \equiv \sum_{\beta=1}^{N_{\alpha}} \rho_{\alpha\beta} e_{\alpha\beta} \quad (202)$$

But

$$\begin{aligned} \sum_{\beta=1}^{N_{\alpha}} \rho_{\alpha\beta} e_{\alpha\beta} \langle \vec{u}_{\alpha\beta} \rangle &= \rho_{\alpha} e_{\alpha} \langle \vec{u}_{\alpha} \rangle + \left[\sum_{\beta=1}^{N_{\alpha}} \rho_{\alpha\beta} e_{\alpha\beta} \langle \vec{u}_{\alpha\beta} \rangle - \rho_{\alpha} e_{\alpha} \langle \vec{u}_{\alpha} \rangle \right] \\ &= \rho_{\alpha} e_{\alpha} \langle \vec{u}_{\alpha} \rangle + \sum_{\beta=1}^{N_{\alpha}} \vec{Q}_{\alpha\beta} \end{aligned} \quad (203)$$

where

$$\vec{Q}_{\alpha\beta} \equiv \rho_{\alpha\beta} e_{\alpha\beta} \langle \vec{u}_{\alpha\beta} - \vec{u}_{\alpha} \rangle \quad (204)$$

is the excitation heat flux vector of species α . $\vec{Q}_{\alpha\beta}$ arises from the fact that the excited states of species α may have different velocity

distributions than the ground state; indeed, because different excited states result from different sets of collisions, it seems probable that the distribution functions of the various excited states will differ dur-

ing some nonequilibrium period. If $f_{\alpha\beta} = \frac{n_{\alpha\beta}}{n_{\alpha}} f_{\alpha}$, then

$\langle \vec{u}_{\alpha\beta} - \vec{u}_{\alpha} \rangle = 0$ and $\vec{Q}_{\alpha\beta} = 0$. In general, however, a diffusive

heat transfer within species α due to the existence of excited states with unequal distribution functions will exist.

Using Equations 203 and 204 in Equation 201 the energy equation becomes

$$\begin{aligned} \frac{\partial}{\partial t} (\rho_{\alpha} \epsilon_{\alpha}) + \vec{\nabla} \cdot (\rho_{\alpha} \langle \vec{u}_{\alpha} \epsilon_{\alpha} \rangle) &= \vec{\nabla} \cdot \left[\rho_{\alpha} \left\langle \vec{u}_{\alpha} \left(\left\langle \frac{\vec{u}_{\alpha}^2}{2} \right\rangle - \frac{\vec{u}_{\alpha}^2}{2} \right) \right\rangle \right] \\ - \vec{\nabla} \cdot \sum_{\beta=1}^{N_{\alpha}} \vec{Q}_{\alpha\beta} + \frac{\rho_{\alpha}}{m_{\alpha}} \langle \vec{F}_{\alpha} \cdot \vec{u}_{\alpha} \rangle + \Delta \left[m_{\alpha} \left(e_{\alpha} + \frac{u_{\alpha}^2}{2} \right) \right] & \quad (205) \end{aligned}$$

where

$$\epsilon_{\alpha} \equiv e_{\alpha} + \left\langle \frac{u_{\alpha}^2}{2} \right\rangle \quad (206)$$

is the total energy per unit mass of species α , and $\Delta \left[m_{\alpha} \left(e_{\alpha} + \frac{u_{\alpha}^2}{2} \right) \right]$ is the time rate of change of the total energy of species α per unit volume at (\vec{r}, t) because of chemical, molecular, and nuclear processes.

Equations 191, 195, and 205 are the required conservation equations. They can be written in more conventional form by use of the pressure tensor and the heat flux vector. The pressure tensor for species α is defined as

$$P_{\alpha\beta}^{ij} = \rho_{\alpha\beta} \langle v_{\alpha\beta}^i v_{\alpha\beta}^j \rangle \quad (207)$$

where the $\vec{v}_{\alpha\beta}$ are given by Equation 127

Summing over all β ,

$$\begin{aligned}
 P_{\alpha}^{ij} &= \sum_{\beta=1}^{N_{\alpha}} P_{\alpha\beta}^{ij} \\
 &= \sum_{\beta=1}^{N_{\alpha}} \rho_{\alpha\beta} \langle (u_{\alpha\beta}^i - \langle u_{\alpha}^i \rangle) (u_{\alpha\beta}^j - \langle u_{\alpha}^j \rangle) \rangle \\
 &= \rho_{\alpha} \langle (u_{\alpha}^i - \langle u_{\alpha}^i \rangle) (u_{\alpha}^j - \langle u_{\alpha}^j \rangle) \rangle \\
 &= \rho_{\alpha} \langle v_{\alpha}^i v_{\alpha}^j \rangle
 \end{aligned} \tag{208}$$

Note that the thermal velocity of an excited particle of species α is referred to the mean velocity of species α , and not to the mean velocity of the excited level:

$$\vec{v}_{\alpha\beta} = \vec{u}_{\alpha\beta} - \langle \vec{u}_{\alpha} \rangle \tag{209}$$

Consider the term

$$I_1^{ij} = \rho_{\alpha} \langle u_{\alpha}^i u_{\alpha}^j \rangle \tag{210}$$

From Equation 208

$$\begin{aligned}
 P_{\alpha}^{ij} &= \rho_{\alpha} \langle u_{\alpha}^i u_{\alpha}^j - u_{\alpha}^j \langle u_{\alpha}^i \rangle - u_{\alpha}^i \langle u_{\alpha}^j \rangle + \langle u_{\alpha}^i \rangle \langle u_{\alpha}^j \rangle \rangle \\
 &= I_1^{ij} - \rho_{\alpha} \left[\langle u_{\alpha}^j \rangle \langle u_{\alpha}^i \rangle + \langle u_{\alpha}^i \rangle \langle u_{\alpha}^j \rangle - \langle u_{\alpha}^i \rangle \langle u_{\alpha}^j \rangle \right]
 \end{aligned}$$

or

$$I_1^{ij} = P_{\alpha}^{ij} + \rho_{\alpha} \langle u_{\alpha}^i \rangle \langle u_{\alpha}^j \rangle \tag{211}$$

Substituting Equations 210 and 211 in Equation 195

$$\frac{\partial}{\partial t}(\rho_{\alpha} \langle u_{\alpha}^i \rangle) + (P_{\alpha}^{ij} + \rho_{\alpha} \langle u_{\alpha}^i \rangle \langle u_{\alpha}^j \rangle)_{,j} = \frac{\rho_{\alpha}}{m_{\alpha}} \langle F_{\alpha}^i \rangle + \Delta [m_{\alpha} u_{\alpha}^i] \quad (212)$$

Now consider the term

$$I_{\alpha}^i = \rho_{\alpha} \left\langle u_{\alpha}^i \left(\left\langle \frac{u_{\alpha}^2}{2} \right\rangle - \frac{u_{\alpha}^2}{2} \right) \right\rangle \quad (213)$$

from Equation 205

The heat flux vector for species α is defined as

$$Q_{\alpha}^i = \frac{\rho_{\alpha}}{2} \langle v_{\alpha}^i v_{\alpha}^j v_{\alpha}^j \rangle + \sum_{\beta=1}^{N_{\alpha}} Q_{\alpha\beta}^i \quad (214)$$

Now

$$\begin{aligned} v_{\alpha}^i v_{\alpha}^j v_{\alpha}^j &= (u_{\alpha}^i - \langle u_{\alpha}^i \rangle) (u_{\alpha}^i - \langle u_{\alpha}^i \rangle) (u_{\alpha}^j - \langle u_{\alpha}^j \rangle) \\ &= (u_{\alpha}^i - \langle u_{\alpha}^i \rangle) (u_{\alpha}^2 - 2u_{\alpha}^j \langle u_{\alpha}^j \rangle + \langle u_{\alpha}^j \rangle^2) \end{aligned}$$

Thus

$$\begin{aligned} \langle v_{\alpha}^i v_{\alpha}^j v_{\alpha}^j \rangle &= \langle u_{\alpha}^i u_{\alpha}^2 \rangle - 2 \langle u_{\alpha}^i u_{\alpha}^j \rangle \langle u_{\alpha}^j \rangle + \langle u_{\alpha}^i \rangle \langle u_{\alpha}^j \rangle^2 \\ &\quad - \langle u_{\alpha}^i \rangle \langle u_{\alpha}^2 \rangle + 2 \langle u_{\alpha}^i \rangle \langle u_{\alpha}^j \rangle \langle u_{\alpha}^j \rangle - \langle u_{\alpha}^i \rangle \langle u_{\alpha}^j \rangle^2 \\ &= \left\langle u_{\alpha}^i (u_{\alpha}^2 - \langle u_{\alpha}^2 \rangle) \right\rangle - 2 \langle u_{\alpha}^j \rangle \left\langle u_{\alpha}^i u_{\alpha}^j - u_{\alpha}^j \langle u_{\alpha}^i \rangle \right\rangle \end{aligned} \quad (215)$$

Using Equation 213 in Equation 215

$$\begin{aligned} \langle v_{\alpha}^i v_{\alpha}^j v_{\alpha}^j \rangle &= -2 \frac{I_{\alpha}^i}{\rho_{\alpha}} - 2 \langle u_{\alpha}^j \rangle \left\langle (u_{\alpha}^i - \langle u_{\alpha}^i \rangle) (u_{\alpha}^j - \langle u_{\alpha}^j \rangle) \right\rangle \\ &\quad - 2 \langle u_{\alpha}^j \rangle \langle u_{\alpha}^j \rangle \left\langle u_{\alpha}^i - \langle u_{\alpha}^i \rangle \right\rangle \end{aligned} \quad (216)$$

Noting that

$$\left\langle u_{\alpha}^i - \langle u_{\alpha}^i \rangle \right\rangle = \langle u_{\alpha}^i \rangle - \langle u_{\alpha}^i \rangle = 0 \quad (217)$$

and using Equation 208, Equation 216 gives

$$\langle v_{\alpha}^i v_{\alpha_j} v_{\alpha}^j \rangle = -2 \frac{I_{\alpha}^i}{\rho_{\alpha}} - 2 \langle u_{\alpha_j} \rangle \frac{P_{\alpha}^{ij}}{\rho_{\alpha}} \quad (218)$$

Substituting Equation 218 in Equation 214

$$Q_{\alpha}^i = -I_{\alpha}^i - P_{\alpha}^{ij} \langle u_{\alpha_j} \rangle + \sum_{\beta=1}^{N_{\alpha}} Q_{\alpha\beta}^i$$

or

$$I_{\alpha}^i = -Q_{\alpha}^i - P_{\alpha}^{ij} \langle u_{\alpha_j} \rangle + \sum_{\beta=1}^{N_{\alpha}} Q_{\alpha\beta}^i \quad (219)$$

Using Equations 213 and 219 in Equation 205 gives

$$\begin{aligned} \frac{\partial}{\partial t} (\rho_{\alpha} e_{\alpha}) + (\rho_{\alpha} e_{\alpha} \langle u_{\alpha}^i \rangle)_{,i} &= -Q_{\alpha,i}^i - (P_{\alpha}^{ij} \langle u_{\alpha_j} \rangle)_{,i} \\ &+ \frac{\rho_{\alpha}}{m_{\alpha}} \langle F_{\alpha}^i u_{\alpha_i} \rangle + \Delta \left[m_{\alpha} \left(e_{\alpha} + \frac{u_{\alpha}^2}{2} \right) \right] \end{aligned} \quad (220)$$

Now consider the term

$$\begin{aligned} I_{\alpha} &= \langle F_{\alpha}^i u_{\alpha_i} \rangle \\ &= \int \sum_{\beta=1}^{N_{\alpha}} f_{\alpha\beta} F_{\alpha}^i u_{\alpha_i} d\vec{u} \end{aligned} \quad (221)$$

As discussed immediately prior to Equation 138, the only velocity dependent force is perpendicular to the velocity, so Equation 221 becomes

$$\begin{aligned} I_{\alpha} &= F_{\alpha}^i \int \sum_{\beta=1}^{N_{\alpha}} f_{\alpha\beta} u_{\alpha_i} d\vec{u} \\ &= F_{\alpha}^i \int f_{\alpha} u_{\alpha_i} d\vec{u} \\ &= F_{\alpha}^i \langle u_{\alpha_i} \rangle \end{aligned} \quad (222)$$

Using Equations 221 and 222, the energy equation becomes

$$\begin{aligned} \frac{\partial}{\partial t} (\rho_\alpha e_\alpha) + \vec{\nabla} \cdot [\rho_\alpha e_\alpha \langle \vec{u}_\alpha \rangle + \vec{P}_\alpha \cdot \langle \vec{u}_\alpha \rangle] \\ = -\vec{\nabla} \cdot \vec{Q}_\alpha + \frac{\rho_\alpha \vec{F}_\alpha}{m_\alpha} \cdot \langle \vec{u}_\alpha \rangle + \Delta \left[m_\alpha \left(e_\alpha + \frac{u_\alpha^2}{2} \right) \right] \end{aligned} \quad (223)$$

where $\Delta \left[m_\alpha \left(e_\alpha + \frac{u_\alpha^2}{2} \right) \right]$ is the time rate of change of energy of species α per unit volume by chemical, molecular, and nuclear processes.

The quantity

$$w_{\alpha*}(\varphi) \equiv \sum_{\beta=1}^{N_\alpha} \int (R_{\alpha\beta*} - \bar{R}_{\alpha\beta*}) \varphi_{\alpha\beta*} d\vec{u}_* \quad (224)$$

gives the rate at which particles of species α carrying property φ_* are generated per unit volume. Let

$$w_* = \text{reference rate of particle generation per unit volume} \quad (225)$$

Then

$$w_\alpha(1) \equiv \sum_{\beta=1}^{N_\alpha} \int \frac{(R_{\alpha\beta*} - \bar{R}_{\alpha\beta*}) d\vec{u}_*}{w_*} \quad (226)$$

and Equation 191 becomes

$$\frac{\partial \rho_\alpha}{\partial t} + \vec{\nabla} \cdot \rho_\alpha \langle \vec{u}_\alpha \rangle = K m_\alpha w_\alpha(1) \quad (227)$$

Similarly, Equation 195 becomes

$$\begin{aligned} \frac{\partial}{\partial t} (\rho_\alpha \langle \vec{u}_\alpha \rangle) + \vec{\nabla} \cdot (\rho_\alpha \langle \vec{u}_\alpha \rangle \langle \vec{u}_\alpha \rangle + \vec{P}_\alpha) \\ = \rho_\alpha \langle \vec{F}_\alpha / m_\alpha \rangle + K m_\alpha w_\alpha(\vec{u}) \end{aligned} \quad (228)$$

and Equation 205 becomes

$$\begin{aligned} \frac{\partial}{\partial t}(\rho_{\alpha} \epsilon_{\alpha}) + \vec{\nabla} \cdot (\rho_{\alpha} \epsilon_{\alpha} \langle \vec{u}_{\alpha} \rangle + \vec{P}_{\alpha} \cdot \langle \vec{u}_{\alpha} \rangle) \\ = - \vec{\nabla} \cdot \vec{Q}_{\alpha} + \rho_{\alpha} (\vec{F}_{\alpha} / m_{\alpha}) \cdot \langle \vec{u}_{\alpha} \rangle \\ + K m_{\alpha} w_{\alpha} (e + u^2/2) \end{aligned} \quad (229)$$

The appropriate nondimensional forms of the conservation equations are Equations 227 through 229.

(This Page is Intentionally Left Blank)

APPENDIX II

FORTRAN GLOSSARY AND FLOW CHARTS

A quantity in parentheses after a definition is the algebraic equivalent of the quantity being defined.

| | |
|--------------|---|
| A(L, J, N) | speed of sound of species N in cell J of column I + L - 1 ($1 \leq L \leq 2$; $1 \leq J \leq \text{MAXJC}$; $1 \leq N \leq \text{NSPEC}$) |
| ARCCS (L, J) | cosine of angle between arc J in column I + L - 1 and positive z axis ($1 \leq L \leq 2$; $1 \leq J \leq \text{MAXJ}$); ($\cos \theta_{i+\frac{1}{2}, j}$) |
| ARCL(L, J) | length of arc J in column I + L - 1 ($1 \leq L \leq 2$; $1 \leq J \leq \text{MAXJ}$) |
| ARCSN(L, J) | sine of angle between arc J in column I + L - 1 and positive z axis ($1 \leq L \leq 2$; $1 \leq J \leq \text{MAXJ}$); ($\sin \theta_{i+\frac{1}{2}, j}$) |
| AREA(L, J) | cross-sectional area of cell J in column I + L - 1 ($1 \leq L \leq 2$; $1 \leq J \leq \text{MAXJ}$) |
| AREARC(L, J) | area of arc face J in column I + L - 1 ($1 \leq L \leq 2$; $1 \leq J \leq \text{MAXJ}$); ($S_{i+\frac{1}{2}, j}$) |
| AREARY(L, J) | ($1 \leq L \leq 4$; $1 \leq J \leq \text{MAXJC}$); ($S_{i, j+\frac{1}{2}}$) |
| AREARY(1, J) | area of face on ray I + 1 of cell J in column I |
| AREARY(2, J) | area of face on ray I + 1 of cell J in column I + 1 |
| AREARY(3, J) | area of face on ray I + 2 of cell J in column I + 1 |
| AREARY(4, J) | area of face on ray 1 of cell J in column 1 |
| CELVOL(L, J) | volume of cell J in column I + L - 1 ($1 \leq L \leq 2$; $1 \leq J \leq \text{MAXJC}$) |
| CS(I) | cosine of angle between ray I and negative z axis ($1 \leq I \leq \text{IBMX}$); ($\cos \alpha_i$) |

| | |
|----------------|--|
| CV(I, J, K) | (1 ≤ I ≤ ICMX; 1 ≤ J ≤ MAXJC; 1 ≤ K ≤ 4 · NSPEC) |
| CV(I, J, 4N-3) | total z-momentum of species N in cell J in column I $((\rho_N V_{Nz})_{i+\frac{1}{2}, j+\frac{1}{2}})$ |
| CV(I, J, 4N-2) | total r-momentum of species N in cell J in column I $((\rho_N V_{Nr})_{i+\frac{1}{2}, j+\frac{1}{2}})$ |
| CV(I, J, 4N-1) | total energy of species N in cell J in column I $((\rho_N V_N^e)_{i+\frac{1}{2}, j+\frac{1}{2}})$ |
| DALPHA (I) | sine of the angle between rays I and I+1 (1 ≤ I ≤ ICMX); $(\sin(\alpha_{i+1} - \alpha_i))$ |
| DEEZEE (I) | distance along z-axis from intersection of ray I to intersection of ray I + 1 (1 ≤ I ≤ ICMX); $(z_{i+1} - z_i)$ |
| DELT | time step |
| DELTAR | r-increment along arc currently being treated |
| DELTAZ | z-increment along arc currently being treated |
| DFRND (I, N) | distance along ray I from reference point to the node formed by the intersection of floating boundary N with ray I (1 ≤ I ≤ IBMX; 2 ≤ N ≤ 4) |
| DNODE(L, J) | (1 ≤ L ≤ 4; 1 ≤ J ≤ MAXJ) |
| DNODE(1, J) | distance along ray I from reference point to the node formed by the intersection of ray I and arc J in column I |
| DNODE(2, J) | distance along ray I + 1 from reference point to the node formed by the intersection of ray I + 1 and arc J in column I |
| DNODE(3, J) | distance along ray I + 1 from reference point to the node formed by the intersection of ray I + 1 and arc J in column I + 1 |
| DNODE(4, J) | distance along ray I + 2 from reference point to the node formed by the intersection of ray I + 2 and arc J in column I + 1 |

| | |
|---------------|--|
| DRBND(I) | r-increment along last arc in column I ($1 \leq I \leq ICMX$); $(\Delta r_{i+\frac{1}{2}, j_{\max}})$ |
| DSTBLY(L) | ($1 \leq L \leq 2$) |
| DSTBLY(1) | minimum distance between the arc boundaries of a cell |
| DSTBLY(2) | minimum distance between the ray boundaries of a cell |
| DST1 | maximum possible ray-segment length |
| DST2 | maximum possible arc-segment length |
| DVOL(J) | volume change of cell J in current column during time-step ($1 \leq J \leq MAXJ$) |
| DZBND(I) | z-increment along last arc in column I ($1 \leq I \leq ICMX$); $(\Delta z_{i+\frac{1}{2}, j_{\max}})$ |
| EB(N, L) | ($1 \leq N \leq NSPEC$; $1 \leq L \leq 2$) |
| EB(N, 1) | internal energy per unit mass of species N on cell boundary currently being treated |
| EB(N, 2) | internal energy per unit mass of species N on first arc of next column downstream |
| EBO(N) | internal energy of species N per unit mass on the boundary for a problem with constant boundary conditions ($1 \leq N \leq NSPEC$) |
| EINT(L, J, N) | internal energy per unit mass of species N in cell J of column I + L - 1 ($1 \leq L \leq 2$; $1 \leq J \leq MAXJC$; $1 \leq N \leq NSPEC$) |
| GAM(L, J, N) | ratio of specific heats of species N in cell J of column I + L - 1 ($1 \leq L \leq 2$; $1 \leq J \leq MAXJC$; $1 \leq N \leq NSPEC$) |
| GAMMA (N) | constant ratio of specific heats for species N treated as a perfect gas ($1 \leq N \leq NSPEC$) |
| GASCST(N) | constant gas constant for species N treated as an ideal gas ($1 \leq N \leq NSPEC$) |

| | |
|--------|--|
| IBCD | number of cycles between which BCD output is desired |
| IBMX | total number of rays |
| ICMX | total number of columns |
| IEXTM | flag denoting time-dependent boundary conditions |
| IECXTM | $\begin{cases} \leq 0 & \text{constant boundary conditions} \\ \geq 1 & \text{time-dependent boundary conditions} \end{cases}$ |
| IGEOM | geometry option word |
| IGEOM | $\begin{cases} 1, & \text{plane geometry} \\ 2, & \text{cylindrical geometry} \\ 3, & \text{spherical geometry} \end{cases}$ |
| IMESH | flag denoting whether or not the mesh moves |
| IMESH | $\begin{cases} \leq 0 & \text{fixed mesh} \\ \geq 1 & \text{floating mesh} \end{cases}$ |
| | (Note: A fixed multi-column mesh in which the cells differ in geometry from column to column must be treated as a floating mesh.) |
| ISLIP | flag denoting whether or not arcs must be continuous at rays |
| ISLIP | $\begin{cases} \leq 0, & \text{arcs are continuous across rays} \\ \geq 1, & \text{arcs are not necessarily continuous across rays} \end{cases}$ |
| KTAPE | tape number for BCD input tape |
| MAXJ | maximum number of arcs permitted in any column of the mesh |
| MAXJC | maximum number of cells permitted in any column of the mesh |
| MTAPE | tape number for binary restart input tape |
| MXFARC | maximum number of floating boundaries permitted in any column of the mesh |

NARC(N, L) arc number of the N^{th} free arc in column $I + L - 1$
 $\text{NAKC}(1, 1) = \text{NARC}(1, 2) = 1$ ($2 \leq N \leq 4; 1 \leq L \leq 2$)

NDIMEN number of dimensions

NDIMEN $\left\{ \begin{array}{l} 1, \text{ one column} \\ 2, \text{ more than one column} \end{array} \right.$

NFRARC(I, N) arc number of the arc which represents floating
 boundary N in column I. $\text{NFRARC}(I, N) = 0$
 if floating boundary N does not occur in column I.
 ($1 \leq I \leq \text{ICMX}; 2 \leq N \leq 4$)

NMOMEN number of momentum equations being treated

NMOMEN $\left\{ \begin{array}{l} 1, \text{ radial momentum only} \\ 2, \text{ radial and axial momentum} \end{array} \right.$

NSPEC number of species under consideration

NTAPE tape number for binary restart output tape

NTOT(L) total number of free arcs in column $I + L - 1$
 ($1 \leq L \leq 2$)

P(L, J, N) partial pressure of species N in cell J of
 column $I + L - 1$ ($1 \leq L \leq 2; 1 \leq J \leq \text{MAXJC};$
 $1 \leq N \leq \text{NSPEC}$)

PB(N, L) ($1 \leq N \leq \text{NSPEC}; 1 \leq L \leq 2$)

PB(N, 1) partial pressure of species N on the cell
 boundary currently being treated

PB(N, 2) partial pressure of species N on the first arc
 of the next column downstream

PBO(N) partial pressure of species N on the boundary
 for a problem with constant boundary conditions
 ($1 \leq N \leq \text{NSPEC}$)

RGAS(L, J, N) gas constant of species N in cell J of column
 $I + L - 1$ ($1 \leq L \leq 2; 1 \leq J \leq \text{MAXJC}; 1 \leq N \leq \text{NSPEC}$)

| | |
|----------------|--|
| RHO(L, J, N) | density of species N in cell J of column $I + L - 1$ ($1 \leq L \leq 2$; $1 \leq J \leq \text{MAXJC}$; $1 \leq N \leq \text{NSPEC}$); (ρ_α) |
| RHOB(N, L) | ($1 \leq N \leq \text{NSPEC}$; $1 \leq L \leq 2$) |
| RHOB(N, 1) | density of species N on the cell boundary currently being treated |
| RHOB(N, 2) | density of species N on the first arc of the next column downstream |
| RHOBO(N) | density of species N on the boundary for a problem with constant boundary conditions |
| SFLUX(L, J, K) | fluxes of mass, momentum, and energy across the surfaces of a cell ($1 \leq L \leq 5$; $1 \leq J \leq \text{MAXJC}$; $1 \leq K \leq 4 \cdot \text{NSPEC}$) |
| L | <ul style="list-style-type: none"> 1, fluxes entering cell J in current column across arc J 2, fluxes entering cell J in current column across arc J + 1 3, fluxes entering cell J in current column across upstream ray 4, fluxes entering cell J in current column across downstream ray 5, fluxes entering cell J in next column across downstream ray of current column |
| K | <ul style="list-style-type: none"> 4N-3, flux of axial momentum of species N 4N-2, flux of radial momentum of species N 4N-1, flux of energy of species N 4N, flux of mass of species N |
| SN(I) | sine of the angle between ray I and the negative z-axis ($1 \leq I \leq \text{IBMX}$); ($\sin \alpha_i$) |
| SORCE(K) | ($1 \leq K \leq 4 \cdot \text{NSPEC}$) |
| SORCE(4N-3) | z body-force on species N in cell being treated |

| | |
|-------------|--|
| SORCE(4N-2) | r body-force plus radial pressure balance on species N in cell being treated |
| SORCE(4N-1) | work and heat added to species N in cell being treated |
| SORCE(4N) | mass source of species N due to chemical reactions |
| SVOL(L) | volume swept out by arc J + 2 - L bounding cell J in current column during the time-step |
| T | time (t) |
| TBCD | time counter for BCD output |
| TBIN | time counter for binary restart output |
| TIBIN | time increment between which binary restart output is desired |
| TULT | time desired at end of run |
| UB(J) | velocity normal to itself of arc J in the current column ($1 \leq J \leq \text{MAXJ}$) |
| UFREE(L, N) | velocity of the free boundary on arc N of column I + L - 1 normal to itself ($1 \leq L \leq 2; 1 \leq N \leq \text{MAXJ}$) |
| UN(L, J, N) | if applied to an arc: velocity normal to arc J of species N in cell J + L - 2 of the current column; if applied to a ray: velocity normal to ray I of species N in cell J of column I + L - 2 ($1 \leq L \leq 2; 1 \leq J \leq \text{MAXJ}; 1 \leq N \leq \text{NSPEC}$) |
| UNB(N, L) | ($1 \leq N \leq \text{NSPEC}; 1 \leq L \leq 2$) |
| UNB(N, 1) | component normal to boundary of velocity of species N on the boundary currently being treated. |
| UNB(N, 2) | component normal to boundary of velocity of species N on first arc of next column downstream |
| UNBO(N) | component normal to boundary of velocity of species N on the boundary for a problem with constant boundary conditions ($1 \leq N \leq \text{NSPEC}$) |

| | |
|-------------|---|
| UR(L, J, N) | radial component of velocity of species N in cell J of column I + L - 1 ($1 \leq L \leq 2$; $1 \leq J \leq \text{MAXJ}$; $1 \leq N \leq \text{NSPEC}$) |
| USTBLY(L) | ($1 \leq L \leq 2$) |
| USTBLY(1) | maximum speed of a characteristic normal to an arc |
| USTBLY(2) | maximum speed of a characteristic normal to a ray |
| UT(L, J, N) | if applied to an arc: velocity tangential to arc J of species N in cell J + L - 2 of the current column; if applied to a ray: velocity tangential to ray I of species N in cell J of column I + L - 2 ($1 \leq L \leq 2$; $1 \leq J \leq \text{MAXJ}$; $1 \leq N \leq \text{NSPEC}$) |
| UTB(N, L) | ($1 \leq N \leq \text{NSPEC}$; $1 \leq L \leq 2$) |
| UTB(N, 1) | component tangential to boundary of velocity of species N on the boundary currently being treated |
| UTB(N, 2) | component tangential to boundary of velocity of species N on first arc of next column downstream |
| UTBO(N) | component tangential to boundary of velocity of species N on the boundary for a problem with constant boundary conditions ($1 \leq N \leq \text{NSPEC}$) |
| UZ(L, J, N) | axial component of velocity of species N in cell J of column I + L - 1 ($1 \leq L \leq 2$; $1 \leq J \leq \text{MAXJ}$; $1 \leq N \leq \text{NSPEC}$) |
| VNODE(L, J) | ($1 \leq L \leq 3$; $1 \leq J \leq \text{MAXJ}$) |
| VNODE(1, J) | velocity along ray I of the node formed by the intersection of ray I and arc J in column I |
| VNODE(2, J) | velocity along ray I + 1 of the node formed by the intersection of ray I + 1 and arc J in column I |
| VNODE(3, J) | velocity along ray I + 1 of the node formed by the intersection of ray I + 1 and arc J in column I + 1 |

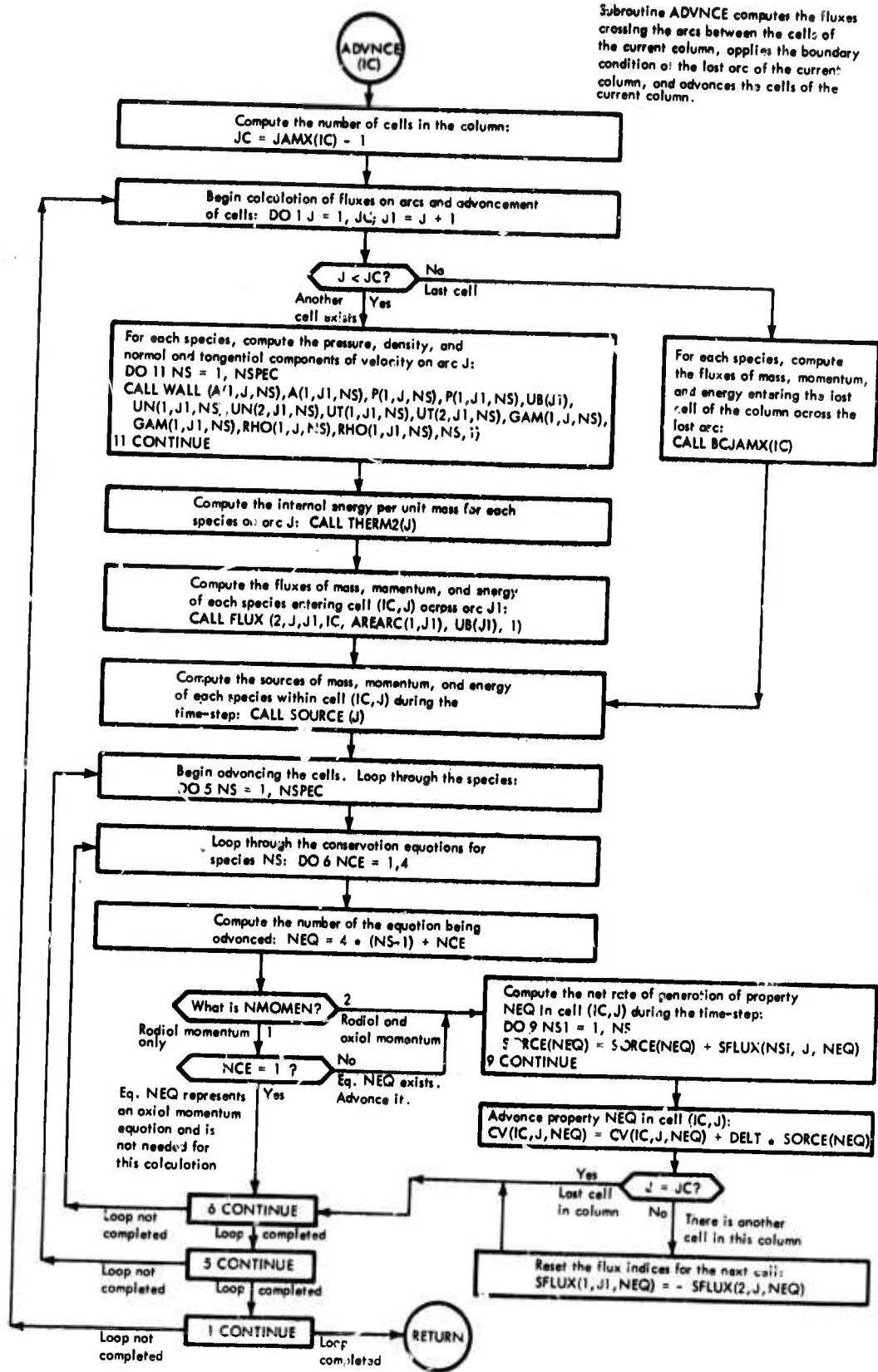


Figure 11. Flow Chart of Subroutine ADVANCE

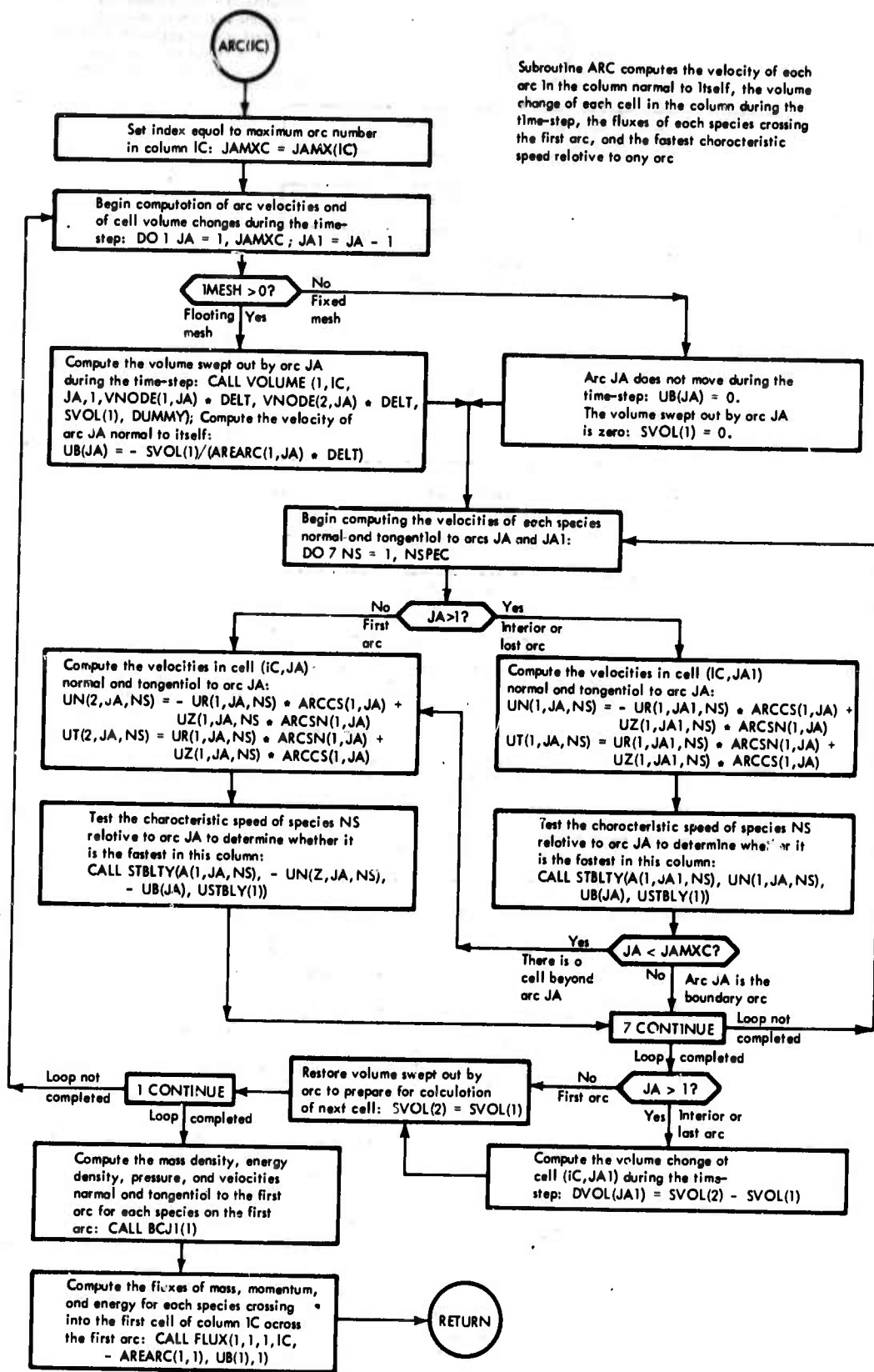


Figure 12. Flow Chart of Subroutine ARC

Subroutine ARCGEO computes the length of a given arc, the sine and cosine of the angle which the arc makes with the positive Z axis, and the area of the cell face formed by the arc.

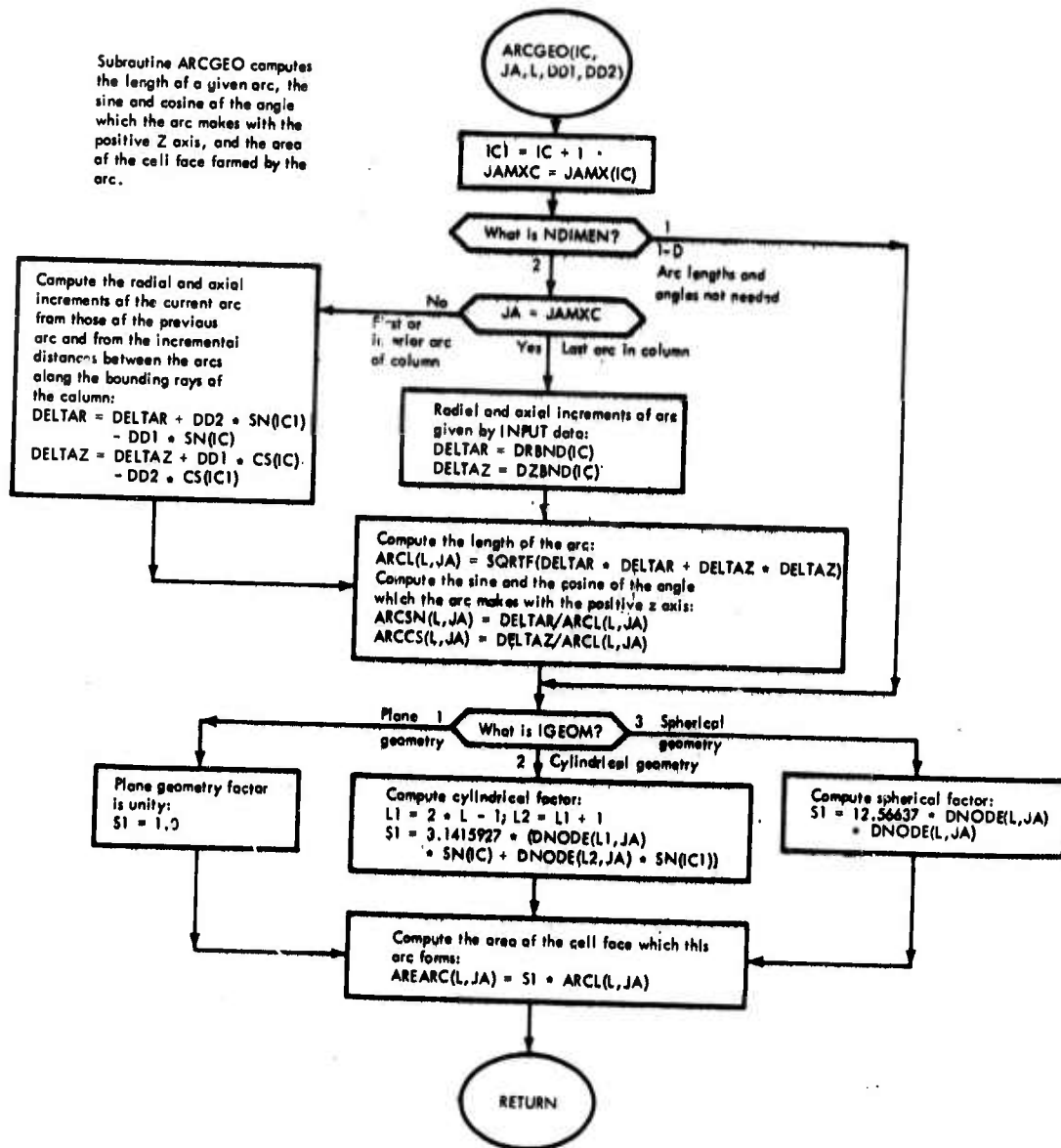


Figure 13. Flow Chart of Subroutine ARCGEO

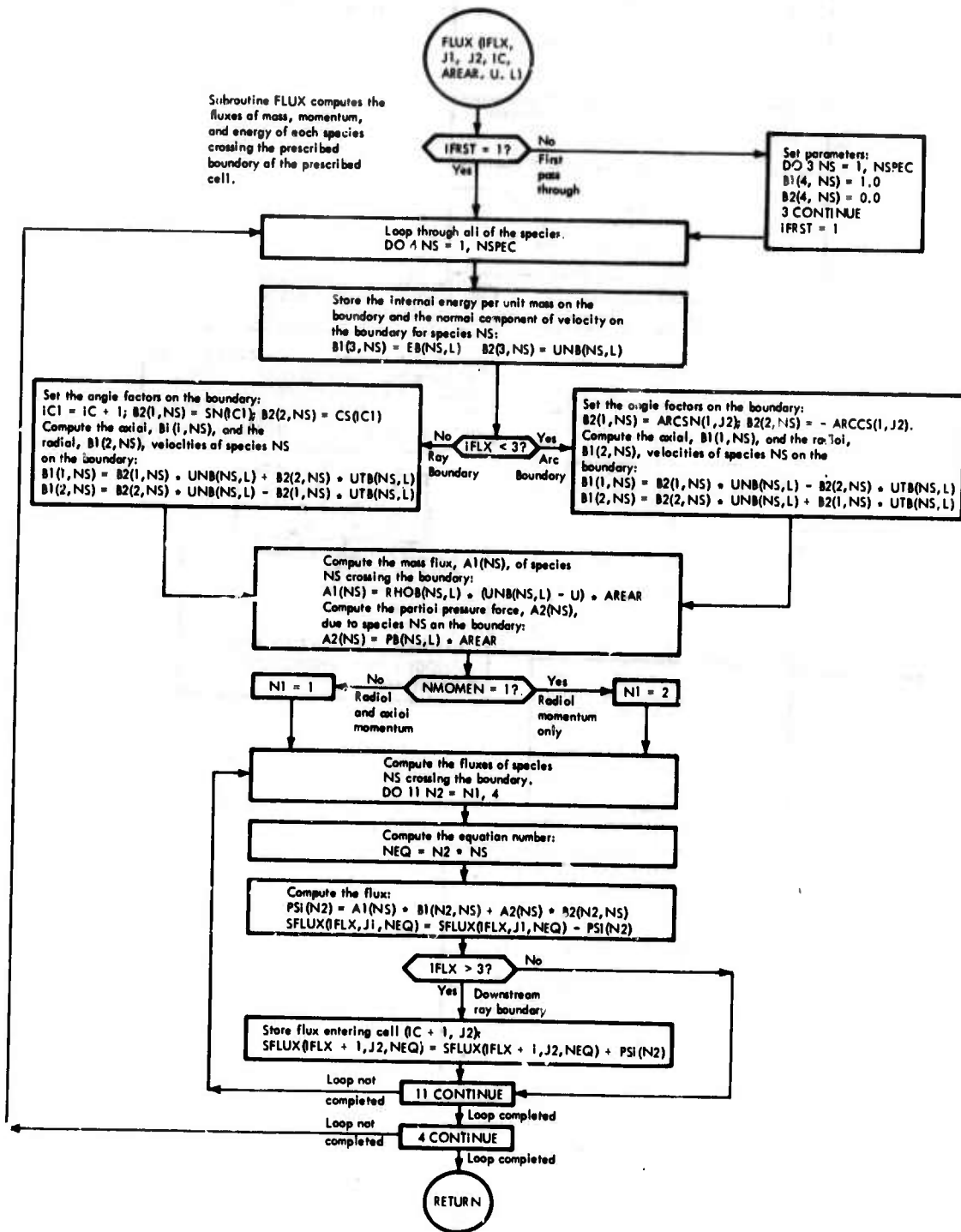


Figure 16. Flow Chart of Subroutine FLUX

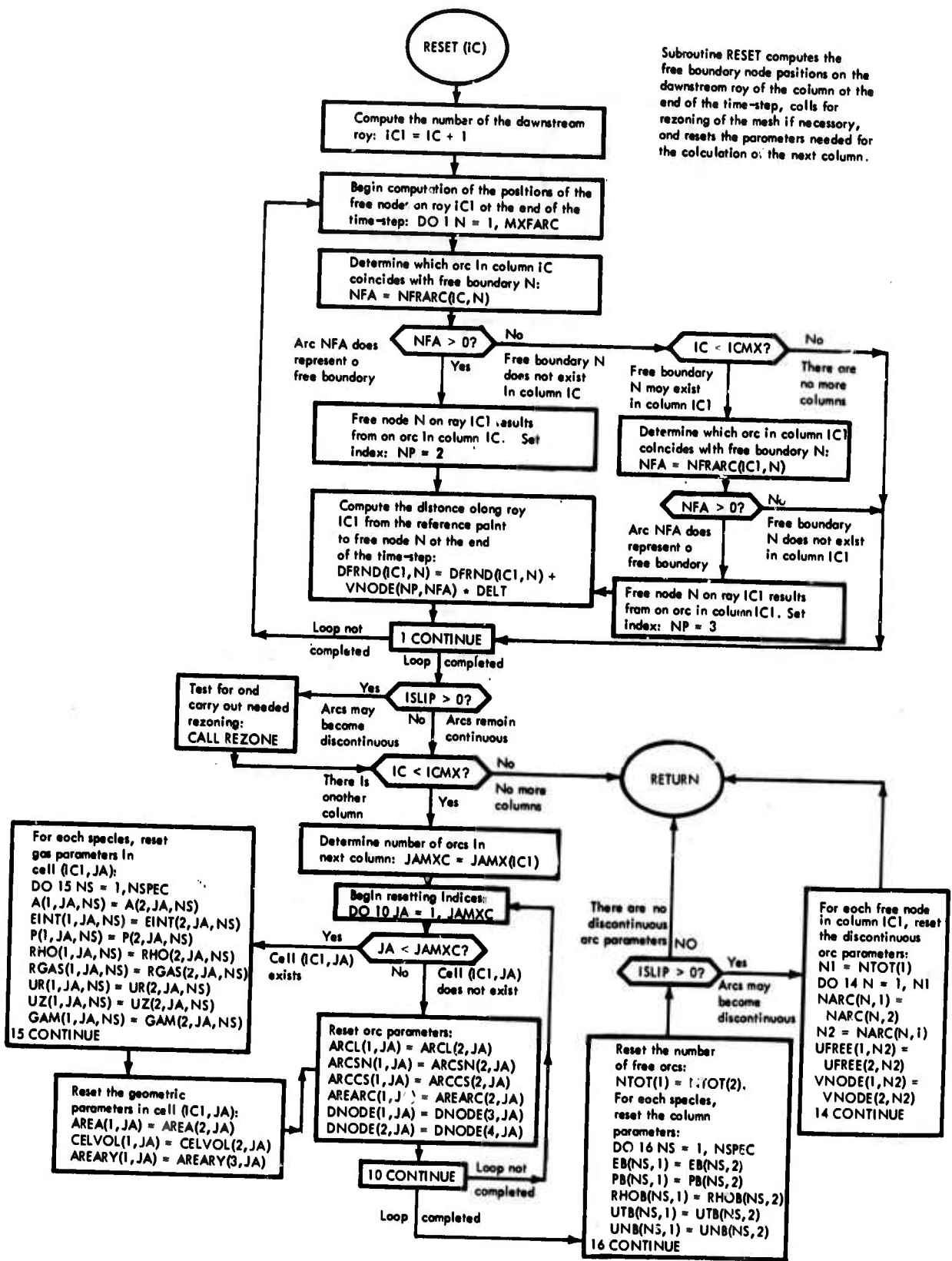


Figure 19. Flow Chart of Subroutine RESET

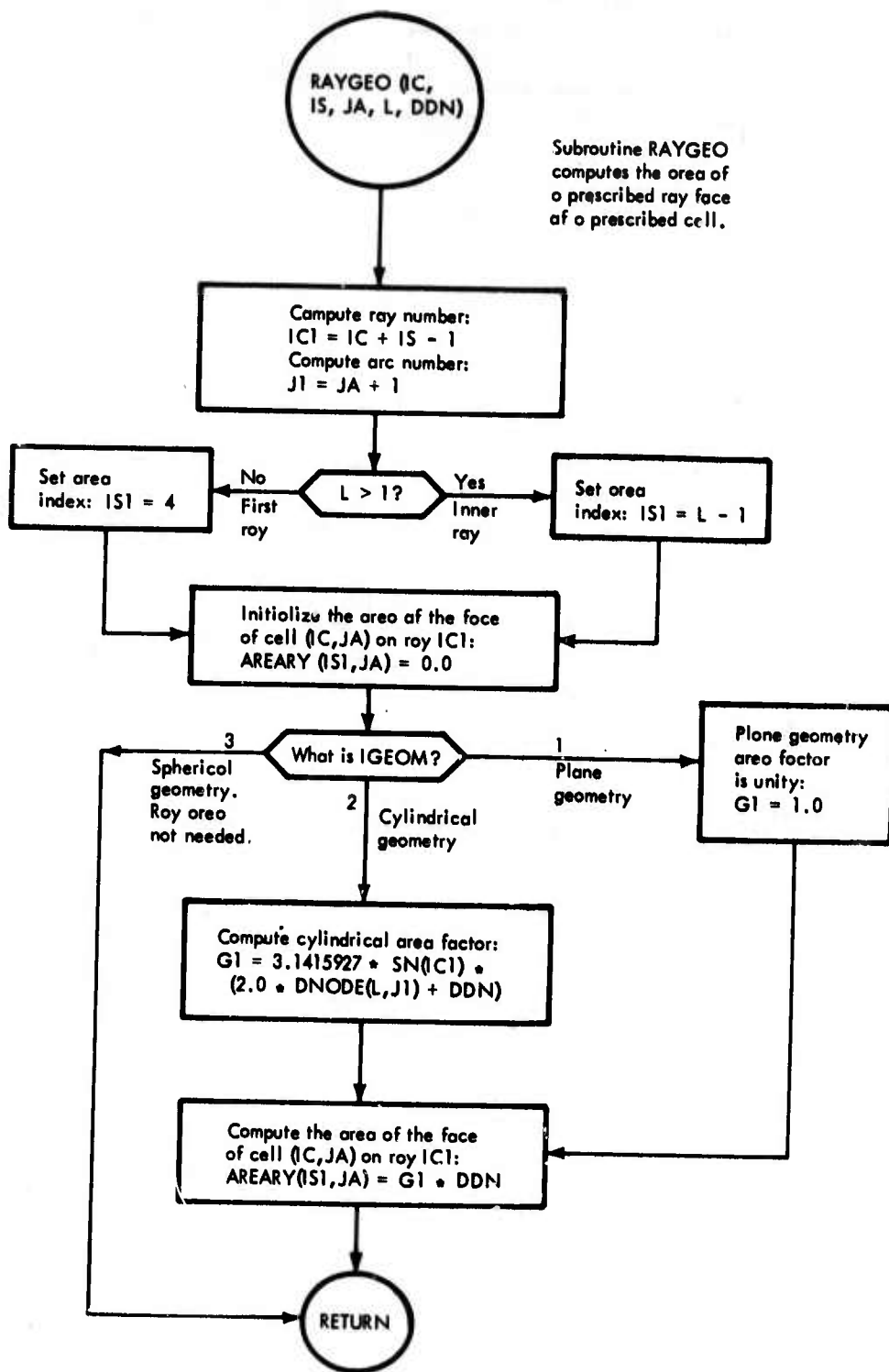
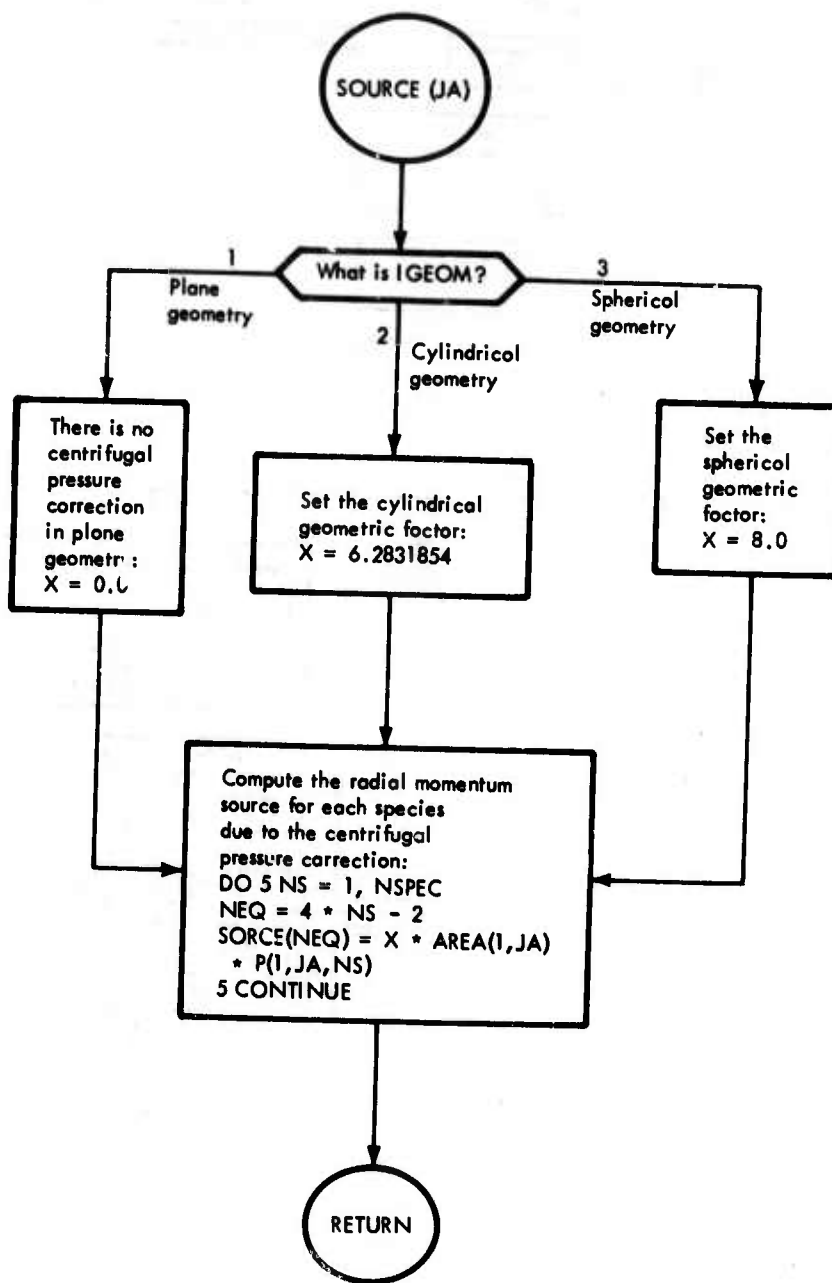


Figure 20. Flow Chart of Subroutine RAYGEO



Subroutine SOURCE computes the sources of mass, momentum, and energy for each species within the given cell. This version of the subroutine is for a chemically inert mixture of gases which do not collide with each other.

Figure 21. Flow Chart of Subroutine SOURCE

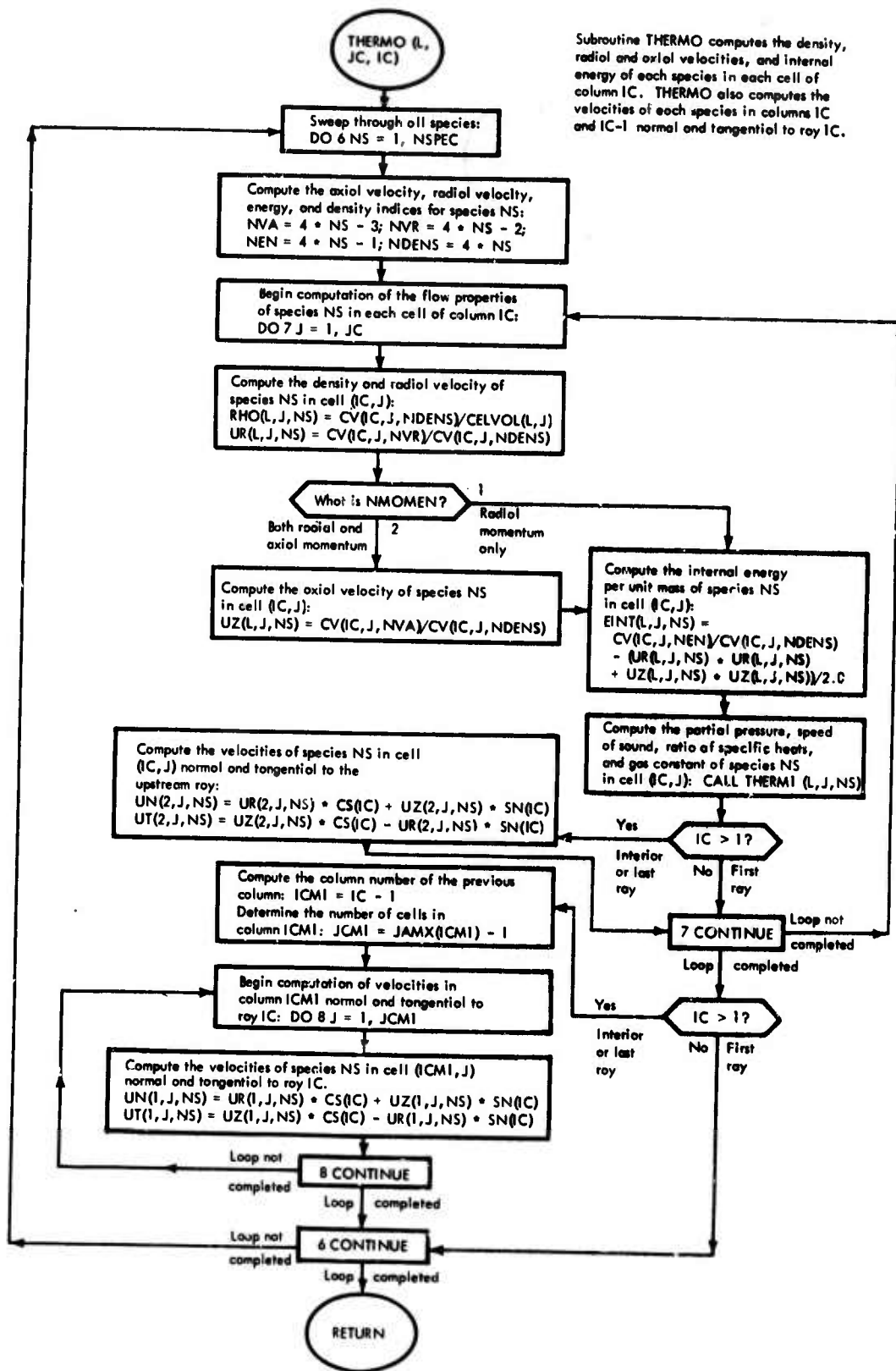


Figure 22. Flow Chart of Subroutine THERMO

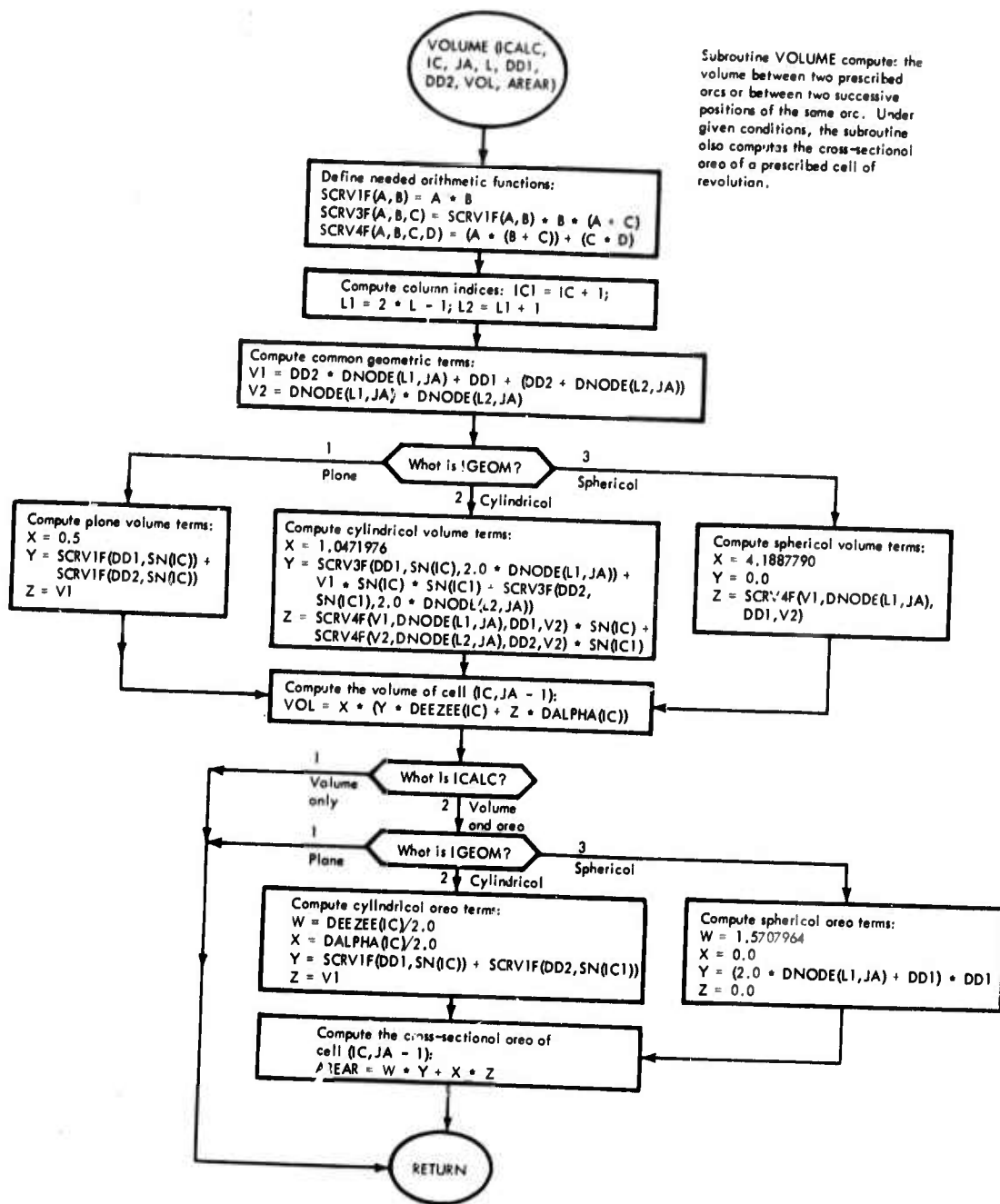


Figure 23. Flow Chart of Subroutine VOLUME

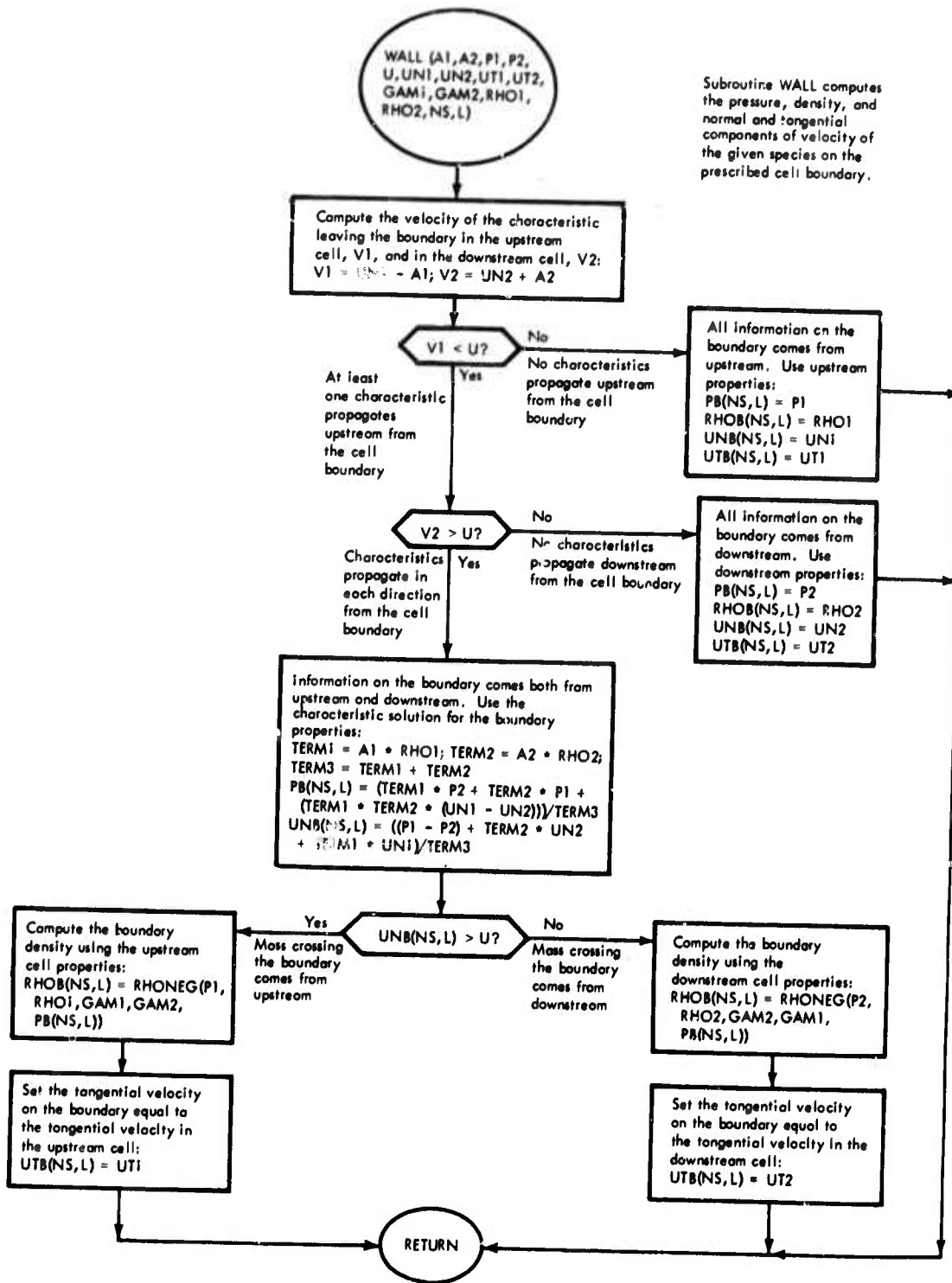


Figure 24. Flow Chart of Subroutine WALL

(This Page is Intentionally Left Blank)

APPENDIX III

EQUATIONS OF RADIATION TRANSPORT

1. GENERAL EQUATIONS

The equations of radiation transport may be derived in the same manner as the equations of hydrodynamics (Appendix I). Thus, the photon distribution function, $f_{R\nu_*}(\vec{r}_*, \vec{c}_*, t_*)$, denotes the number density of photons at point (\vec{r}_*, t_*) having velocities in the increment $d\vec{c}_*$ about \vec{c}_* and frequencies in the increment $d\nu_*$ about ν_* (the subscript asterisks denote quantities with physical dimensions). The number density of photons at point (\vec{r}_*, t_*) is then

$$n_{R\nu_*} = \int f_{R\nu_*}(\vec{r}_*, \vec{c}_*, t_*) d\vec{c}_* \quad (230)$$

where the integration is carried out over all velocity space. The total number density of photons of all frequencies is

$$n_{R*} = \int_0^\infty n_{R\nu_*} d\nu_* \quad (231)$$

Since the energy carried by a photon is $h_*\nu_*$, the total radiative energy density at point (\vec{r}_*, t_*) is

$$e_{R*} = \int_0^\infty h_*\nu_* n_{R\nu_*} d\nu_* \quad (232)$$

In equilibrium, however, it can be shown that the value of e_{R*} is (Section 4 of Chapter XI, Reference 2)

$$e_{R*} = 4\sigma_* T_*^4 / c_* \quad (233)$$

Thus, an appropriately normalized radiative energy density is

$$e_R = \frac{e_{R*}}{4\sigma_* T_*^4 / c_*} \quad (234)$$

The energy density of photons of frequency ν_* , $e_{R\nu_*}$, may be defined by the relation

$$e_{R*} = \int_0^\infty e_{R\nu_*} d\nu_* \quad (235)$$

Defining the normalized value of $e_{R\nu}$ by the relation

$$e_R = \int_0^\infty e_{R\nu} d\nu \quad (236)$$

and using Equations 232 through 236, there results

$$e_{R\nu} = \frac{h_* \nu_* n_{R\nu_*}}{4\sigma_* T_*^4 / c_* \nu_{R*}} \quad (237)$$

The radiant heat flux vector at point (\vec{r}_*, t_*) is defined as

$$\vec{Q}_{R*} = \int_0^\infty d\nu_* \int d\vec{c}_* h_* \nu_* \vec{c}_* f_{R\nu_*} \quad (238)$$

By direct comparison with Equations 232 and 234, the appropriate normalization for \vec{Q}_R is seen to be

$$\vec{Q}_R = \frac{\vec{Q}_{R*}}{4\sigma_* T_*^4} \quad (239)$$

Proceeding as in Equations 235 through 237, the normalized heat flux vector for photons of frequency ν_* is seen to be

$$\vec{Q}_{R\nu} = \frac{\int h_* \nu_* \vec{c}_* f_{R\nu*} d\vec{c}_*}{4\sigma_* T_*^4 / \nu R_*} \quad (240)$$

Definitions 230 , 237 , and 240 involve moments of the photon distribution function. This distribution function is given by a Boltzmann-like equation similar to the Boltzmann equation in Appendix I; since photons cannot accelerate, however, the form of the equation for photons is slightly simpler. As derived in Reference 2 (Section 3 of Chapter XI), the equation for the photon distribution function is

$$\frac{\partial}{\partial t_*} f_{R\nu*} + \vec{c}_* \cdot \vec{\nabla}_* f_{R\nu*} = \left(\frac{\partial f_{R\nu*}}{\partial t_*} \right)_{\text{interactions}} \quad (241)$$

where the term $\left(\frac{\partial f_{R\nu*}}{\partial t_*} \right)_{\text{interactions}}$ accounts for all changes in the distribution function due to scattering, absorption, and emission.

Integrating Equation 241 over all values of \vec{c}_* ,

$$\int \frac{\partial}{\partial t_*} f_{R\nu*} d\vec{c}_* + \int \vec{\nabla}_* \cdot f_{R\nu*} \vec{c}_* d\vec{c}_* = \int \left(\frac{\partial f_{R\nu*}}{\partial t_*} \right)_{\text{interactions}} d\vec{c}_* \quad (242)$$

where

$$\vec{\nabla}_* \cdot \vec{c}_* = 0 \quad (243)$$

because \vec{r}_* and \vec{c}_* are independent variables. Interchanging the differential and integral operators and normalizing according to Equation 237 , Equation 242 gives

$$\frac{\partial e_{R\nu}}{\partial t} + c \vec{\nabla} \cdot \vec{Q}_{R\nu} = \left(\frac{\partial e_{R\nu}}{\partial t} \right)_{\text{interactions}} \quad (244)$$

Taking the first moment of Equation 241 by multiplying by \vec{c}_* and integrating over \vec{c}_* gives

$$\frac{\partial}{\partial t_*} \int \vec{c}_* f_{R\nu_*} d\vec{c}_* + \vec{\nabla}_* \cdot \int \vec{c}_* \vec{c}_* f_{R\nu_*} d\vec{c}_* = \left(\frac{\partial}{\partial t_*} \int \vec{c}_* f_{R\nu_*} d\vec{c}_* \right)_{\text{interactions}} \quad (245)$$

Multiplying by $h_* \nu_* \nu_{R_*}$, dividing by $4\sigma_* T_*^4$, and using Equation 240 gives

$$\frac{\partial}{\partial t_*} \vec{Q}_{R\nu} + \vec{\nabla}_* \cdot \frac{\int \vec{c}_* \vec{c}_* h_* \nu_* f_{R\nu_*} d\vec{c}_*}{4\sigma_* T_*^4 / \nu_{R_*}} = \left(\frac{\partial}{\partial t_*} \vec{Q}_{R\nu} \right)_{\text{interactions}} \quad (246)$$

The radiative pressure tensor is defined as (Equation 2.13, Chapter XI, Reference 2)

$$\vec{\vec{P}}_{R\nu_*} = \int h_* \nu_* f_{R\nu_*} \frac{\vec{c}_* \vec{c}_*}{c_*} d\vec{c}_* \quad (247)$$

where

$$c_* = |\vec{c}_*| \quad (248)$$

Since pressure is an energy density, it is convenient to normalize $\vec{\vec{P}}_{R\nu}$ in the same fashion as $e_{R\nu}$; thus, as in Equation 237,

$$\vec{\vec{P}}_{R\nu} = \frac{\vec{\vec{P}}_{R\nu_*}}{4\sigma_* T_*^4 / c_* \nu_{R_*}} \quad (249)$$

Introducing Equation 249 into Equation 246

$$\frac{\partial \vec{Q}_{R\nu}}{\partial t} + \frac{L_*}{U_*} \vec{\nabla}_* \cdot \vec{\vec{P}}_{R\nu} c_* = \left(\frac{\partial \vec{Q}_{R\nu}}{\partial t} \right)_{\text{interactions}}$$

or

$$\frac{\partial \vec{Q}_{R\nu}}{\partial t} + c \vec{\nabla} \cdot \vec{\vec{P}}_{R\nu} = \left(\frac{\partial \vec{Q}_{R\nu}}{\partial t} \right)_{\text{interactions}} \quad (250)$$

2. SPECIFIC TERMS

a. Interaction Terms

The interaction terms on the right-hand side of Equations 244 and 250 represent sources of radiative energy and heat flux due to absorption, emission, and scattering. These terms depend upon the properties of the material through which the photons are propagating, and can be expressed in terms of absorption, emission, and scattering coefficients. The following discussion of these effects is based upon Reference 19 (Sections 3 through 5).

b. Absorption

The volume rate at which species α absorbs photons of frequency ν is given by the product of the photon flux, $c_* f_{R\nu_*}$; the absorption coefficient per unit mass, $\kappa_{\nu\alpha_*}$; and the density, ρ_{α_*} :

$$\left(\frac{\partial}{\partial t_*} f_{R\nu_*}\right)_{\text{abs}} = - \sum_{\alpha} \rho_{\alpha_*} \kappa_{\nu\alpha_*} c_* f_{R\nu_*} \quad (251)$$

Multiplying by $h_* \nu_*$, integrating over velocity directions, and using Equations 230 and 237 gives

$$\left(\frac{\partial e_{R\nu}}{\partial t}\right)_{\text{abs}} = - \frac{L_*}{U_*} \sum_{\alpha} \rho_{\alpha_*} \kappa_{\nu\alpha_*} c_* e_{R\nu} \quad (252)$$

Introducing the Bouguer number,

$$B_u = \rho_* \kappa_* L_* \quad (253)$$

where κ_* is a reference absorption coefficient, Equation 252 becomes

$$\left(\frac{\partial e_{R\nu}}{\partial t}\right)_{\text{abs}} = -c B_u e_{R\nu} \sum_{\alpha} \rho_{\alpha} \kappa_{\nu\alpha} \quad (254)$$

Treating the heat flux vector similarly,

$$\begin{aligned} \left(\frac{\partial \vec{Q}_{R\nu}}{\partial t}\right)_{\text{abs}} &= -\frac{L_*}{U_*} \frac{\int h_* \nu_* \vec{c}_* f_{R\nu_*} d\vec{c}_*}{4\sigma_* T_*^4 / \nu R_*} \sum_{\alpha} \rho_{\alpha_*} \kappa_{\nu\alpha_*} c_* \\ &= -c B_u \vec{Q}_{R\nu} \sum_{\alpha} \rho_{\alpha} \kappa_{\nu\alpha} \end{aligned} \quad (255)$$

c. Spontaneous Emission

The rate at which unit mass of species α emits energy at frequency ν in the direction \vec{c}_* is given by the emission coefficient, $\bar{j}_{\nu\alpha_*}$. Thus,

$$\frac{\partial}{\partial t_*} (f_{R\nu_*} h_* \nu_*)_{\text{sp em}} = \sum_{\alpha} \rho_{\alpha_*} \bar{j}_{\nu\alpha_*} \quad (256)$$

Integrating Equation 256 over all \vec{c}_* , dividing by $4\sigma_* T_*^4 / c_* \nu R_*$, and using Equations 230 and 237 gives

$$\left(\frac{\partial e_{R\nu}}{\partial t}\right)_{\text{sp em}} = \frac{L_*}{U_*} \frac{\sum_{\alpha} \rho_{\alpha_*} j_{\nu\alpha_*}}{4\sigma_* T_*^4 / c_* \nu R_*} \quad (257)$$

where

$$j_{\nu\alpha_*} = \int \bar{j}_{\nu\alpha_*} d\vec{c}_* \quad (258)$$

in the net rate of emission of radiant energy at frequency ν per unit mass of species α . Defining

$$j_{\nu\alpha} = \frac{j_{\nu\alpha*}}{4\kappa_*\sigma_*T_*^4/c_*\nu R_*} \quad (259)$$

and using Equation 253 , there results

$$\left(\frac{\partial e_{R\nu}}{\partial t}\right)_{\text{sp em}} = c B_u \sum_{\alpha} \rho_{\alpha} j_{\nu\alpha} \quad (260)$$

If $\bar{j}_{\nu\alpha*}$ is not a function of the direction of energy emission, as seems reasonable for spontaneous emission, there will be no net direction of the emitted energy; thus, there is no change in the heat-flux vector due to spontaneous emission:

$$\left(\frac{\partial \vec{Q}_{R\nu}}{\partial t}\right)_{\text{sp em}} = 0 \quad (261)$$

d. Induced Emission

The rate per unit volume at which species α is stimulated into emitting photons of frequency ν_* in the direction \vec{c}_* is given by the product of the photon flux, $c_* f_{R\nu_*}$; the coefficient of induced emission per unit mass, $J_{\nu\alpha*}$; and the density, $\rho_{\alpha*}$:

$$\left(\frac{\partial f_{R\nu_*}}{\partial t_*}\right)_{\text{In em}} = \sum_{\alpha} \rho_{\alpha*} J_{\nu\alpha*} c_* f_{R\nu_*} \quad (262)$$

Equation (262) is similar to Equation 251 for absorption; thus, by analogy with Equations 254 and 255 ,

$$\left(\frac{\partial e_{R\nu}}{\partial t}\right)_{\text{In em}} = c B_u e_{R\nu} \sum_{\alpha} \rho_{\alpha} J_{\nu\alpha} \kappa_{\nu\alpha} \quad (263)$$

and

$$\left(\frac{\partial \vec{Q}_{R\nu}}{\partial t}\right)_{\text{In em}} = c B_u \vec{Q}_{R\nu} \sum_{\alpha} \rho_{\alpha} J_{\nu\alpha} \kappa_{\nu\alpha} \quad (264)$$

e. Scattering

Since scattering changes the direction of a photon but does not involve the absorption of energy, it cannot change the radiative energy density at a point:

$$\left(\frac{\partial e_{R\nu}}{\partial t}\right)_{\text{scat}} = 0 \quad (265)$$

The effect of scattering on the heat-flux vector may be determined by considerations similar to those for absorption. The differential rate at which photons of frequency ν_* are scattered by solid angle ω out of direction \vec{c}_* by species α is defined as

$$d\left(\frac{\partial f_{R\nu_*}}{\partial t_*}\right)_{\text{scat}} = -\sum_{\alpha} c_* f_{R\nu_*} \rho_{\alpha} \bar{S}_{\nu\alpha_*}(\omega) d\omega \quad (266)$$

where $\bar{S}_{\nu\alpha_*}(\omega)$ is the cross section for scattering one photon through the solid angle ω . The net heat-flux loss from direction c_* is thus

$$\begin{aligned} \left(\frac{\partial}{\partial t} f_{R\nu_*} h_* \nu_* \vec{c}_*\right)_{\text{scat}} &= -c_* h_* \nu_* \vec{c}_* \sum_{\alpha} \rho_{\alpha} f_{R\nu_*} \int \bar{S}_{\nu\alpha_*}(\omega) d\omega \\ &= -c_* h_* \nu_* f_{R\nu_*} \vec{c}_* \sum_{\alpha} \rho_{\alpha} S_{\nu\alpha_*} \end{aligned} \quad (267)$$

where

$$S_{\nu\alpha_*} = \int \bar{S}_{\nu\alpha_*}(\omega) d\omega \quad (268)$$

is the cross section for scattering a photon into any direction. Integrating Equation 267 over all \vec{c}_* and using Equation 240

$$\begin{aligned} \left(\frac{\partial \vec{Q}_{R\nu}}{\partial t}\right)_{\text{scat}} &= -\frac{L_*}{U_*} \frac{c_* h_* \nu_* \sum_{\alpha} \rho_{\nu} S_{\nu\alpha} \int f_{R\nu} \vec{c}_* d\vec{c}_*}{4\sigma_* T_*^4 / \nu R_*} \\ &= -c B_u \vec{Q}_{R\nu} \sum_{\alpha} \rho_{\alpha} S_{\nu\alpha} \kappa_{\nu\alpha} \end{aligned} \quad (269)$$

Equation 269 shows that scattering cannot change the direction of the heat-flux vector. Thus, the radiative energy approaching a scattering region may be divided into pencils of radiation coming from many different directions; Equation 269 shows that each of these pencils will be attenuated by the same attenuation constant, $c B_u \sum_{\alpha} \rho_{\alpha} S_{\nu\alpha} \kappa_{\nu\alpha}$. Consequently, the ratio of the number of photons in any one pencil to the number in any other pencil will be unchanged as a result of the scattering. The net heat-flux vector, therefore, will not change direction as a result of the scattering.

f. Final Equations

Combining Equations 244, 254, 260, 263, and 265 gives the equation for the radiative energy density:

$$\frac{1}{c} \frac{\partial e_{R\nu}}{\partial t} + \vec{\nabla} \cdot \vec{Q}_{R\nu} = -B_u \sum_{\alpha} \rho_{\alpha} \left[\kappa_{\nu\alpha} e_{R\nu} (1 - J_{\nu\alpha}) - j_{\nu\alpha} \right] \quad (270)$$

Similarly, combining Equations 250, 255, 261, and 269 gives the equation for the radiative heat-flux vector:

$$\frac{1}{c} \frac{\partial \vec{Q}_{R\nu}}{\partial t} + \vec{\nabla} \cdot \vec{P}_{R\nu} = -B_u \vec{Q}_{R\nu} \sum_{\alpha} \rho_{\alpha} \kappa_{\nu\alpha} (1 - J_{\nu\alpha} + S_{\nu\alpha}) \quad (271)$$

g. Energy Absorbed by One Species

The net rate at which radiant energy is absorbed into internal energy of species α is obtained by integrating Equations 254, 260, and 263 over all frequencies:

$$\left(\frac{\partial e_R}{\partial t}\right)_{\text{abs by } \alpha} = c B_u \rho_\alpha \int \left[e_{R\nu}^\alpha (1 - J_{\nu\alpha}) - j_{\nu\alpha} \right] d\nu \quad (272)$$

as written in Equation 272, the radiative energy density is normalized with respect to radiative parameters; that is, the normalization is as shown in Equation 234. The hydrodynamic energy density, however, is normalized by the term $\rho_* U_*^2$. Changing the normalization of Equation 272 accordingly,

$$\begin{aligned} \left(\frac{\partial e_R}{\partial t}\right)_{\text{abs by } \alpha} &= \frac{4\sigma_* T_*^4 / c_*}{\rho_* U_*^2} c B_u \int \left[e_{R\nu}^\alpha (1 - J_{\nu\alpha}) - j_{\nu\alpha} \right] d\nu \\ &= B_o B_u \int \left[e_{R\nu}^\alpha (1 - J_{\nu\alpha}) - j_{\nu\alpha} \right] d\nu \end{aligned} \quad (273)$$

where

$$B_o = \frac{4\sigma_* T_*^4}{\rho_* U_*^3} \quad (274)$$

is the Boltzmann number.

APPENDIX IV
MAXWELL'S EQUATIONS

For convenient computational application to a wide variety of problems, Maxwell's equations must be normalized into a form which can be related to a similarly wide variety of initial conditions.

1. RATIONALIZED MKS UNITS

Maxwell's equations in rationalized mks units are given in Table I-1 of Reference 20 as

$$\epsilon_{0*} \vec{\nabla}_* \cdot \vec{E}_* = q_* \quad (275)$$

$$\vec{\nabla}_* \cdot \vec{B}_* = 0 \quad (276)$$

$$\vec{\nabla}_* \times \vec{E}_* = - \frac{\partial \vec{B}_*}{\partial t_*} \quad (277)$$

and

$$\vec{\nabla}_* \times \vec{B}_* = \mu_{0*} \left(\vec{j}_* + \epsilon_{0*} \frac{\partial \vec{E}_*}{\partial t_*} \right) \quad (278)$$

Equations 275 through 278 are to be normalized into a form convenient for studying the flow of ionized gases. For this purpose, the reference for the charge density is taken as the reference particle density multiplied by the charge of the electron, and the reference electric field intensity is taken as the field intensity which this reference charge density would generate if divided into positive and negative charges separated by a Debye length. Since the Debye length represents the distance of charge separation at which the energy density of the electric

field equals the energy density of the thermal motion, it is felt that this choice of normalization will yield a nondimensional electric field of order unity throughout the gas. The magnetic flux-density is then normalized by equating the energy density of the reference magnetic flux-density to that of the reference electric field intensity.

The reference charge density, q_{R*} , is thus

$$q_{R*} = N_* q_{e*} \quad (279)$$

Assuming that the length scale for variations in the electric field is the Debye length, L_{D*} , Equation 275 gives

$$\epsilon_{o*} \frac{E_*}{L_{D*}} = q_{R*} \quad (280)$$

or

$$E_* = \frac{N_* q_{e*} L_{D*}}{\epsilon_{o*}} \quad (281)$$

The Debye length can be estimated by equating the energy density of the field E_* to the thermal energy density of a gas without internal structure at a characteristic temperature T_* :

$$\frac{\epsilon_{o*} E_*^2}{2} = \frac{3}{2} N_* k_* T_* \quad (282)$$

Substituting Equation 281 into Equation 282 and solving for L_{D*} gives

$$L_{D*} = \left(\frac{3k_* T_* \epsilon_{o*}}{N_* q_{e*}^2} \right)^{1/2} \quad (283)$$

The reference magnetic flux-density is now computed by equating the energy density of the reference electric field intensity to that of the reference magnetic flux-density:

$$\frac{B_*^2}{2\mu_{o*}} = \frac{\epsilon_{o*} E_*^2}{2}$$

or

$$B_* = E_* (\mu_{o*} \epsilon_{o*})^{1/2} \quad (284)$$

Applying normalizations 279 and 280 to Equation 275 ,

$$\frac{\epsilon_{o*}}{L_*} \vec{\nabla} \cdot \vec{E} \frac{N_* q_{e*} L_{D*}}{\epsilon_{o*}} = q N_* q_{e*}$$

or

$$\vec{\nabla} \cdot \vec{E} = \mathcal{L} q \quad (285)$$

where

$$\mathcal{L} = L_* / L_{D*} \quad (286)$$

Similarly, Equation 276 becomes

$$\vec{\nabla} \cdot \vec{B} = 0 \quad (287)$$

Using normalizations 281 and 284 in Equation 277 gives

$$\frac{E_*}{L_*} \vec{\nabla} \times \vec{E} = - \frac{E_*}{c_*} \frac{U_*}{L_*} \frac{\partial \vec{B}}{\partial t}$$

or

$$\vec{\nabla} \times \vec{E} = - \frac{1}{c} \frac{\partial \vec{B}}{\partial t} \quad (288)$$

Choosing

$$\vec{j}_* = N_* q_{e*} U_* \quad (289)$$

as the reference current density, Equation 278 becomes

$$\frac{\vec{\nabla}}{L_*} \times \frac{N_* q_{e*} L_{D*}}{\epsilon_{o*} c_*} \vec{B} = \mu_{o*} \left(N_* q_{e*} U_* \vec{j} + \frac{N_* q_{e*} L_{D*} U_*}{L_*} \frac{\partial \vec{E}}{\partial t} \right)$$

or

$$\vec{\nabla} \times \vec{B} = \frac{\mathcal{L} \vec{j}}{c} + \frac{1}{c} \frac{\partial \vec{E}}{\partial t} \quad (290)$$

2. GAUSSIAN UNITS

Maxwell's equations in Gaussian units with the current density measured in esu are given in Table I-1 of Reference 20 as

$$\vec{\nabla}_* \cdot \vec{E}_* = 4\pi q_* \quad (291)$$

$$\vec{\nabla}_* \cdot \vec{B}_* = 0 \quad (292)$$

$$\vec{\nabla}_* \times \vec{E}_* = -\frac{1}{c_*} \frac{\partial \vec{B}_*}{\partial t_*} \quad (293)$$

$$\vec{\nabla}_* \times \vec{B}_* = \frac{4\pi \vec{j}_*}{c_*} + \frac{1}{c_*} \frac{\partial \vec{E}_*}{\partial t_*} \quad (294)$$

As for the rationalized mks units, the reference charge density is defined as

$$q_{R*} = N_* q_{e*} \quad (295)$$

For the reference electric field intensity, Equation 291 then gives

$$\begin{aligned}
 E_* &= 4\pi N_* q_{e*} L_{D*} \\
 &= \frac{N_* q_{e*} L_{D*}}{\epsilon_{o*}}
 \end{aligned}
 \tag{296}$$

if

$$\epsilon_{o*} = \frac{1}{4\pi}
 \tag{297}$$

in Gaussian units.

Equating the energy density of the reference electric field to the reference thermal energy density of the gas,

$$\frac{E_*^2}{8\pi} = \frac{3}{2} N_* k_* T_*
 \tag{298}$$

Substituting from Equation 296 and solving for L_{D*} ,

$$\begin{aligned}
 L_{D*} &= \left(\frac{3 k_* T_*}{4\pi N_* q_{e*}^2} \right)^{1/2} \\
 &= \left(\frac{3 k_* T_* \epsilon_{o*}}{N_* q_{e*}^2} \right)^{1/2}
 \end{aligned}
 \tag{299}$$

Computing the reference magnetic flux-density by equating the energy density of the reference electric field to that of the reference magnetic field,

$$\frac{B_*^2}{8\pi} = \frac{E_*^2}{8\pi}$$

or

$$B_* = E_* (\mu_{o*} \epsilon_{o*})^{1/2}
 \tag{300}$$

if

$$\mu_{0*} = 4\pi \quad (301)$$

in Gaussian units.

Applying normalizations 295 and 296 to Equation 291 ,

$$\vec{\nabla} \cdot \vec{E} = \Sigma q \quad (302)$$

Similarly, Equation 292 becomes

$$\vec{\nabla} \cdot \vec{B} = 0 \quad (303)$$

Using normalizations 296 and 300 in Equation 293 gives

$$\frac{\vec{\nabla}}{L_*} \times \vec{E} E_* = - \frac{1}{c_*} E_* \frac{U_*}{L_*} \frac{\partial \vec{B}}{\partial t}$$

or

$$\vec{\nabla} \times \vec{E} = - \frac{1}{c} \frac{\partial \vec{B}}{\partial t} \quad (304)$$

Choosing

$$j_* = N_* q_{e*} U_* \quad (305)$$

as the reference current density, Equation 294 becomes

$$\frac{\vec{\nabla}}{L_*} \times E_* \vec{B} = \frac{4\pi N_* q_{e*}}{c} \vec{j} + \frac{E_*}{c L_*} \frac{\partial \vec{E}}{\partial t}$$

or

$$\vec{\nabla} \times \vec{B} = \frac{\Sigma \vec{j}}{c} + \frac{1}{c} \frac{\partial \vec{E}}{\partial t} \quad (306)$$

3. FORCE AND WORK TERMS

Normalized expressions also are required for the force exerted on and the work done to a charged particle by the electromagnetic fields.

In rationalized mks units, the force on a charged particle is (Table I-1, Reference 20)

$$\vec{F}_{\alpha*}^{\downarrow} = q_{\alpha*} (\vec{E}_{*} + \vec{u}_{\alpha*} \times \vec{B}_{*}) \quad (307)$$

and the work done on the particle is

$$\vec{F}_{\alpha*}^{\downarrow} \cdot \vec{u}_{\alpha*} = q_{\alpha*} \vec{E}_{*} \cdot \vec{u}_{\alpha*} \quad (308)$$

The force is normalized with respect to mechanical units:

$$\vec{F}_{\alpha}^{\downarrow} = \frac{\vec{F}_{\alpha*}^{\downarrow}}{(M_* U_*^2 / L_*)} \quad (309)$$

Inserting normalizations 281, 284 and 309 into Equation 307 gives

$$\vec{F}_{\alpha}^{\downarrow} = \frac{N_* q_{e*} L_* E_*}{\rho_* U_*^2} q_{\alpha} \left[\vec{E} + U_* \vec{U}_{\alpha} \times \vec{B} (\mu_{o*} \epsilon_{o*})^{1/2} \right] \quad (310)$$

Using the fact that

$$\mu_{o*} \epsilon_{o*} = \frac{1}{c_*^2} \quad (311)$$

in rationalized mks units, Equation 310 becomes

$$\vec{F}_{\alpha}^{\downarrow} = \frac{q_{\alpha}}{m} \left(\vec{E} + \frac{\vec{u}_{\alpha} \times \vec{B}}{c} \right) \quad (312)$$

where

$$\mathfrak{m} = \left(\frac{\rho_* u_*}{N_*} \right) \left(\frac{q_{e_*} E_* L_*}{U_*} \right) \quad (313)$$

The normalization of the work term, Equation 308, is obviously identical:

$$\vec{F}_\alpha \cdot \vec{u}_\alpha = \frac{q_\alpha}{\mathfrak{m}} \vec{E} \cdot \vec{u}_\alpha \quad (314)$$

In Gaussian units, the force is (Table I-1, Reference 20)

$$\vec{F}_{\alpha*} = q_{\alpha*} \left(\vec{E}_* + \frac{\vec{u}_*}{c_*} \times \vec{B}_* \right) \quad (315)$$

Inserting normalizations 296, 300, and 309 into Equation 315 gives

$$\vec{F}_\alpha = \frac{N_* q_{e_*} L_* E_*}{\rho_* U_*^2} q_\alpha \left[\vec{E} + \frac{\vec{u}}{c} \times \vec{B} (\mu_{o_*} \epsilon_{o_*})^{1/2} \right] \quad (316)$$

Using Equation 313 plus the fact that

$$\mu_{o_*} \epsilon_{o_*} = 1 \quad (317)$$

in Gaussian units, Equation 316 becomes

$$\vec{F}_\alpha = \frac{q_\alpha}{\mathfrak{m}} \left(\vec{E} + \frac{\vec{u} \times \vec{B}}{c} \right) \quad (318)$$

Since Equation 308 is valid for the work in Gaussian units as well as in rationalized mks units, it is clear that Equation 314 is the correct normalized form of the work term for Gaussian units as well as for rationalized mks units.

APPENDIX V
INTEGRATION OF THE EQUATIONS

The integral equations developed in Subsection III-1 have two general forms; these are

$$\int_V dV \int_{\Delta t} dt \left[\frac{\partial \phi}{\partial t} + \vec{\nabla} \cdot \vec{\psi} + \vec{f}_1 \right] = 0 \quad (319)$$

and

$$\int_V dV \int_{\Delta t} dt \left[\frac{\partial \psi}{\partial t} + \vec{\nabla} \cdot \vec{\chi} + \vec{\nabla} \times \vec{\omega} + \vec{f}_2 \right] = 0 \quad (320)$$

Equations 319 and 320 are to be integrated over a cell volume, V , and over a time step, Δt , in plane, cylindrical, and spherical coordinates.

1. EQUATION 319

The first term of Equation 319 may be written as

$$\begin{aligned} \int_V dV \int_{\Delta t} dt \frac{\partial \phi}{\partial t} &= \int_{t_0}^{t_1} \frac{\partial \phi}{\partial t} \int_V dV = \int_{t_0}^{t_1} dt \left[V(t) \frac{\partial \phi}{\partial t} \right] \\ &= \int_{t_0}^{t_1} dt \left[\frac{\partial}{\partial t} (\phi V) - \phi \frac{\partial V}{\partial t} \right] \end{aligned} \quad (321)$$

where $\partial \phi / \partial t$ is assumed uniform throughout the cell, and the cell volume is a function of time because the mesh moves.

If the cell surface moves with velocity \vec{W} , the rate of change of cell volume over a small increment of cell surface is

$$d\left(\frac{\partial V}{\partial t}\right) = \vec{W} \cdot \hat{\nu} dS \quad (322)$$

where $\hat{\nu}$ is the unit outward normal to the cell surface. Assuming that property ϕ is constant on each element of the cell surface during the time step, the rate at which property ϕ changes due to the motion of surface element dS is

$$d\left(\phi \frac{\partial V}{\partial t}\right) = \phi \vec{W} \cdot \hat{\nu} dS \quad (323)$$

Integrating Equation 323,

$$\phi \frac{\partial V}{\partial t} = \int_S \phi \vec{W} \cdot \hat{\nu} dS \quad (324)$$

Inserting Equation 324 in Equation 321,

$$\int_V dV \int_{\Delta t} dt \frac{\partial \phi}{\partial t} = (\phi V) \Big|_{t_0}^{t_1} - \int_{t_0}^{t_1} dt \int_S \phi \vec{W} \cdot \hat{\nu} dS \quad (325)$$

Replacing the surface integral by a summation over the faces of the cell, and assuming that the properties on each face of the cell remain constant during the time step, Equation 325 becomes

$$\int_V dV \int_{\Delta t} dt \frac{\partial \phi}{\partial t} = (\phi V) \Big|_{t_0}^{t_1} - \Delta t \sum_{\substack{\text{cell} \\ \text{faces}}} \phi W_n S \quad (326)$$

where W_n is the component of \vec{W} normal to the cell face.

Using Green's theorem on the second term of Equation 319 gives

$$\int_V dV \int_{\Delta t} dt \vec{v} \cdot \vec{\psi} = \int_{\Delta t} dt \int_S \vec{\psi} \cdot \hat{v} dS = \Delta t \sum_{\substack{\text{cell} \\ \text{faces}}} \psi_n S \quad (327)$$

where

$$\psi_n = \vec{\psi} \cdot \hat{v} \quad (328)$$

and $\vec{\psi}$ has been assumed constant on each cell face during the time step.

The last term in Equation 319 is integrated under the assumption that the source term, \mathcal{S}_1 , is constant throughout the cell volume for the entire time step:

$$\int_V dV \int_{\Delta t} dt \mathcal{S}_1 = \mathcal{S}_1 \int_0^{\Delta t} dt V(t) \quad (329)$$

But using Equation 324,

$$\begin{aligned} V(t) &= V(0) + \int_0^t dt \int_S dS \vec{w} \cdot \hat{v} \\ &= V(0) + t \sum_{\substack{\text{cell} \\ \text{faces}}} w_n S \end{aligned} \quad (330)$$

Substituting Equation 330 into Equation 329,

$$\int_V dV \int_{\Delta t} dt \mathcal{S}_1 = \Delta t \cdot \mathcal{S}_1 \left[V(t_0) + \frac{\Delta t}{2} \sum_{\substack{\text{cell} \\ \text{faces}}} w_n S \right] \quad (331)$$

Combining Equations 326, 327, and 331, the integrated form of Equation 319 is

$$\begin{aligned}
 (\varphi V)_{t_1} = & (\varphi V)_{t_0} + \Delta t \left\{ \sum_{\text{cell faces}} \left[\left(\varphi - \frac{\Delta t \cdot \mathcal{L}_1}{2} \right) W_n - \psi_n \right] S \right. \\
 & \left. - \mathcal{L}_1 V_{t_0} \right\} \quad (332)
 \end{aligned}$$

2. EQUATION 320

Equation 320 is a vector equation and, because of the rotation of the unit vectors in curvilinear coordinates, Green's theorem is not applicable to vector integrands. Consequently, it is necessary to separate Equation 320 into its scalar components, and apply Green's theorem separately to each component. As can be seen from the symmetry of the computational cells illustrated in Figure 1, it suffices to consider the x and z components of Equation 320 for plane and cylindrical geometry, and it suffices to consider only the x component for spherical geometry. Consideration of the remaining components will not yield new information because of the symmetries involved.

Let $\hat{\ell}$ denote a unit vector in either the x or z direction. Then the required components of Equation 320 are given by

$$\int_V dV \int_{\Delta t} dt \left[\hat{\ell} \cdot \frac{\partial \vec{\psi}}{\partial t} + \hat{\ell} \cdot \vec{\nabla} \cdot \vec{\chi} + \hat{\ell} \cdot \vec{\nabla} \times \vec{\omega} + \hat{\ell} \cdot \vec{\mathcal{L}}_2 \right] = 0 \quad (333)$$

Noting that $\hat{\ell}$ is a constant vector,

$$\hat{\ell} \cdot \frac{\partial \psi}{\partial t} = \frac{\partial}{\partial t} (\hat{\ell} \cdot \vec{\psi}) \quad (334)$$

$$\hat{l} \cdot \vec{\nabla} \cdot \vec{\chi} = \vec{\nabla} \cdot (\hat{l} \cdot \vec{\chi}) \quad (335)$$

and

$$\hat{l} \cdot \vec{\nabla} \times \vec{\omega} = \vec{\omega} \cdot \vec{\nabla} \times \hat{l} + \vec{\nabla} \cdot \vec{\omega} \times \hat{l} = \vec{\nabla} \cdot (\vec{\omega} \times \hat{l}) \quad (336)$$

Applying Green's theorem to Equation 336 gives

$$\int_V dV \hat{l} \cdot \vec{\nabla} \times \vec{\omega} = \int_S dS \hat{\nu} \cdot \vec{\omega} \times \hat{l} \quad (337)$$

by use of the vector identities. Combining Equations 333 through 335 and 337,

$$\int_V dV \int_{\Delta t} dt \left[\frac{\partial}{\partial t} (\hat{l} \cdot \vec{\psi}) + \hat{l} \cdot \vec{J}_2 \right] + \int_S dS \int_{\Delta t} dt \hat{\nu} \cdot (\hat{l} \cdot \vec{\chi} + \vec{\omega} \times \hat{l}) = 0 \quad (338)$$

Equation 338 cannot be approximated in the same manner as Equation 320 because the integrands contain geometric factors which are not constant throughout the cells in curvilinear coordinates. Thus, the z and x components of Equation 338 must be considered separately.

a. z Component of Equation 338

As discussed above, the z component of Equation 338 is required only for the plane and cylindrical geometries. As shown in Figure 1, however, the angles between the z axis and the normals to the cell sides are constant for a given cell regardless of the value of y or θ . Consequently, the integrands in the z component of Equation 338 are constant, and the equation may be approximated analogously to

Equation 319. Using Equation 325, the symbol r to represent either x in plane geometry or r in cylindrical geometry, and the symbol θ to represent either y in plane geometry or θ in cylindrical geometry, the z component of Equation 338 becomes

$$\begin{aligned}
 (\psi_z V)_{t_1} = & (\psi_z V)_{t_0} + \Delta t \left\{ \sum_{\text{cell faces}} \left[\left(\psi_z - \frac{\Delta t \mathcal{L}_{2z}}{2} \right) W_n \right. \right. \\
 & \left. \left. - \left(\chi_{zz} \nu_z + \chi_{zr} \nu_r + \omega_{\theta} \nu_r \right) \right] S - \mathcal{L}_{2z} V_{t_0} \right\} \quad (339)
 \end{aligned}$$

where

$$\nu_{\theta} = 0 \quad (340)$$

for the cells shown in Figure 1. Here, ν_r is the direction cosine between the outward normal to the cell face and the r (or x) axis, and ν_z is the direction cosine between the outward normal to the cell face and the z axis.

b. r Component of Equation 338

In the cylindrical and spherical geometries, reference to Figure 1 shows that the angle between the x axis and the normal to a side of the cell is not constant over the entire side of the cell. Consequently, the detailed integrations must be carried out for these two geometries.

For plane geometry, however, these geometric factors are constant on the sides of the cells, and the integrated equation may be written down by analogy to Equation 339 :

$$\begin{aligned}
 (\psi_x V)_{t_1} &= (\psi_x V)_{t_0} + \Delta t \left\{ \sum_{\text{faces}} \left[\left(\psi_x - \frac{\Delta t}{2} \mathcal{L}_{2x} \right) W_n \right. \right. \\
 &\quad \left. \left. - \left(\chi_{xx} \nu_x + \chi_{xz} \nu_z - \omega_y \nu_z \right) S - \mathcal{L}_{2x} V_{t_0} \right] \right\} \quad (341)
 \end{aligned}$$

In carrying out the integration for the cylindrical and spherical geometries, it must be remembered that the radius, r , is never negative while the x coordinate may be negative. Consequently, these integrations must be carried out only over the half cell for which x is positive.

For the cylindrical geometry, the half cell of integration is given by

$$-\frac{\pi}{2} \leq \theta \leq \frac{\pi}{2} \quad (342)$$

Thus, Equation 338 becomes

$$\begin{aligned}
 &\int_{\Delta r} dr \int_{\Delta z} dz \int_{-\pi/2}^{\pi/2} r d\theta \int_{\Delta t} dt \left[\frac{\partial}{\partial t} (\psi_r \cos \theta - \psi_\theta \sin \theta) \right. \\
 &\quad \left. + \mathcal{L}_{2r} \cos \theta - \mathcal{L}_{2\theta} \sin \theta \right] + \left[\int_{A(\theta=\pi/2)} dA \int_{\Delta t} dt \right. \\
 &\quad \left. + \int_{A(\theta=-\pi/2)} dA \int_{\Delta t} dt + \int_C dl \int_{-\pi/2}^{\pi/2} R(l) d\theta \int_{\Delta t} dt \right] \\
 &\quad \left[(\chi_{rr} \nu_r + \chi_{r\theta} \nu_\theta + \chi_{rz} \nu_z) \cos \theta - (\chi_{\theta r} \nu_r + \chi_{\theta\theta} \nu_\theta \right. \\
 &\quad \left. + \chi_{\theta z} \nu_z) \sin \theta + (\omega_z \nu_\theta - \omega_\theta \nu_z) \cos \theta - (\omega_r \nu_z \right. \\
 &\quad \left. - \nu_r \omega_z) \sin \theta \right] = 0 \quad (343)
 \end{aligned}$$

where $\int_C d\ell$ denotes the line integral around the cell at fixed θ , $R(\ell)$ is the value of r on this path, and A is the cross-sectional area of the cell as shown in Figure 2.

On the face $A(\theta = \pi/2)$,

$$\nu_r = \nu_z = 0 \quad (344)$$

and

$$\nu_\theta = 1 \quad (345)$$

On the face $A(\theta = -\pi/2)$,

$$\nu_r = \nu_z = 0 \quad (346)$$

and

$$\nu_\theta = -1 \quad (347)$$

On the faces $-\pi/2 < \theta < \pi/2$,

$$\nu_\theta = 0 \quad (348)$$

and

$$\nu_r = \nu_z = \text{constants}$$

Using Equations 344 through 348 in Equation 343 and performing the θ integration,

$$\begin{aligned} \int_{\Delta t} dt \left\{ \int_{\Delta r} dr \int_{\Delta z} dz 2r \left(\frac{\partial \psi}{\partial t} + \mathcal{L}_{2r} \right) - \int_{A(\theta=\pi/2)} dA \chi_{\theta\theta} \right. \\ \left. - \int_{A(\theta=-\pi/2)} dA \chi_{\theta\theta} + 2 \int_C R(\ell) d\ell \left(\chi_{rr} \nu_r \right. \right. \\ \left. \left. + \chi_{rz} \nu_z - \omega_\theta \nu_z \right) \right\} = 0 \quad (349) \end{aligned}$$

Noting that

$$\int_V dV = \int_{\Delta r} dr \int_{\Delta z} dz \int_0^{2\pi} r d\theta \quad (350)$$

and

$$\int_S dS = \int_C dl \int_0^{2\pi} R(t) d\theta \quad (351)$$

for the full cell, Equation 349 becomes

$$\int_V dV \int_{\Delta t} dt \left(\frac{\partial \psi_r}{\partial t} + \mathcal{L}_{2r} \right) + \int_S dS \int_{\Delta t} dt \left(\chi_{rr} \nu_r + \chi_{rz} \nu_z - \omega_\theta \nu_z \right) - 2\pi \int_{\Delta t} dt \int_A dA \chi_{\theta\theta} = 0 \quad (352)$$

The integrated form of Equation 352 can be written by analogy to Equation 339:

$$(\psi_r V)_{t_1} = (\psi_r V)_{t_0} + \Delta t \left\{ \sum_{\text{faces}} \left[\left(\psi_r - \frac{\Delta t}{2} \mathcal{L}_{2r} \right) W_n - \left(\chi_{rr} \nu_r + \chi_{rz} \nu_z - \omega_\theta \nu_z \right) S + 2\pi A \chi_{\theta\theta} - \mathcal{L}_{2r} V_{t_0} \right] \right\} \quad (353)$$

The integration for spherical geometry is handled similarly to that for cylindrical geometry. In the spherical case, the half cell of integration is given by

$$-\pi/2 \leq \theta \leq \pi/2 \quad \text{and} \quad -\pi/2 \leq \varphi \leq \pi/2 \quad (354)$$

In this coordinate system, the x component of Equation 338 becomes

$$\begin{aligned}
& \int_{\Delta t} dt \left\{ \int_{r_1}^{r_2} r d\varphi \int_{-\pi/2}^{\pi/2} r \cos \varphi d\theta \left[\frac{\partial}{\partial t} (\psi_r \cos \varphi \cos \theta - \psi_\theta \sin \theta \right. \right. \\
& \quad - \psi_\varphi \sin \varphi \cos \theta) + \mathcal{L}_{2r} \cos \varphi \cos \theta - \mathcal{L}_{2\theta} \sin \theta \\
& \quad \left. \left. - \mathcal{L}_{2\varphi} \sin \varphi \cos \theta \right] + \left[\int_{A(\theta=\pi/2)} dA + \int_{A(\theta=-\pi/2)} dA \right. \right. \\
& \quad + \int_{-\pi/2}^{\pi/2} r_1 d\varphi \int_{-\pi/2}^{\pi/2} r_1 \cos \varphi d\theta \\
& \quad \left. \left. + \int_{-\pi/2}^{\pi/2} r_2 d\varphi \int_{-\pi/2}^{\pi/2} r_2 \cos \varphi d\theta \right] \cdot \left[(\chi_{rr} \nu_r + \chi_{r\theta} \nu_\theta \right. \right. \\
& \quad + \chi_{r\varphi} \nu_\varphi) \cos \varphi \cos \theta - (\chi_{\theta r} \nu_r + \chi_{\theta\theta} \nu_\theta \\
& \quad + \chi_{\theta\varphi} \nu_\varphi) \sin \theta - (\chi_{\varphi r} \nu_r + \chi_{\varphi\theta} \nu_\theta + \chi_{\varphi\varphi} \nu_\varphi) \sin \varphi \cos \theta \\
& \quad + (\omega_{\varphi\theta} \nu_\theta - \omega_{\theta\varphi} \nu_\varphi) \cos \varphi \cos \theta - (\omega_r \nu_\varphi - \omega_{\varphi r}) \sin \theta \\
& \quad \left. \left. - (\omega_{\theta r} \nu_r - \omega_r \nu_\theta) \sin \varphi \cos \theta \right] \right\} = 0 \quad (355)
\end{aligned}$$

where r_1 is the radius of the inner face of the cell and $r_2 = r_1 + \Delta r$ is the radius of the outer face.

On the face $A(\theta = \pi/2)$,

$$\nu_r = \nu_\varphi = 0 \quad (356)$$

and

$$\nu_\theta = 1 \quad (357)$$

On the face $A(\theta = -\pi/2)$,

$$\nu_r = \nu_\varphi = 0 \quad (358)$$

and

$$\nu_\theta = -1 \quad (359)$$

On the faces $r_1 = \text{constant}$ and $r_2 = \text{constant}$,

$$\nu_\theta = \nu_\varphi = 0 \quad (360)$$

and

$$\nu_r = \text{constant} \quad (361)$$

Substituting Equations 356 through 360 into Equation 355 and carrying out the angular integrations,

$$\begin{aligned} \int_{\Delta t} dt \left\{ \int_{r_1}^{r_2} r^2 dr \left[\pi \frac{\partial \psi_r}{\partial t} + \pi \nu_{2r} \right] - \int_{A(\theta=\pi/2)} dA \chi_{\theta\theta} \right. \\ \left. - \int_{A(\theta=-\pi/2)} dA \chi_{\theta\theta} + \left[r_1^2 \nu_{r1} + r_2^2 \nu_{r2} \right] \right. \\ \left. \cdot \left[\pi \chi_{rr} \right] \right\} = 0 \quad (362) \end{aligned}$$

Noting that

$$\int_V dV = 4\pi \int_{r_1}^{r_2} r^2 dr \quad (363)$$

and

$$\int_S dS = 4\pi r^2 \quad (364)$$

for the full cell, Equation 362 becomes

$$\int_V dV \int_{\Delta t} dt \left(\frac{\partial \psi_r}{\partial t} + \mathcal{L}_{2r} \right) + \int_S dS \int_{\Delta t} dt \chi_{rr} \nu_r - 8 \int_{\Delta t} dt \int_A dA \chi_{\theta\theta} = 0 \quad (365)$$

The integrated form of Equation 365 can be written by analogy to Equation 339 :

$$(\psi_r V)_{t_1} = (\psi_r V)_{t_0} + \Delta t \left\{ \sum_{\text{faces}} \left[\left(\psi_r - \frac{\Delta t}{2} \mathcal{L}_{2r} \right) W_n - \chi_{rr} \nu_r \right] S + 8A \chi_{\theta\theta} - \mathcal{L}_{2r} V_{t_0} \right\} \quad (366)$$

By letting r and θ represent x and y in plane geometry, defining

$$\nu_z = 0 \quad (367)$$

in spherical geometry, and defining

$$\eta = \begin{cases} 0 & \text{in plane geometry} \\ \pi & \text{in cylindrical geometry} \\ 4 & \text{in spherical geometry} \end{cases} \quad (368)$$

it is possible to combine Equations 341 , 353 and 366 into one form:

$$(\psi_r V)_{t_1} = (\psi_r V)_{t_0} + \Delta t \left\{ \sum_{\text{faces}} \left[\left(\psi_r - \frac{\Delta t}{2} \mathcal{L}_{2r} \right) W_n - \left(\chi_{rr} \nu_r + \chi_{rz} \nu_z - \omega_{\theta} \nu_z \right) \right] S + 2\eta A \chi_{\theta\theta} - \mathcal{L}_{2r} V_{t_0} \right\} \quad (369)$$

APPENDIX VI CHARACTERISTICS

The field properties on the cell faces are evaluated by the use of characteristics. The theory of characteristics for the hydrodynamic equations of a perfect gas in equilibrium is given in Reference 4. In this appendix, the theory of characteristics is extended to a mixture of gases out of equilibrium, to the equations of radiation transport, and to Maxwell's equations.

1. HYDRODYNAMIC EQUATIONS

The gas in each cell of the mesh is assumed to be at a constant state; this state is characterized by a pressure tensor defined by (see Equation 207, Appendix I)

$$\underline{\underline{P}}_{\alpha} = \rho_{\alpha} \langle \vec{v}_{\alpha} \vec{v}_{\alpha} \rangle \quad (370)$$

and a kinetic temperature defined by (see Equation 2.13, Chapter IX, Reference 2),

$$\frac{3}{2} k_* T_{\alpha*} = \frac{1}{2} m_{\alpha*} \langle v_{\alpha*}^2 \rangle$$

or

$$\frac{3}{2} k T_{\alpha} = \frac{1}{2} m_{\alpha} \langle v_{\alpha}^2 \rangle \quad (371)$$

The normal pressure of species α is defined by

$$\begin{aligned}
 P_{\alpha} &= \frac{1}{3} \vec{P}_{\alpha} : \vec{I} \\
 &= \frac{\rho_{\alpha}}{3} \langle \vec{v}_{\alpha} \cdot \vec{v}_{\alpha} \rangle
 \end{aligned}
 \tag{372}$$

Equations 371 and 372 give

$$P_{\alpha} = n_{\alpha} k T_{\alpha}
 \tag{373}$$

as the kinetic relation for the species α in the cell in question.

Now consider a plane with a constant flow on each side as depicted in Figure 25

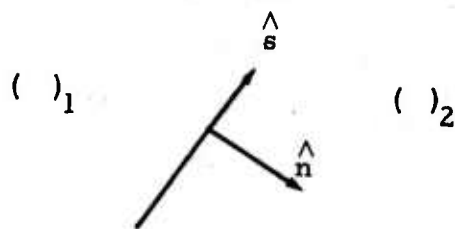


Figure 25. Surface Coordinate System

where \hat{n} and \hat{s} are unit vectors in the directions normal and tangential to the plane, respectively.

In terms of these coordinates, Equation 19 is

$$\frac{\partial \rho_{\alpha}}{\partial t} + \frac{\partial}{\partial n} (\rho_{\alpha} \langle u_{\alpha n} \rangle) = \mathcal{L}_{\alpha}^{(1)}
 \tag{374}$$

where Equation 25 has been used, and Equation 20 is

$$\frac{\partial}{\partial t} (\rho_{\alpha} \langle u_{\alpha n} \rangle) + \frac{\partial}{\partial n} (\rho_{\alpha} \langle u_{\alpha n} \rangle^2 + P_{\alpha n n}) = \mathcal{L}_{\alpha n}^{(2)}
 \tag{375}$$

where Equation 26 has been used.

But

$$P_{\alpha nn} = \frac{1}{3} \vec{P}_{\alpha} : \vec{I} = P_{\alpha} \quad (376)$$

where the assumption of constant flow within the cell implies that the pressure tensor is isotropic.

The First Law of Thermodynamics gives

$$de_{\alpha} = T_{\alpha} dS_{\alpha} - P_{\alpha} d\left(\frac{1}{\rho_{\alpha}}\right) \quad (377)$$

This version of the first law (with the various species decoupled) is valid for the flow across a boundary because the effects of collisions are volume effects and disappear from the integrals for sufficiently small cell size. Thus, the several species may be considered to flow across the cell boundaries without interfering with one another.

Now

$$\begin{aligned} de_{\alpha} &= \left(\frac{\partial e_{\alpha}}{\partial T_{\alpha}}\right)_{\rho_{\alpha}} dT_{\alpha} + \left(\frac{\partial e_{\alpha}}{\partial(1/\rho_{\alpha})}\right)_{T_{\alpha}} d(1/\rho_{\alpha}) \\ &= c_{v\alpha} dT_{\alpha} + \left(\frac{\partial e_{\alpha}}{\partial(1/\rho_{\alpha})}\right)_{T_{\alpha}} d(1/\rho_{\alpha}) \end{aligned} \quad (378)$$

also

$$\left(\frac{\partial e_{\alpha}}{\partial(1/\rho_{\alpha})}\right)_{T_{\alpha}} = T_{\alpha} \left(\frac{\partial S_{\alpha}}{\partial(1/\rho_{\alpha})}\right)_{T_{\alpha}} - P_{\alpha} \quad (379)$$

Forming

$$F_{\alpha} \equiv e_{\alpha} - T_{\alpha} S_{\alpha} \quad (380)$$

it is clear that

$$\left(\frac{\partial F_\alpha}{\partial(1/\rho_\alpha)}\right)_{T_\alpha} = \left(\frac{\partial e_\alpha}{\partial(1/\rho_\alpha)}\right)_{T_\alpha} - T_\alpha \left(\frac{\partial S_\alpha}{\partial(1/\rho_\alpha)}\right)_{T_\alpha} = -P_\alpha \quad (381)$$

and

$$\begin{aligned} \left(\frac{\partial F_\alpha}{\partial T_\alpha}\right)_{\rho_\alpha} &= \left(\frac{\partial e_\alpha}{\partial T_\alpha}\right)_{\rho_\alpha} - S_\alpha - T_\alpha \left(\frac{\partial S_\alpha}{\partial T_\alpha}\right)_{\rho_\alpha} \\ &= c_{v\alpha} - S_\alpha - T_\alpha \left(\frac{\partial S_\alpha}{\partial T_\alpha}\right)_{\rho_\alpha} \end{aligned} \quad (382)$$

But the First Law gives

$$\left(\frac{\partial e_\alpha}{\partial T_\alpha}\right)_{\rho_\alpha} = T_\alpha \left(\frac{\partial S_\alpha}{\partial T_\alpha}\right)_{\rho_\alpha} = c_{v\alpha}$$

Thus

$$\left(\frac{\partial F_\alpha}{\partial T_\alpha}\right)_{\rho_\alpha} = -S_\alpha \quad (383)$$

Equations 381 and 383 give

$$\left(\frac{\partial P_\alpha}{\partial T_\alpha}\right)_{\rho_\alpha} = \left(\frac{\partial S_\alpha}{\partial(1/\rho_\alpha)}\right)_{T_\alpha} \quad (384)$$

Thus

$$de_\alpha = T_\alpha dS_\alpha - P_\alpha d(1/\rho_\alpha)$$

or

$$\begin{aligned} de_{\alpha} &= c_{v\alpha} dT_{\alpha} + \left(\frac{\partial e_{\alpha}}{\partial (1/\rho_{\alpha})} \right)_{T_{\alpha}} d(1/\rho_{\alpha}) \\ &= c_{v\alpha} dT_{\alpha} + \left[T_{\alpha} \left(\frac{\partial P_{\alpha}}{\partial T_{\alpha}} \right)_{\rho_{\alpha}} - P_{\alpha} \right] d(1/\rho_{\alpha}) \end{aligned} \quad (385)$$

or

$$c_{v\alpha} dT_{\alpha} - T_{\alpha} dS_{\alpha} = - T_{\alpha} \left(\frac{\partial P_{\alpha}}{\partial T_{\alpha}} \right)_{\rho_{\alpha}} d(1/\rho_{\alpha}) \quad (386)$$

Thus

$$\left(\frac{\partial T_{\alpha}}{\partial (1/\rho_{\alpha})} \right)_{S_{\alpha}} = - \frac{T_{\alpha}}{c_{v\alpha}} \left(\frac{\partial P_{\alpha}}{\partial T_{\alpha}} \right)_{\rho_{\alpha}} \quad (387)$$

By use of Equation 373 ,

$$\left(\frac{\partial P_{\alpha}}{\partial T_{\alpha}} \right)_{\rho_{\alpha}} = n_{\alpha} \kappa \quad (388)$$

Thus, Equation 387 becomes

$$\left(\frac{\partial T_{\alpha}}{\partial (1/\rho_{\alpha})} \right)_{S_{\alpha}} = - \frac{T_{\alpha}}{c_{v\alpha}} n_{\alpha} \kappa = - P_{\alpha} / c_{v\alpha} \quad (389)$$

Now consider

$$\begin{aligned} \left(\frac{\partial P_{\alpha}}{\partial (1/\rho_{\alpha})} \right)_{S_{\alpha}} &= \left[\frac{\partial}{\partial (1/\rho_{\alpha})} \left(\frac{\rho_{\alpha} \kappa T_{\alpha}}{m_{\alpha}} \right) \right]_{S_{\alpha}} \\ &= \frac{\kappa}{m_{\alpha}} \left\{ T_{\alpha} \left[\frac{\partial \rho_{\alpha}}{\partial (1/\rho_{\alpha})} \right]_{S_{\alpha}} + \rho_{\alpha} \left[\frac{\partial T_{\alpha}}{\partial (1/\rho_{\alpha})} \right]_{S_{\alpha}} \right\} \end{aligned}$$

or

$$\begin{aligned} \left(\frac{\partial P_\alpha}{\partial(1/\rho_\alpha)} \right)_{S_\alpha} &= \frac{\kappa}{m_\alpha} \left\{ -T_\alpha \rho_\alpha^2 - \frac{P_\alpha \rho_\alpha}{c_{v\alpha}} \right\} \\ &= \frac{\kappa T_\alpha \rho_\alpha^2}{m_\alpha} \left[1 + \frac{\kappa}{m_\alpha c_{v\alpha}} \right] \end{aligned} \quad (390)$$

Using Equation 373 in Equation 390,

$$\left(\frac{\partial P_\alpha}{\partial(1/\rho_\alpha)} \right)_{S_\alpha} = -\frac{P_\alpha}{(1/\rho_\alpha)} \left(1 + \frac{\kappa}{m_\alpha c_{v\alpha}} \right) = -\frac{\gamma_\alpha P_\alpha}{(1/\rho_\alpha)} \quad (391)$$

where

$$\gamma_\alpha \equiv 1 + \frac{\kappa}{m_\alpha c_{v\alpha}} \quad (392)$$

Ignoring volume effects, which do not contribute to the surface flux terms, Equation 374 becomes

$$\frac{\partial \rho_\alpha}{\partial t} + \langle u_{\alpha n} \rangle \frac{\partial \rho_\alpha}{\partial n} + \rho_\alpha \frac{\partial}{\partial n} \langle u_{\alpha n} \rangle = 0 \quad (393)$$

If the changes between regions (1) and (2) are small (ensured by sufficiently small cell size), the flow processes will be nearly isentropic. Thus,

$$\frac{\partial \rho_\alpha}{\partial t} \cong \left(\frac{\partial \rho_\alpha}{\partial P_\alpha} \right)_{S_\alpha} \frac{\partial P_\alpha}{\partial t} \quad (394)$$

But

$$\left(\frac{\partial \rho_\alpha}{\partial P_\alpha} \right)_{S_\alpha} = \frac{1}{\left(\frac{\partial P_\alpha}{\partial \rho_\alpha} \right)_{S_\alpha}} = \frac{\partial \rho_\alpha / \partial(1/\rho_\alpha)}{\left(\frac{\partial P_\alpha}{\partial(1/\rho_\alpha)} \right)_{S_\alpha}} \quad (395)$$

and

$$\frac{\partial(1/\rho_\alpha)}{\partial\rho_\alpha} = -\frac{1}{\rho_\alpha} \quad (396)$$

Thus, Equations 391, 395, and 396 give

$$\left(\frac{\partial\rho_\alpha}{\partial P_\alpha}\right)_{S_\alpha} = \frac{-\rho_\alpha^2}{-\gamma_\alpha P_\alpha \rho_\alpha} = \frac{1}{a_\alpha^2} \quad (397)$$

where

$$a_\alpha = (\gamma_\alpha P_\alpha / P_\alpha)^{1/2} \quad (398)$$

is the local speed of sound for species α .

Using Equation 397, Equation 396 becomes

$$\frac{\partial\rho_\alpha}{\partial t} = \frac{1}{a_\alpha^2} \frac{\partial P_\alpha}{\partial t} \quad (399)$$

Similarly

$$\frac{\partial\rho_\alpha}{\partial n} = \frac{1}{a_\alpha^2} \frac{\partial P_\alpha}{\partial n} \quad (400)$$

Defining

$$M_\alpha = \frac{\langle u_{\alpha n} \rangle}{a_\alpha} \quad (401)$$

Equation 393 becomes

$$\frac{1}{\rho_{\alpha} a_{\alpha}} \frac{\partial P_{\alpha}}{\partial t} + a_{\alpha} \frac{\partial}{\partial n} \langle u_{\alpha n} \rangle + \frac{M_{\alpha}}{\rho_{\alpha}} \frac{\partial P_{\alpha}}{\partial n} = 0 \quad (402)$$

In the same way, Equation 375 becomes

$$\frac{M_{\alpha}}{\rho_{\alpha} a_{\alpha}} \frac{\partial P_{\alpha}}{\partial t} + \frac{\partial}{\partial t} \langle u_{\alpha n} \rangle + 2 \langle u_{\alpha n} \rangle \frac{\partial}{\partial n} \langle u_{\alpha n} \rangle + \frac{(M_{\alpha}^2 + 1)}{\rho_{\alpha}} \frac{\partial P_{\alpha}}{\partial n} = 0 \quad (403)$$

Adding and subtracting Equation 402 to Equation 403 :

$$\begin{aligned} \frac{\partial}{\partial t} \langle u_{\alpha n} \rangle + \frac{M_{\alpha} \pm 1}{\rho_{\alpha} a_{\alpha}} \frac{\partial P_{\alpha}}{\partial t} + a_{\alpha} (2M_{\alpha} \pm 1) \frac{\partial}{\partial n} \langle u_{\alpha n} \rangle \\ + \frac{(M_{\alpha}^2 + 1 \pm M_{\alpha})}{\rho_{\alpha}} \frac{\partial P_{\alpha}}{\partial n} = 0 \end{aligned} \quad (404)$$

Multiplying Equation 402 by M_{α} and subtracting from Equation 404 :

$$\begin{aligned} \frac{\partial}{\partial t} \langle u_{\alpha n} \rangle \pm \frac{1}{\rho_{\alpha} a_{\alpha}} \frac{\partial P_{\alpha}}{\partial t} + a_{\alpha} (M_{\alpha} \pm 1) \frac{\partial}{\partial n} \langle u_{\alpha n} \rangle \\ + \frac{(1 \pm M_{\alpha})}{\rho_{\alpha}} \frac{\partial P_{\alpha}}{\partial n} = 0 \end{aligned} \quad (405)$$

Rearranging

$$\begin{aligned} \left[\frac{\partial}{\partial t} \langle u_{\alpha n} \rangle \pm \frac{1}{\rho_{\alpha} a_{\alpha}} \frac{\partial P_{\alpha}}{\partial t} \right] + a_{\alpha} (M_{\alpha} \pm 1) \left[\frac{\partial}{\partial n} \langle u_{\alpha n} \rangle \right. \\ \left. \pm \frac{1}{\rho_{\alpha} a_{\alpha}} \frac{\partial P_{\alpha}}{\partial n} \right] = 0 \end{aligned} \quad (406)$$

Define

$$J_{\alpha\pm} \equiv \langle u_{\alpha n} \rangle \pm \int^P \alpha \frac{dP}{\rho_{\alpha} a_{\alpha}} \quad (407)$$

Then the final characteristic equation is

$$\frac{\partial J_{\alpha\pm}}{\partial t} + a_{\alpha} (M_{\alpha} \pm 1) \frac{\partial}{\partial n} J_{\alpha\pm} = 0 \quad (408)$$

Over an interval of constant a_{α} and M_{α} , Equation 408 has the solutions

$$J_{\alpha\pm} = J_{\alpha\pm} \left[n - a_{\alpha} (M_{\alpha} \pm 1) t \right] \quad (409)$$

Thus, $J_{\alpha+}$ is constant along the phase paths

$$n - a_{\alpha} (M_{\alpha} + 1) t = \text{constant}$$

or

$$n = n_0 + a_{\alpha} (M_{\alpha} + 1) t \quad (410)$$

and $J_{\alpha-}$ is constant along the trajectories

$$n - a_{\alpha} (M_{\alpha} - 1) t = \text{constant}$$

or

$$n = n_0 + a_{\alpha} (M_{\alpha} - 1) t \quad (411)$$

2. RADIATION TRANSPORT EQUATIONS

The characteristics for the equations of radiation transport are found in the same manner as for the equations of

hydrodynamics. The mathematical derivation appears much simpler in the present case, however, because the equations are linear.

As in the case of the hydrodynamic equations, the volume source terms do not enter into the determination of surface properties. Thus, assuming constant radiative properties in a cell and using the same (n, s) coordinates as used for the hydrodynamic equations, Equations 25 and 26 become

$$\frac{\partial e_{R\nu}}{\partial t} + c \frac{\partial Q_{R\nu n}}{\partial n} = 0 \quad (412)$$

and

$$\frac{\partial Q_{R\nu n}}{\partial t} + \frac{c}{3} \frac{\partial e_{R\nu}}{\partial n} = 0 \quad (413)$$

Equation 35 has been used in reducing Equation 26 to Equation 413. Multiplying Equation 412 by a constant, a , and adding and subtracting Equation 413 to the resulting equation gives

$$\frac{\partial}{\partial t} \left(a e_{R\nu} \pm Q_{R\nu n} \right) + c \frac{\partial}{\partial n} \left(a Q_{R\nu n} \pm \frac{e_{R\nu}}{3} \right) = 0 \quad (414)$$

Rearranging

$$\frac{\partial}{\partial t} \left(e_{R\nu} \pm Q_{R\nu n} / a \right) \pm \frac{c}{3a} \frac{\partial}{\partial n} \left(e_{R\nu} \pm 3a Q_{R\nu n} \right) = 0 \quad (415)$$

The arguments of the differential operators in Equation 415 are identical if

$$\frac{1}{a} = 3a$$

or

$$a = 1/\sqrt{3} \quad (416)$$

Defining

$$J_{\nu\pm} = e_{R\nu} \pm \sqrt{3} Q_{R\nu n} \quad (417)$$

and using Equations 416 and 417 in Equation 415 gives

$$\frac{\partial J_{\nu\pm}}{\partial t} \pm \frac{c}{\sqrt{3}} \frac{\partial J_{\nu\pm}}{\partial n} = 0 \quad (418)$$

Equation 413 has the solutions

$$J_{\nu\pm} = J_{\nu\pm}(n \mp ct/\sqrt{3}) \quad (419)$$

Thus, $J_{\nu+}$ is constant on the trajectories

$$n = n_0 + ct/\sqrt{3} \quad (420)$$

and $J_{\nu-}$ is constant on the trajectories

$$n = n_0 - ct/\sqrt{3} \quad (421)$$

3. MAXWELL'S EQUATIONS

As in the case of the hydrodynamic equations, the characteristics for Maxwell's equations are found by neglecting source effects in the equations; thus, the appropriate forms of Equations 29 and 30 are

$$\frac{\partial \vec{B}}{\partial t} + c \vec{\nabla} \times \vec{E} = 0 \quad (422)$$

and

$$\frac{\partial \vec{E}}{\partial t} - c \vec{\nabla} \times \vec{B} = 0 \quad (423)$$

The presence of the vector product in these equations necessitates the defining of a rectangular Cartesian coordinate system on the surface of the cell as depicted in Figure 26:

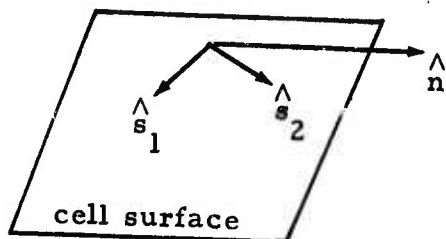


Figure 26. Three-Dimensional Surface Coordinate System

As illustrated, the coordinates (n, s_1, s_2) form a right-handed system.

Remembering that the assumption of uniform field properties on each side of the cell surface implies that the only derivatives which exist are $\partial/\partial t$ and $\partial/\partial n$, Equations 422 and 423 reduce to

$$\frac{\partial B_{s_1}}{\partial t} - c \frac{\partial E_{s_2}}{\partial n} = 0 \quad (424)$$

$$\frac{\partial B_{s_2}}{\partial t} + c \frac{\partial E_{s_1}}{\partial n} = 0 \quad (425)$$

$$\frac{\partial E_{s_1}}{\partial t} + c \frac{\partial B_{s_2}}{\partial n} = 0 \quad (426)$$

and

$$\frac{\partial E_{s_2}}{\partial t} - c \frac{\partial B_{s_1}}{\partial n} = 0 \quad (427)$$

Adding and subtracting Equations 424 and 427 gives

$$\frac{\partial}{\partial t} (B_{s_1} \pm E_{s_2}) \mp c \frac{\partial}{\partial n} (B_{s_1} \pm E_{s_2}) = 0 \quad (428)$$

Similarly, Equations 425 and 426 give

$$\frac{\partial}{\partial t} (B_{s_2} \pm E_{s_1}) \pm c \frac{\partial}{\partial n} (B_{s_2} \pm E_{s_1}) = 0 \quad (429)$$

Defining

$$J_{1\pm} = B_{s_1} \pm E_{s_2} \quad (430)$$

Equation 428 shows that J_{1+} is constant along the path

$$n = n_0 - ct \quad (431)$$

while J_{1-} is constant along the path

$$n = n_0 + ct \quad (432)$$

Similarly, defining

$$J_{2\pm} = B_{s_2} \pm E_{s_1} \quad (433)$$

Equation 429 shows that J_{2+} is constant along the path

$$n = n_0 + ct \quad (434)$$

while J_{2-} is constant along the path

$$n = n_0 - ct \quad (435)$$

(This Page is Intentionally Left Blank)

APPENDIX VII
GEOMETRICAL FORMULAE

The formulae for the cell geometry are developed as outlined in Subsection III-5c. To minimize loss of significant figures, all distances along a ray are measured from arc $j = j_{\max}$ (the closest arc to the z axis). It is convenient to define the distance between two successive arcs (Figure 2):

$$\Delta d_{i,j+1/2} = d_{i,j} - d_{i,j+1} \quad (436)$$

The radial and axial increments on arc j in column $i+1/2$ are

$$\begin{aligned} \Delta r_{i+1/2,j} &= \Delta r_{i+1/2,j+1} + \Delta d_{i+1,j+1/2} \sin \alpha_{i+1} \\ &\quad - \Delta d_{i,j+1/2} \sin \alpha_i \end{aligned} \quad (437)$$

and

$$\begin{aligned} \Delta z_{i+1/2,j} &= \Delta z_{i+1/2,j+1} + \Delta d_{i,j+1/2} \cos \alpha_i \\ &\quad - \Delta d_{i+1,j+1/2} \cos \alpha_{i+1} \end{aligned} \quad (438)$$

The length of arc j in column $i+1/2$ is

$$l_{i+1/2,j} = \left[(\Delta r_{i+1/2,j})^2 + (\Delta z_{i+1/2,j})^2 \right]^{1/2} \quad (439)$$

and the angle that this arc makes with respect to the positive z direction is given by

$$\sin \beta_{i+1/2, j} = \Delta r_{i+1/2, j} / l_{i+1/2, j} \quad (440)$$

and

$$\cos \beta_{i+1/2, j} = \Delta z_{i+1/2, j} / l_{i+1/2, j} \quad (441)$$

It is convenient to define the following auxiliary formulae:

$$(\mathfrak{J}_1)_i = \Delta d_{i, j+1/2} \sin \alpha_i \quad (442)$$

$$\mathfrak{J}_2 = d_{i, j+1} \Delta d_{i+1, j+1/2} + d_{i+1, j+1} \Delta d_{i, j+1/2} + \Delta d_{i, j+1/2} \Delta d_{i+1, j+1/2} \quad (443)$$

$$(\mathfrak{J}_3)_i = (\mathfrak{J}_1)_i (2d_{i, j+1} + \Delta d_{i, j+1/2}) \sin \alpha_i \quad (444)$$

$$(\mathfrak{J}_4)_i = \mathfrak{J}_2 (d_{i, j+1} + \Delta d_{i, j+1/2}) + \mathfrak{J}_5 \Delta d_{i, j+1/2} \quad (445)$$

$$\mathfrak{J}_5 = d_{i, j+1} d_{i+1, j+1} \quad (446)$$

In terms of these auxiliary formulae, the volume of cell $(i+1/2, j+1/2)$ is given by

$$V_{i+1/2, j+1/2} = g_1 (V_1 \Delta z + V_2 \sin \Delta \alpha) \quad (447)$$

where in plane geometry

$$g_1 = 1/2 \quad (448)$$

$$V_1 = (\mathfrak{J}_1)_i + (\mathfrak{J}_1)_{i+1} \quad (449)$$

$$V_2 = \mathfrak{J}_2 \quad (450)$$

$$\Delta z = z_{i+1} - z_i \quad (451)$$

$$\sin \Delta \alpha = \sin(\alpha_{i+1} - \alpha_i) \quad (452)$$

in cylindrical geometry

$$g_1 = \pi/3 \quad (453)$$

$$V_1 = (J_3)_i + J_2 \sin \alpha_i \sin \alpha_{i+1} + (J_3)_{i+1} \quad (454)$$

$$V_2 = (J_4)_i \sin \alpha_i + (J_4)_{i+1} \sin \alpha_{i+1} \quad (455)$$

$$\Delta z = z_{i+1} - z_i \quad (456)$$

$$\sin \Delta \alpha = \sin(\alpha_{i+1} - \alpha_i) \quad (457)$$

and in spherical geometry

$$g_1 = 4\pi/3 \quad (458)$$

$$V_1 = 0 \quad (459)$$

$$V_2 = J_4 \quad (460)$$

$$\Delta z = 0 \quad (461)$$

$$\sin \Delta \alpha = 1 \quad (462)$$

The surface area of arc j in column $i+1/2$ is

$$S_{i+1/2, j} = S_1 S_2 \quad (463)$$

where in plane geometry

$$S_1 = 1 \quad (464)$$

$$S_2 = l_{i+1/2, j} \quad (465)$$

in cylindrical geometry

$$S_1 = \pi (l_{i+1/2, j} \sin \alpha_{i+1} + d_{i, j} \sin \alpha_i) \quad (466)$$

and in spherical geometry

$$S_1 = 4\pi d_j^2 \quad (468)$$

$$S_2 = 1 \quad (469)$$

The area of the face of cell $(i+1/2, j+1/2)$ on ray i is

$$S_{i,j+1/2} = g_1 \Delta d_{i,j+1/2} \quad (470)$$

where in plane geometry

$$g_1 = 1 \quad (471)$$

in cylindrical geometry

$$g_1 = \pi(2d_{i,j+1} + \Delta d_{i,j+1/2}) \sin \alpha_i \quad (472)$$

and in spherical geometry

$$g_1 = 0 \quad (473)$$

Note that spherical geometry does not require $S_{i,j+1/2}$.

The cross-sectional area of cell $(i+1/2, j+1/2)$ is

$$A_{i+1/2, j+1/2} = g_2 S_3 + g_3 S_4 \quad (474)$$

where in plane geometry

$$g_2 = g_3 = 0 \quad (475)$$

(plane geometry does not require $A_{i+1/2, j+1/2}$)

in cylindrical geometry

$$g_2 = (z_{i+1} - z_i) / 2 \quad (476)$$

$$g_3 = \sin(\alpha_{i+1} - \alpha_i) / 2 \quad (477)$$

$$S_3 = (\mathfrak{J}_1)_i + (\mathfrak{J}_1)_{i+1} \quad (478)$$

$$S_4 = \mathfrak{J}_2 \quad (479)$$

and in spherical geometry

$$g_2 = \pi/2 \quad (480)$$

$$g_3 = 0 \quad (481)$$

$$S_3 = (2d_{j+1} + \Delta d_{j+1/2}) \Delta d_{j+1/2} \quad (482)$$

APPENDIX VIII
STATISTICAL ANALYSIS

The following table shows the results of the statistical analysis of the data obtained in the experiments described in the preceding pages. The results are given in the form of the standard deviation of the mean, the standard error of the mean, and the confidence interval for the mean. The results are given in the form of the standard deviation of the mean, the standard error of the mean, and the confidence interval for the mean.

(183) $\sigma = \sqrt{\frac{1}{n} \sum_{i=1}^n (x_i - \bar{x})^2}$

(184) $\sigma_{\bar{x}} = \frac{\sigma}{\sqrt{n}}$

(This Page is Intentionally Left Blank)

Integration Equation 481 over a unit cube and over the volume of a unit cube in three-dimensional space.

(185)
$$\int_0^1 \int_0^1 \int_0^1 (x^2 + y^2 + z^2) dx dy dz = \frac{1}{2}$$

The results of the statistical analysis of the data obtained in the experiments described in the preceding pages are given in the form of the standard deviation of the mean, the standard error of the mean, and the confidence interval for the mean.

(186)
$$\int_0^1 \int_0^1 \int_0^1 (x^2 + y^2 + z^2) dx dy dz = \frac{1}{2}$$

APPENDIX VIII
STABILITY ANALYSIS

The equations of radiation transport in characteristic form, Equations 418 of Appendix VI, and Maxwell's equations in characteristic form, Equations 428 and 429 of Appendix VI, are all of the general form

$$\frac{\partial J_{\pm}}{\partial t} \pm c \frac{\partial J_{\pm}}{\partial r} = 0 \quad (483)$$

where

$$c > 0 \quad (484)$$

Integrating Equation 483 over a time step and over the volume of a cell in a fixed one-dimensional mesh gives

$$J_{\pm}^{n+1/2} = J_{\pm n+1/2} \mp c \Delta t \left[J_{\pm}^{n+1} - J_{\pm}^n \right] \quad (485)$$

where cell $(n+1/2)$ is bounded by cell surfaces n and $n+1$, lowered indices denote properties evaluated at the beginning of the time step, and raised indices denote properties evaluated at the end of the time step.

To study the growth of any one Fourier component of J_{\pm} , it is convenient to assume an exponential variation:

$$J_{\pm n+1/2} = J_{\pm} \exp i \left[k(n+1/2) \Delta r - \omega m \Delta t \right] \quad (486)$$

where k is the wave number and ω is the frequency of the Fourier component under study.

According to Equation 483, J_+ propagates in the positive r direction while J_- propagates in the negative r direction. Thus, the characteristic boundary properties are

$$J_+^n = J_+^{n-1/2} \quad (487)$$

and

$$J_-^n = J_-^{n+1/2} \quad (488)$$

Substituting 486 through 488 into Equation 485 yields the two equations

$$J_{+n+1/2} = J_+^{n+1/2} \left[1 + c \Delta t (1 - e^{-ik\Delta r}) \right] \quad (489)$$

and

$$J_{-n+1/2} = J_-^{n+1/2} \left[1 - c \Delta t (e^{ik\Delta r} - 1) \right] \quad (490)$$

Using the notation

$$\tau = c \Delta t \quad (491)$$

$$a = 1 - \cos k \Delta r \quad (492)$$

$$b = \sin k \Delta r \quad (493)$$

Equations 489 and 490 can be written in the matrix form

$$\begin{bmatrix} J_+^{n+1/2} \\ J_-^{n+1/2} \end{bmatrix} = \begin{bmatrix} G \end{bmatrix} \cdot \begin{bmatrix} J_{+n+1/2} \\ J_{-n+1/2} \end{bmatrix} \quad (494)$$

where the amplification matrix, G , is given by

$$G = \begin{bmatrix} \frac{1}{1 + \tau(a + ib)} & 0 \\ 0 & \frac{1}{1 + \tau(a - ib)} \end{bmatrix} \quad (495)$$

The matrix G is a normal matrix, since, if G^* denotes the Hermitian conjugate of G , it is obvious that

$$GG^* = G^*G = I \quad (496)$$

Since G is a normal matrix, the necessary and sufficient condition for the stability of Equations 485 is that the eigenvalues of the matrix G satisfy the relation (Equation 4.25, Reference 14)

$$|\lambda| \leq 1 + O(\Delta t) \quad (497)$$

or, for the present application

$$\lambda\lambda^* \leq 1 \quad (498)$$

The eigenvalues of the matrix G are

$$\lambda = \frac{1}{1 + \tau(a \pm ib)} \quad (499)$$

Consequently, for either eigenvalue,

$$\lambda\lambda^* = \frac{1}{[1 + \tau(a + ib)][1 + \tau(a - ib)]} \quad (500)$$

and requirement 498 gives

$$1 \leq (1 + a\tau)^2 + b^2 \tau^2 \quad (501)$$

Because $a \geq 0$ according to Equation 492, inequality 501 is satisfied for all $\tau \geq 0$. Thus, Equation 485 is stable for any positive time step.

REFERENCES

1. Chapman, S. and T. G. Cowling, The Mathematical Theory of Non-Uniform Gases, The University Press, Cambridge, 1958.
2. Vincenti, W. G. and C. H. Kruger, Jr., Introduction to Physical Gas Dynamics, John Wiley and Sons, Inc., New York, 1965.
3. McNamara, W., Axisymmetric Interaction of a Blast Wave with the Shock Layer of a High-Speed Blunt Body, Aeroelastic and Structures Research Lab., Mass. Inst. of Tech., ASRL TR 121-15 (also BSD TR 66-280), February, 1966.
4. Courant, R. and K. O. Friedrichs, Supersonic Flow and Shock Waves, Interscience Publishers, Inc., New York, 1948.
5. McNamara, W., "FLAME Computer Code for the Axisymmetric Interaction of a Blast Wave with a Shock Layer on a Blunt Body," J. Spacecraft and Rockets, v. 4 n. 6, pp. 790-795, June, 1967.
6. Bell, G. I., "The Capture and Loss of Electrons by Fission Fragments," Phys. Rev., v. 90, p. 548, 1953.
7. Bohr, N. and J. Lindhard, "Electron Capture and Loss by Heavy Ions Penetrating through Matter," K. Danske Vidensk. Selsk. Mat. fys. Medd., v. 28 n. 7, 1954.
8. Firsov, O. B., "A Qualitative Interpretation of the Mean Excitation Energy in Atomic Collisions," JETP, v. 9, p. 1076, 1959.
9. Fite, W. L., Experimental Studies on Heavy Ion Exchange in Air, AFWL-TR-181, February, 1966.
10. Kieffer, L. J. and G. H. Dunn, "Electron Impact Ionization Cross-Section Data for Atoms, Atomic Ions, and Diatomic Molecules: I. Experimental Data," Rev. Mod. Phys., v. 38, p. 1, 1966.

DOCUMENT CONTROL DATA - R & D

(Security classification of title, body of abstract and indexing annotation must be entered when the overall report is classified)

1. ORIGINATING ACTIVITY (Corporate author)

General Electric Company TEMPO
Santa Barbara, California

2a. REPORT SECURITY CLASSIFICATION

Unclassified

2b. GROUP

3. REPORT TITLE

NUCLEAR INTERFERENCE STUDIES II:
A Physics Code For The Dynamics Of High-Altitude Nuclear Bursts

4. DESCRIPTIVE NOTES (Type of report and inclusive dates)

1 March 1967 through 31 December 1967

5. AUTHOR(S) (First name, middle initial, last name)

W. McNamara
D. H. Archer
T. A. Hoffman

6. REPORT DATE

August 1968

7. TOTAL NO. OF PAGES

188

7b. NO. OF REFS

20

8a. CONTRACT OR GRANT NO.

F29601-67-C-0059

9a. ORIGINATOR'S REPORT NUMBER(S)

AFWL-TR-67-150

b. PROJECT NO.

ARPA Order No. 727

9b. OTHER REPORT NO(S) (Any other numbers that may be assigned
to this report)

67TMP-111

10. DISTRIBUTION STATEMENT

This document is subject to special export controls and each transmittal to foreign governments or foreign nationals may be made only with prior approval of AFWL (WLRT), Kirtland AFB, NMex 87117. Distribution is limited because of the technology discussed in the report.

11. SUPPLEMENTARY NOTES

12. SPONSORING MILITARY ACTIVITY

AFWL (WLRT)
Kirtland AFB, NMex 87117

13. ABSTRACT

(Distribution Limitation Statement No. 2)

A computational code is developed for investigating the dynamics of high-altitude nuclear bursts. The code can treat either one- or two-dimensional problems having either plane, cylindrical, or spherical symmetries. Electromagnetic and radiation transport effects are included, as are the effects of charge and current distributions. The numerical procedure computes the change during a time step of a property within a computational cell in terms of the fluxes of the property crossing the faces of the cell during the time step. The fluxes are computed by the method of characteristics. Use of a moving mesh permits the code to follow contact discontinuities in the field properties. Procedures for incorporating nonequilibrium thermodynamics are developed.

14.

KEY WORDS

LINK A

LINK B

LINK C

ROLE

WT

ROLE

WT

ROLE

WT

Finite-Difference Methods

Method of Characteristics

Plasma Physics

Air/Debris Coupling in Explosions

Hydro Code